Phil. Trans. R. Soc. Lond. B **298**, 355–393 (1982) [355]
Printed in Great Britain

THE MORPHOLOGY OF THE BIPOLAR CELLS, AMACRINE CELLS AND GANGLION CELLS IN THE RETINA OF THE TURTLE *PSEUDEMYS SCRIPTA ELEGANS*

BY HELGA KOLB

Department of Physiology, University of Utah College of Medicine, Salt Lake City, Utah 84108, *U.S.A.*

(*Communicated by P. Fatt, F.R.S. – Received 27 October* 1981)

[Plates 1–5]

CONTENTS

The morphology of the neurons that contribute to the inner plexiform layer of the retina of the turtle *Pseudemys scripta elegans* has been studied by light microscopy of whole-mount material stained by the method of Golgi. Cells have been distinguished on the basis of criteria that include dendritic branching patterns, dendritic morphology, dendritic tree sizes and stratification of processes in the inner plexiform layer. Many of the neurons have dendritic trees oriented parallel to and a few exhibit an orthogonal orientation with the linear visual streak present in the retina of this species. The neurons of the turtle retina have been compared, where possible, with the neurons of the lizard retina as described by Cajal. The findings are discussed in relation to other vertebrate retinas, and correlations are made with recent electrophysiological recordings of the turtle retina. Comments are made with regard to the significance of orientation of neurons relative to the linear visual streak.

Introduction

Morphological descriptions of the retina of the red-eared slider, *Pseudemys scripta elegans*, have dealt primarily with the distribution of oil droplets and photoreceptor types (Liebman & Granda 1971; Granda & Haden 1970; Brown 1969; Gallego & Perez-Arroya 1976) and the first synaptic level where the photoreceptors contact horizontal and bipolar cells (Lasansky 1969, 1971; Leeper 1978*a*, *b*). A recent quantitative study of the ganglion cells (Peterson & Ulinski 1979) has added information on the total number of ganglion cells and their distribution according to cell body size. However, that study did not concentrate on the various morphological types of ganglion cell present in this species' retina. Likewise, little is known of the morphology of the different types of bipolar and amacrine cells. Yet the retina of the *Pseudemys* turtle is particularly favourable for intracellular recording (Baylor & Fuortes 1970; Baylor *et al.* 1971; Baylor & Hodgkin 1973; Simon 1973; Fuortes & Simon 1974; Schwartz 1973; Marchiafava 1979; Marchiafava & Torre 1978), and many investigators are now marking cells with intracellular dyes to make correlations between morphology and physiology (Simon 1973; Saito *et al.* 1974; Schwartz 1973; Normann *et al.* 1979; Marchiafava & Weiler 1980; Jensen & DeVoe 1980, 1981). Clearly a more complete description of the neurons of the *Pseudemys* retina would be valuable.

Intracellular recordings from horizontal cell axon terminals (LI units based upon physiological criteria) in the linear visual streak region of the turtle retina disclosed an interesting correlation between oriented morphology of these axon terminals and their oriented anisotropic receptive fields (Normann *et al.* 1979). The turtle is only one of a variety of species with a prominent visual streak in its retina. In fact, visual streaks may be more or less developed extensions of the circular area centralis found in the retinas of most vertebrates (e.g. birds, rabbits, sheep, cats and ground squirrels) (Hughes 1977), and thus observation of cells in the visual streak may be of importance for visual processing in other species. For this reason the orientation of cells relative to the specialized streak region has received particular attention in this Golgi study of turtle retina. It is hoped that ultimately such information could help our understanding of how a neuron's shape influences its receptive field properties.

Where possible the cells of the turtle retina described in this paper have been compared with Cajal's (1933) description of the cells of the lizard retina: however, more cell types are described than have been previously reported in the reptilian retina. Thus, I describe nine types of bipolar cell, many of which have multistratified axon terminals in the inner plexiform layer, 27 different types of amacrine cell, each characterized by distinctive dendritic morphology and specific stratification levels, and 21 different morphological types of ganglion cell.

The study describes the cell types that have been seen in 30 well impregnated retinas of the turtle. However, the possibility of additional, as yet uncharacterized cell types must be borne in mind. Many of the cells were seen frequently, but some were only seen on one or two occasions. To try to draw quantitative conclusions concerning frequency of cell types from a Golgi study is thought to be a futile endeavour, and even to conclude that cells that are only seen once or twice are 'rare' can be equally problematic. The cells illustrated in this paper are the best examples and sometimes the only examples. It must, therefore, be clearly stated that the nomenclature used in this paper is in reference to the illustrated cells and not intended to be taken as an authoritative classification of the cells of the inner plexiform layer of the turtle retina. Future morphological and physiological studies will be needed to decide finally whether each cell described in this paper is a unique functional type.

Materials and methods

Thirty retinas of the red-eared slider, *Pseudemys scripta elegans*, were used for this study. The eyes were enucleated under dim room lighting and hemisected. The vitreous humor was first drained from the eye cup and remaining tough strands were severed with scissors. Three or four cuts were made with a razor blade from the edge towards the centre of the eye cup to flatten the preparation. The flattened eye cup was then placed retina side down on a Millipore filter (diameter 2.5 cm, pore diameter 0.45 μm) and pressed flat to ensure that all parts of the retina adhered to the filter. After 1–2 min, the sclera and choroid plus pigment epithelium could be peeled back, the optic nerve was severed and the isolated retina remained flattened to the Millipore filter, ganglion side against the filter. Several retina–Millipore filter preparations were sandwiched between pieces of regular filter paper and glass slides. The sandwiched tissue was processed through the Golgi–Colonnier method (Colonnier 1964) after an initial fixation for 2 h in 3% glutaraldehyde in 0.1 M phosphate buffer. After dehydration and clearing in cedar wood oil each retina–Millipore filter preparation was mounted filter side, i.e. ganglion side, up, in Permount on a glass slide for viewing in the light microscope as a whole mount.

Well impregnated cells were examined and drawn with the aid of a camera lucida. Their position or orientation relative to the linear visual streak (l.v.s.) was measured with an eyepiece graticule. Stratification of dendrites or axon terminals within the inner plexiform layer (i.p.l.) was determined by measuring the thickness of the i.p.l. which varies according to retinal location, dividing this figure by 5 and thence estimating the borders of Cajal's (1933) five strata (S1–S5) in which the impregnated profiles were branching. In the linear visual streak region of the turtle retina the i.p.l. is 75–90 μm thick, while in peripheral retina the i.p.l. is only 45–60 μm thick (plate 1, figures 18, 19). In this study the five strata are considered to be of equal thickness. Most of the drawings were made by using an achromatic ×40 long working distance oil objective. Most of the cells are reproduced in the figures at the same magnification with their orientation relative to the l.v.s. and their distance from the streak indicated.

Observations

Bipolar cells of the turtle retina

I have seen at least nine different morphological types of bipolar cell in the retina of the turtle. They can be recognized as different types primarily by the shape and stratification of their axon terminals. All the bipolar cell types appear to have a process projecting from one of the major dendrites in the outer plexiform layer (o.p.l.), into the outer nuclear layer, to end at the level of the outer limiting membrane. Such processes are Landolt clubs (Landolt 1871). Two of the nine types of bipolar cell have unistratified axon terminals while the remainder have bi- or tristratified axon terminals. Figure 1 shows the appearance of a typical example of each bipolar type. Most of the examples are from in or near the l.v.s. (indicated by the black bar on this and subsequent figures). Unfortunately, in drawings of whole mounts the multistratified axon terminals are difficult to represent and thus the schematic drawing of figure 2 is included to show this feature of the bipolar cells' morphologies. Bipolar cells in or near the l.v.s. take an oblique course away from their dendritic trees for distances as great as 150 μm, fanning out from the l.v.s.

B1 and B2 (figures 1, 2) both have axon terminals branching in the most vitread portion of the i.p.l. B1 is differentiated from B2 by its more planar, widely branching axon terminal

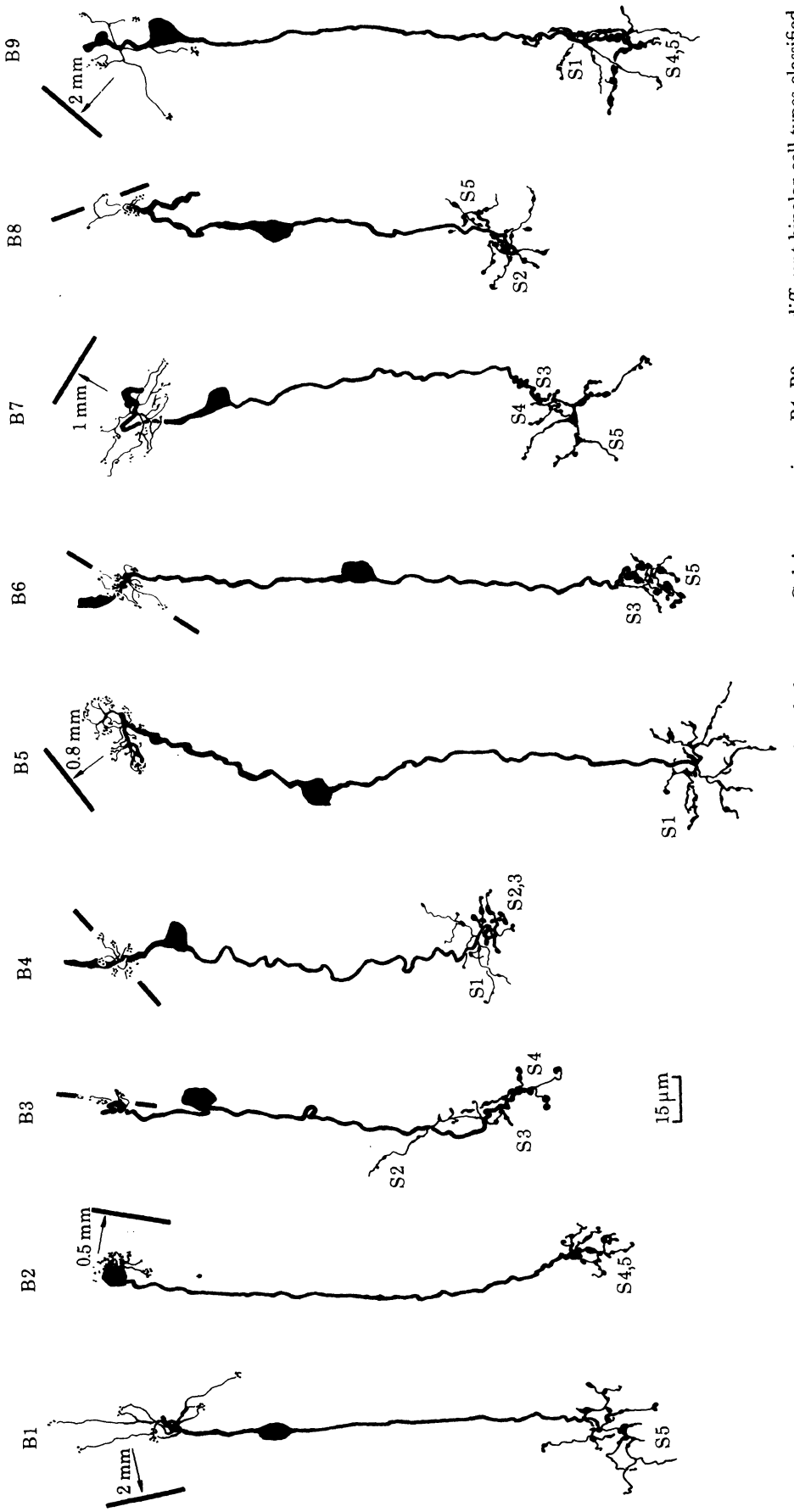

FIGURE 1. Camera lucida drawings of bipolar cells of the turtle retina as seen in whole-mount Golgi preparations. B1–B9 are different bipolar cell types classified according to their axonal branching in the i.p.l. All have Landolt clubs. Examples of a B3 and a B6 are illustrated in figure 26, plate 2. The strata of branching of the axon in the inner plexiform layer are shown. Distance from the l.v.s. is indicated on the arrow and the orientation of the streak is indicated by the solid black bar in this and all following figures.

consisting of spidery branches restricted to stratum 5 (S5). B2, on the other hand, has a distinctly varicose axon terminal directed more in the vertical direction, branching through S4 and S5. B1 of figure 1 is located in midperipheral retina (2 mm from the l.v.s.) and consequently has a larger dendritic spread than B2. However, examples of B1 seen in the streak (not illustrated) indicate that they may have a 35–40 μm dendritic field. It is probable that B1 bipolar cells have larger dendritic fields than other bipolars in all areas of retina. Most of the other

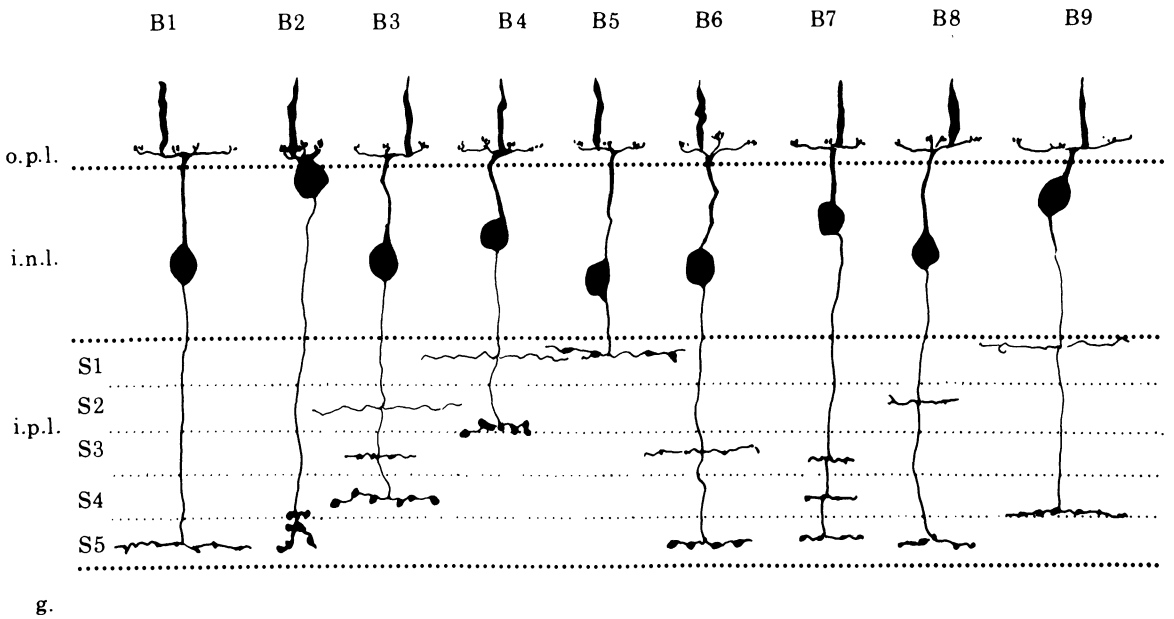

FIGURE 2. Summary drawing of the bipolar cell types of the turtle retina as seen in vertical view. The stratification of the axon terminals of the different cell types are more clearly represented than in the whole-mount view (figure 1). Abbreviations: o.p.l., outer plexiform layer; i.n.l., inner nuclear layer; i.p.l., inner plexiform layer; g., ganglion cell layer.

bipolar cell types had dendritic fields measuring between 15 and 25 μm where they occur on the l.v.s. B2 is characterized by a cell body lying sclerad in the inner nuclear layer (i.n.l.) at the level of the horizontal cell bodies or, as seen on numerous occasions, displaced to the outer nuclear layer. Its dendritic span is small (20 μm) and composed of many short dendrites ending in many clusters of terminals. Thus, B2 typically has a more compact and bushy dendritic tree than any of the other bipolar types.

B3 has a tristratified axon terminal with a branch in each of the three middle strata of the i.p.l., S2–S4. The axon branches become progressively more varicose and less spread out as they go from S2 to S4. The cell body of B3 lies in the centre of the i.n.l. and the small dendritic tree consists of fine dendrites and delicate clusters of terminals projecting to the photoreceptor pedicles (figures 1, 2; plate 2, figure 26). B4 is a bipolar with a bistratified axon terminal restricted to the upper half of the i.p.l. closer to the amacrine cells. The branches in S1 are of very fine calibre and spread over a larger area than the more beaded branches that lie on the S2/3 border. The cell body is large and lies fairly high in the i.n.l. under the horizontal cell somata. In the l.v.s. the dendritic spread is 15 μm but in more peripheral locations it can be 40 μm.

The bipolar cell with a unistratified wide-spreading axon terminal in S1 under the amacrine cell bodies is here designated B5. In appearance the axon terminal of B5 resembles that of B1 but the terminals differ in branching on opposite sides of the i.p.l. B5 typically has a low-lying cell body, just above the amacrine cell bodies in the i.n.l., and a 30–35 μm dendritic spread when it occurs in the l.v.s. (figure 1). No examples of far peripheral B5 cells have been seen in the present turtle material.

Bipolar cells B6–B9 are all multistratified (figures 1, 2), differing in the specific strata at which their axons branch. Like B3 and B4, the axonal branches in the strata closer to the amacrine cells are wider-spreading and less sturdy or varicose than the branches in the lower strata, with the exception of B7. B6 has a small-diameter spread of its axon terminal with fine branches in S3 and distinctly varicose endings in S5. B6 has a cell body lying close to the amacrine cells in the i.n.l. and a very small dendritic field where it occurs in the l.v.s. (15 μm, figure 1; plate 2, figure 26). However, examples from far peripheral retina have dendritic trees of 120 μm.

The axon of B7 branches in the three inner (proximal to the ganglion cells) strata, S3–S5 of the i.p.l. The B7 bipolars outside of the streak, which are the only examples that have been seen, have axon terminal branches increasing in spread with depth. Thus, the branches in S5 ramify furthest. The dendritic trees of peripheral B7 cells cover 45 μm of the outer plexiform layer with fine curly dendrites that appear to give off terminals *en passant* before ending in other clusters of terminals. B8 has a small (22 μm) dendritic spread (figure 1), a low-lying cell body and an extensive bistratified axon terminal. The stratification of B8 axon terminals is easy to determine as they consist of two definite slim planar processes branching in S2 and S5.

Finally, B9 is a bipolar cell type of which only a few examples have been observed in peripheral retina. Its simple wide-spreading fine dendrites bear small clusters of terminals. The dendrites appear to be selective for a widely spaced cone (or rod) population. The cell body of B9 lies high in the i.n.l., just beneath the horizontal cell bodies (figures 1, 2) and its axon terminal is, like B8, rather divergent to different areas of the neuropil of the i.p.l. Thus, the upper slim twigs branch in S1 while the lower, coarser processes straddle the S4/5 border.

Judging from stratification of their axon terminals, Cajal (1933) described equivalent bipolar cells to B1–B4 and B6–B8 in lizard retina: however, there does not appear to be a description of cells like B5 and B9. On the other hand, Cajal (1933) did describe two bipolar types in lizard not seen here in turtle retina.

Amacrine cells of the turtle retina

Amacrine cells of the turtle retina are extremely diverse in morphology (plates 1–3) and it becomes necessary to classify them into categories having some feature in common. Dendritic field size has been chosen. Dendritic fields of some retinal neurons in the mammalian retina are known to increase in size with eccentricity from the area centralis (Boycott & Kolb 1973*a*; Boycott & Wässle 1974). Similarly, in turtle retina, horizontal cells are known to increase dramatically in size from the l.v.s. (Leeper 1978*a*, *b*; Normann & Kolb 1981). A similar increase will be seen for certain amacrine and ganglion cells in the present study. However, such data are difficult to obtain for every cell type to be described in this paper; so the dendritic field size groups for amacrine cells must be regarded as approximate and based on measurements on cells lying within 2 mm of the l.v.s. The turtle amacrine cells observed here have been arbitrarily allocated to narrow-field groups (30–150 μm), small-field groups (150–300 μm), medium-field groups (300–500 μm) and wide-field groups (over 500 μm).

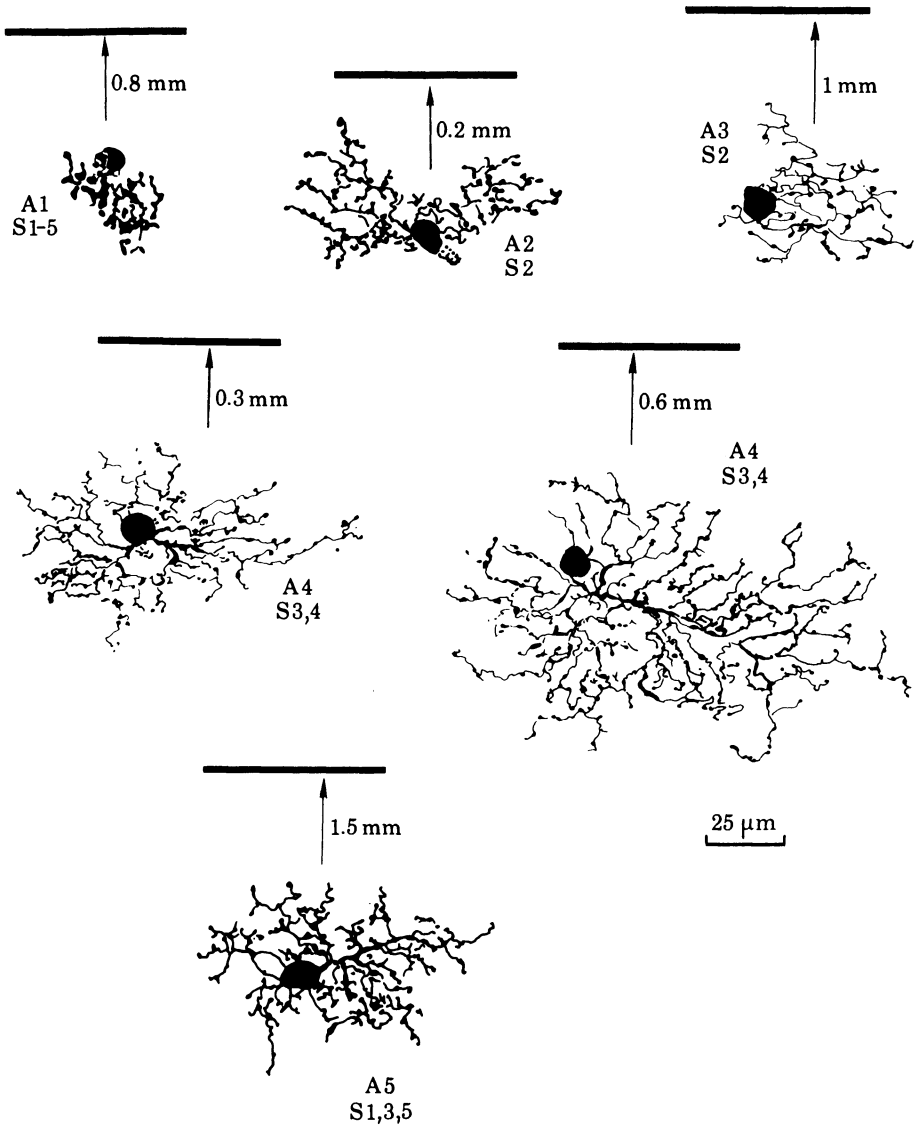

FIGURE 3. Camera lucida drawings of narrow-field amacrine cells of the turtle retina. See text for further details. The strata in which the dendrites branch are indicated in this and all following figures. A2, A4 and A5 are illustrated in light micrographs on plate 2.

Narrow-field amacrine cells

Amacrine cells in this group have dendritic field sizes of 30–150 μm. Only five such amacrine types have been observed in this whole-mount turtle retinal material.

A1 is a narrow-field diffuse amacrine variety. Its cell body measures 7 μm in diameter and its narrow dendritic tree consists of a tufted group of varicosities branching through the vertical depth of the i.p.l. (S1–S5) (figure 3). A2, by comparison, has a 80 μm wide dendritic tree consisting of a similar arbor of tufted branches, but the dendrites are organized on a single plane in S2 of the i.p.l. (figure 3; plate 2, figure 27). Both A1 and A2 are similar to the cells depicted as fig. 5a and 5b or 5c on pl. III in Cajal's (1933) description of the lizard retina.

Amacrine cell A3 is considered a different type from A2 even though it branches in the same stratum (S2), because of its more delicate appearing dendritic tree (figure 3). The slender

processes are notably beaded and contain less appendages than those of A2. The A3 cell illustrated has a 9 μm cell body and a 56 μm dendritic spread.

A4 attains a larger dendritic spread than the other narrow-field varieties, measuring between 80 and 150 μm. The round, 9 μm cell body gives rise to one or more dendrites that pass to the middle of the i.p.l. (S3 and S4) before breaking up into a loosely tufted group of intertwined dendrites bearing many appendages (figure 3; plate 2, figure 31). A5, on the other hand, is a tristratified amacrine with three definite planes of branching (S1, S2 and S5) of the tufted varicose dendritic tree (figure 3; plate 2, figures 32–34). The dendritic field size of A5 is approximately 50 μm but in the example of figure 3 it takes an oblique course and thus appears much bigger. Cell A4 is possibly a counterpart of fig. 4a, pl. III, of Cajal's (1933) lizard material.

Small-field amacrine cells

A6–A12 (figure 4) have been placed in the category of amacrine cells having dendritic tree diameters between 150 and 300 μm.

Amacrine A6 is the only member of the small-field group with a diffusely spreading dendritic tree branching at all levels of the i.p.l. (figure 4). Its rather fine dendrites branch sparingly and are quite beaded, arising from two or three major dendrites springing from the lower vitread surface of the 9 μm cell body. Both A7 and A8 stratify high on a precise plane just beneath the amacrine cell bodies in S1. Nevertheless, they are distinctly different morphological types, for A7 has coarse knobbly dendrites and the secondary dendrites bear short spines (figure 4; plate 1, figure 23), while A8 has a wavy dendritic tree with stout major dendrites and delicate secondary branches curving in and out. Both A7 and A8 have most of their dendritic trees directed towards the l.v.s. and the dendrites of the A8 cell actually pass across the streak. A6 and A8 appear to be oriented orthogonal to the streak while A7 is oriented oblique to the streak.

A9 like A7 and A8 is very narrowly stratified but its dendrites occupy the border between S3 and S4. The flattened (11 μm × 5 μm) cell body gives rise to stout major dendrites that pass to the S3/4 border where they branch into a loosely organized ramification of slender dendrites (figure 4). In contrast A10 is broadly stratified, branching through the lower i.p.l., S3 and S5 (figure 4). The round, 10 μm cell body has a single descending apical dendrite which ultimately splits into three and branches profusely, with large beaded varicosities characterizing the secondary dendrites (figure 4).

The final two amacrine cells of the small-field group, A11 and A12, are bi- and tristratified respectively. A11 has a very curious branching pattern. The dendrites of A11 branching in S2 and S5 have different morphologies. Thus, the top layer, restricted to S2, is composed of four wavy dendrites covering a 200 μm × 250 μm field and the lower layer is composed of dendrites arising from the top four branches (arrows, figure 4), each breaking up into a compact cluster of dendrites. Each cluster of lower dendrites covers only a 50–75 μm area of neuropil. Unfortunately, only one example of an A11 cell has been seen in this Golgi study of turtle retina, but it appears to have a distinct enough morphology to be considered a unique cell type.

The tristratified amacrine A12 has been seen on several occasions (plate 2, figures 28–30). In figure 4, dendrites of the top layer, branching in S1, are indicated as fine dotted profiles, of the layer in S3 as coarse dots and of the vitread layer in S5 as solid profiles. The dendritic trees of each stratum appear morphologically similar, composed of delicate wavy dendrites bearing occasional appendages (plate 2, figures 28–30). Their dendritic spreads also appear to be approximately the same (130 μm × 150 μm) and each layer arises from the main branch

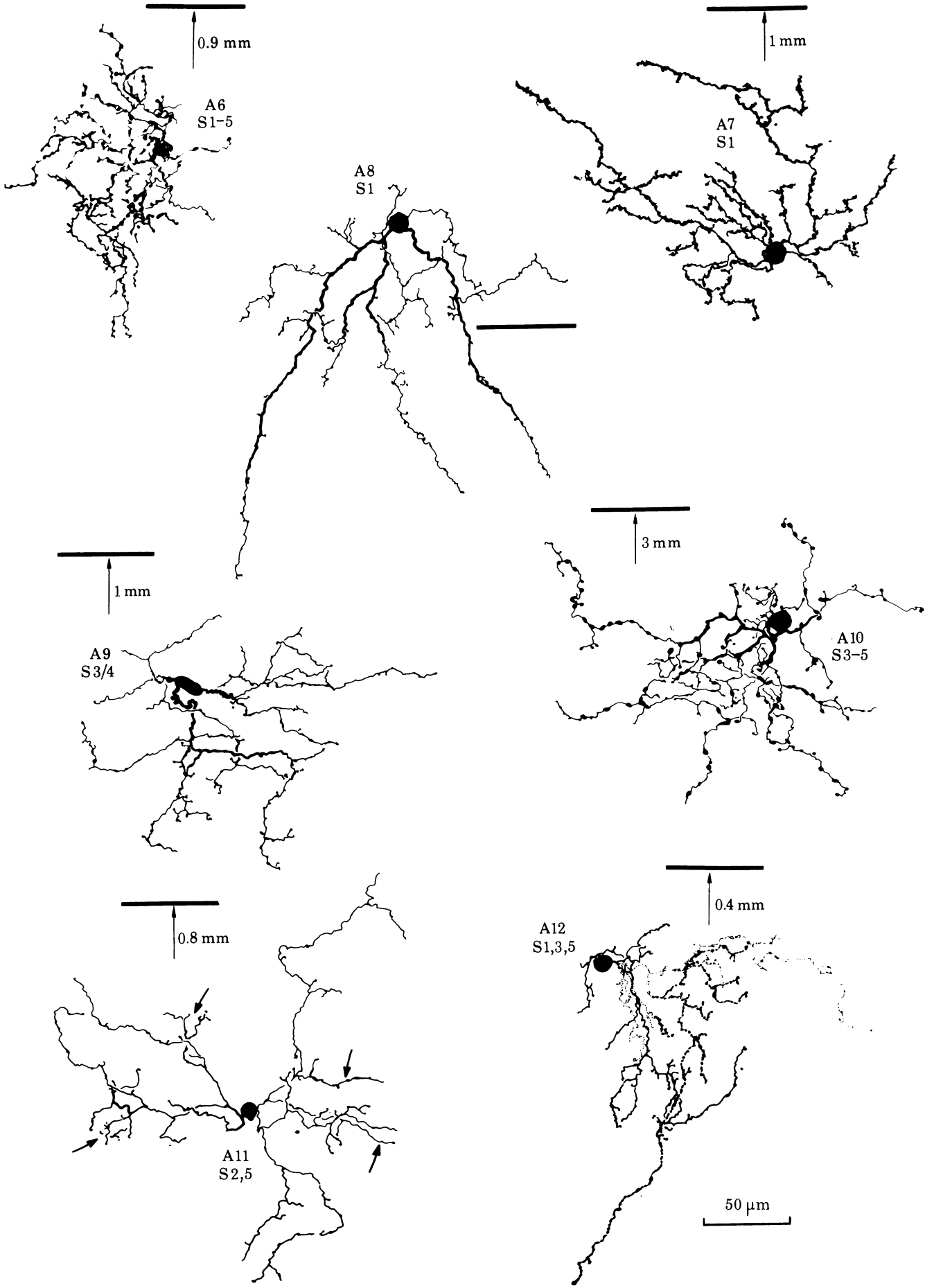

FIGURE 4. Camera lucida drawings of small-field amacrine cells of the turtle retina. A6 is a diffuse cell; A7–A9 are monostratified, while A10 is broadly stratified; A11 is bistratified, with dendritic clusters in S5 arrowed; A12 is tristratified, with the lowest tier of dendrites (S5) as solid lines, the middle tier (S3) as heavy dotted lines and the top tier (S1) as fine dotted lines. A7 and A12 are illustrated in light micrographs on plates 1 and 2.

beneath the round, 10 μm cell body. Interestingly, the dendrites stratifying in S3 and S5 appear to be oriented orthogonal to the streak while the dendrites in S1 appear to be more parallel in orientation (A12, figure 4; plate 2, figures 28–30).

Medium-field amacrine cells

A13–A15 belong to the medium-field group of amacrine cells with 300–500 μm dendritic field dimensions. A13 has a small (10 μm) cell body and an oval 350 μm × 200 μm dendritic field with the long axis oriented parallel to the l.v.s. (figure 5). In the example illustrated in figure 5, one of the major dendrites is incomplete while the others branch profusely in S2 giving rise to a jumbled dendritic tree of overlapping branches. A14, on the other hand, has a very simple polar branching pattern (figure 5). The small, 9 μm, cell body gives rise to two major dendrites passing in opposite directions in S1. These are relatively devoid of spines and appendages and break up into daughter branches that dip down to form curved profiles in S3. The cell (A14) lies along the border of the l.v.s. and is oriented precisely parallel to the streak.

Only one of the amacrine cell type here designated A15 has been seen in the turtle material. This example (A15, figure 5) is characterized by a large-diameter cell body (11 μm × 15 μm) and stout major dendrites that ramify on the S1/2 border with a radiate dichotomous branching pattern. Primarily the tips, but occasionally more central portions of the dendritic tree, produce very fine tapering processes (dotted profiles, figure 5) that dip down to ramify on the border between S4 and S5. Probably A15 should be considered a bistratified amacrine cell. It bears some resemblance to Cajal's cell of fig. 5, pl. III, from lizard retina.

Wide-field amacrine cells

Most of the amacrine cell types in the turtle retina have large simple radiate dendritic trees. Thus, amacrines A16–A27 have dendritic fields greater than 500 μm in diameter. Indeed some amacrine varieties have dendrites that cover 2 mm of retina (see below).

A16 has the simplest morphology of all the amacrine cells of the turtle retina (figure 6; plate 1, figures 24, 25). Such amacrine cells were not uncommon in the present material. The small, 10 μm cell body is flattened and produces only two dendrites from either side, which pass down to the most vitread level of the i.p.l. (S5), to travel in opposite directions without branching. The two dendrites bear an occasional appendage and finally taper to slim beaded profiles. The dendritic field, from the tip of one dendrite to the tip of the other, measures approximately 1.45 mm. A17 (figure 6) is a complementary cell to A16, which branches in the sclerad portion of the i.p.l. in S1. However, A17 has a few branches from its otherwise essentially bipolar dendritic tree. The dendrites cover a 1.4 mm region of retina, as measured from the ends of each major dendrite. The cell body of A18 is slightly larger (9 μm × 14 μm) than those of either A16 or A17, and gives rise to several major dendrites that fan out with a simple dichotomous dendritic tree (900 μm) lying just beneath the amacrine cell bodies in S1 (figure 6; plate 3, figure 37). Cajal's cell fig. 4f, pl. III, is probably comparable to A18 in lizard retina, and it is possible that his cell fig. 5d is the equivalent of A16, although it appears to have more branches in lizard.

Amacrine cells A19 and A20 appear to be morphological counterparts that branch in two different strata of the i.p.l. Thus, A19 has a 13 μm cell body and irregular angular dendrites, spreading over a 1 mm field stratifying in S1 (figure 7; plate 1, figure 21). A20, on the other hand, has dendrites restricted to the middle of the i.p.l. in S3. The dendritic spread of the

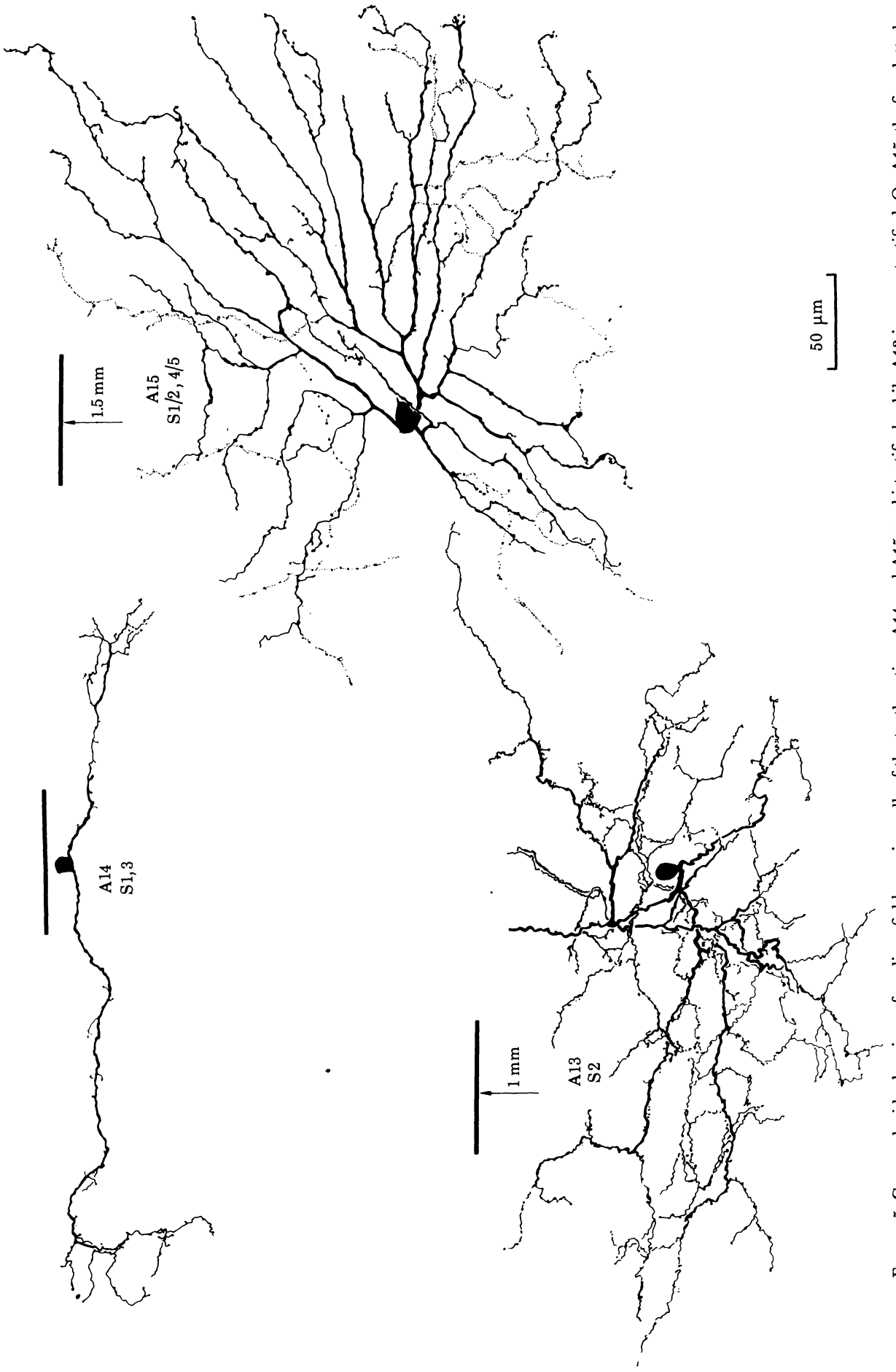

FIGURE 5. Camera lucida drawings of medium-field amcrine cells of the turtle retina. A14 and A15 are bistratified, while A13 is monostratified. On A15, the fine dotted lines are the dendrites that pass down to the S4/5 border. A14 has a very striking orientation parallel to the edge of the l.v.s.

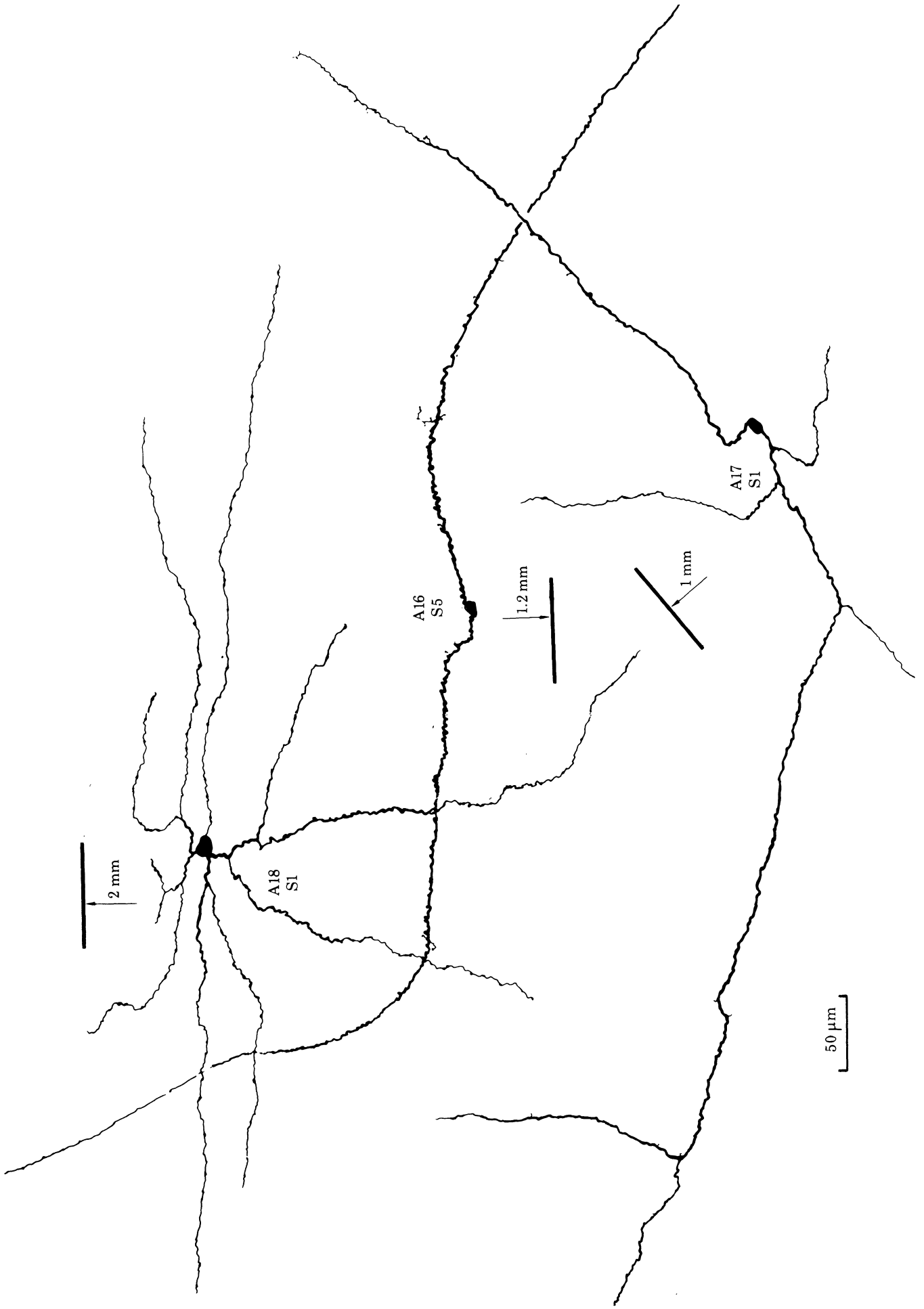

FIGURE 6. Camera lucida drawings of wide-field amacrine cells of the turtle retina. These monostratified amacrine cells have either a simple bipolar (A16, A17) or a sparsely branched (A18) dendritic tree. A16 and A18 are illustrated on plates 1 and 3.

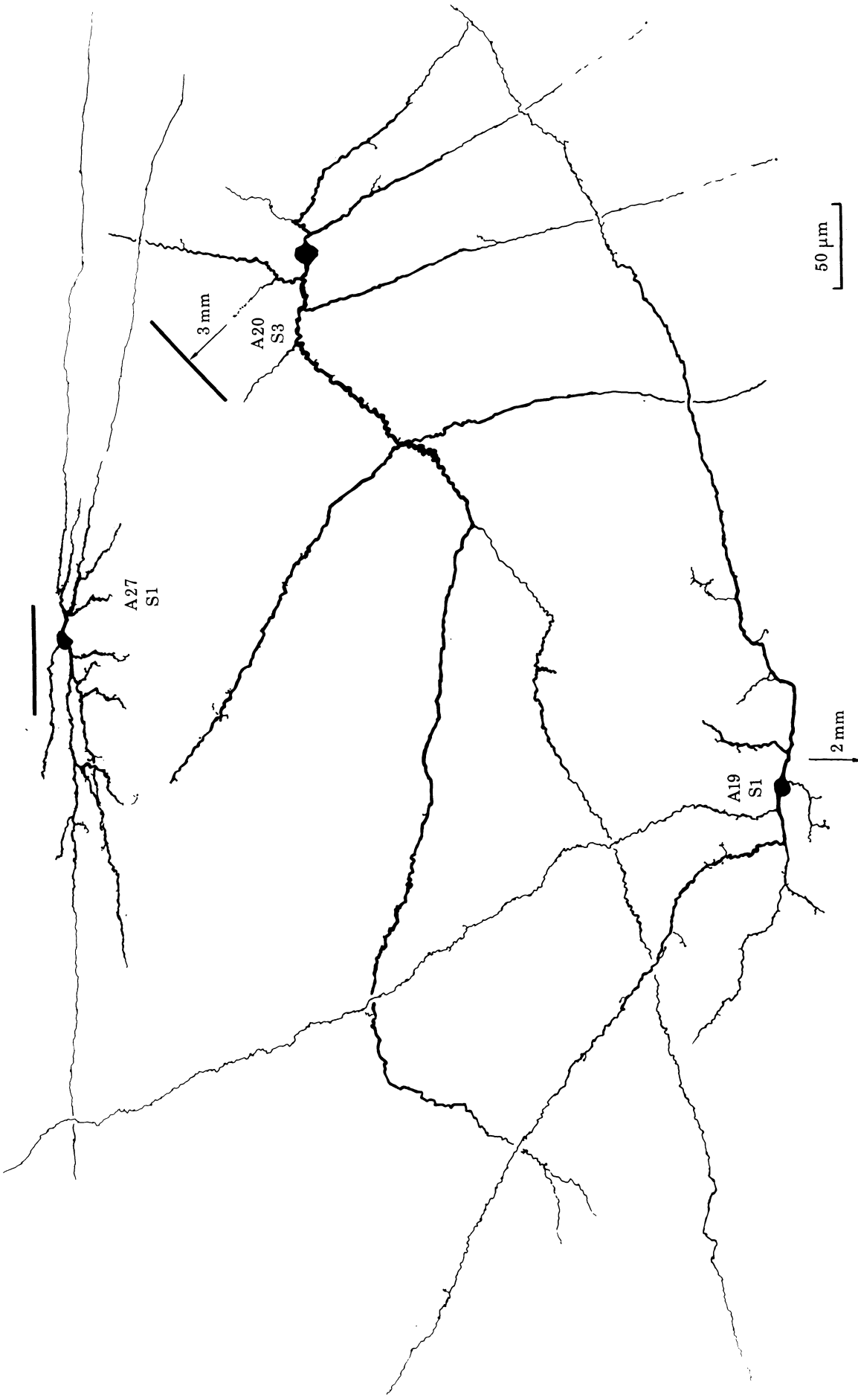

FIGURE 7. Camera lucida drawings of wide-field amacrine cells of the turtle retina. A19 and A20 are monostratified cells with dendrites arising at 90° from the parent dendrite. A27 occurs along the edge of the l.v.s. and has fine extensions of the dendrites travelling for hundreds of micrometres. A19 and A20 are illustrated on plate 1.

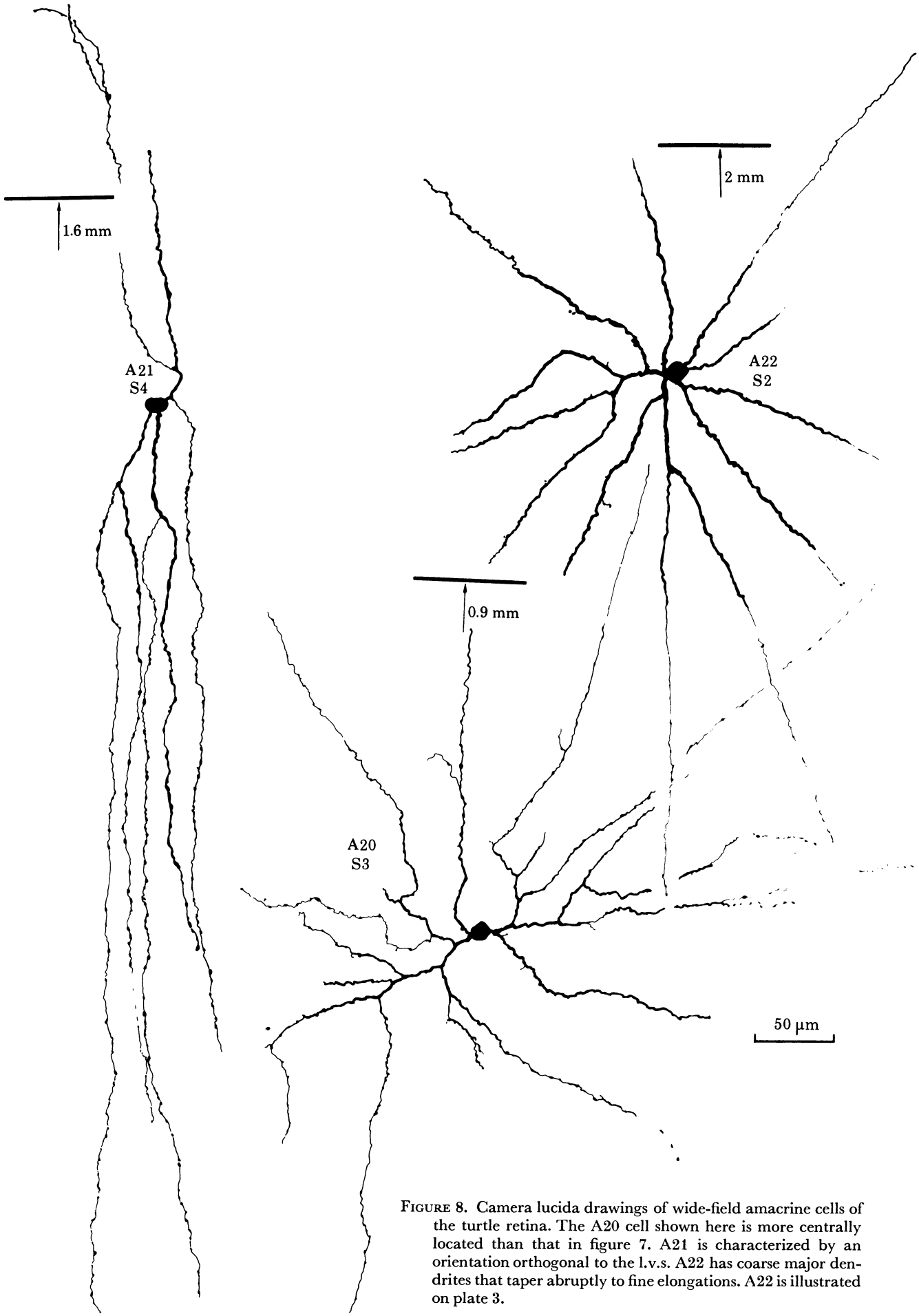

FIGURE 8. Camera lucida drawings of wide-field amacrine cells of the turtle retina. The A20 cell shown here is more centrally located than that in figure 7. A21 is characterized by an orientation orthogonal to the l.v.s. A22 has coarse major dendrites that taper abruptly to fine elongations. A22 is illustrated on plate 3.

peripheral (3 mm from l.v.s.) A20 in figure 7 is approximately 1 mm, while a more centrally located A20 amacrine (2 mm from l.v.s.) in figure 8 has a 650 μm dendritic tree. The latter cell has a more complete, filled-in dendritic tree. However, both examples, like A19, have an irregular dichotomous branching pattern with each branch being given off at right angles from the parent branch. All three amacrine cell types have dendritic trees oriented with their long axis parallel to the l.v.s. A20 bears some resemblance to a large amacrine cell of the lizard retina as seen in Cajal's (1933) fig. 4h, pl. III.

An amacrine cell oriented exactly orthogonal to the l.v.s. has been observed in this turtle whole-mount material. A21 (figure 8) has a wide dendritic spread (950 μm) but all the simple, essentially straight-running, dendrites pass orthogonally towards or away from the streak region. All the dendrites remain strictly at the same level of the i.p.l. in S4 (figure 8). Only a single example of the A21 has been observed. A21 may be the cell fig. 4c, pl. III, in Cajal's (1933) description.

A very distinctive amacrine cell seen in the turtle retina is A22 (figure 8; plate 3, figure 36). It is almost certainly equivalent to the giant amacrine cell of lizard retina as described by Cajal (1933) in fig. 5f, pl. III. A22 is characterized by a large (12 μm) very round cell body which gives rise to three or four main dendrites. On the S2/3 border in the i.p.l. the thick main dendrites (2.5 μm) branch dichotomously once or twice and the secondary dendrites ramify straight out from the central point like spokes of a wheel. The tips of the major dendrites narrow abruptly and continue as very fine profiles running for hundreds of micrometres. The fine tips are not impregnated in most Golgi-stained A22 cells and thus the full extent of such an amacrine cell's dendritic field is rarely seen. Another example at lower magnification is shown in figure 9 to be compared with other radiate wide-field amacrine cell types.

The remaining amacrines A23–A27 have extremely large dendritic fields covering between 1 and 3 mm (figure 9). The very symmetrical radiate cells A23 and A24 stratify high in the i.p.l. close to the amacrine cells. A23 has a burst of slender dendrites emerging from the small 10 μm cell body. All of these branch immediately and approximately 24–26 secondary dendrites radiate like spokes of a wheel in lower S1, covering an essentially circular area with a 1–2 mm diameter (plate 3, figure 35). A24 differs slightly from A23 in morphology (figure 9; plate 3, figure 37). Its larger cell body (12 μm) produces fewer dendrites than does A23. These also split immediately into two or three branches so that a total of about 18 branches radiate out symmetrically from the central point. The dendrites of A24 cells stratify on the S2/3 border and appear to cover a 1.5–2.0 mm field. A25 and A26 become progressively simpler in having fewer radiating dendrites than A23 and A24. My impression is that these cells become less complex as they stratify more vitread. Thus, A25 has only nine radiating dendrites from the midpoint and A26 only six such dendrites. A25 stratifies on the S3/4 border with the largest dendritic field seen for any amacrine cell in the turtle retina, at 2.7 mm. A26 stratifies in S5, running over the surface of the ganglion cell bodies. Only one example of A26 has been seen (illustrated in figure 9) and its dendritic tree is smaller than those of the other radiating cells, being only 1.0 mm in diameter. All the radiating amacrine cell types (A22–A26) appear to have essentially symmetrical round dendritic fields and they show no evidence of orientation relative to the streak (figure 9). Cajal (1933) described cells such as A23 (fig. 4b, pl. III) A24 (fig. 4g, pl. III; fig. 1, pl. IV), A25 (fig. 4d, pl. III) and A26 (unlabelled cell branching in S5, pl. III) in lizard retina.

The final wide-field amacrine cell A27 (figures 7, 9) has only been observed on the edge of the

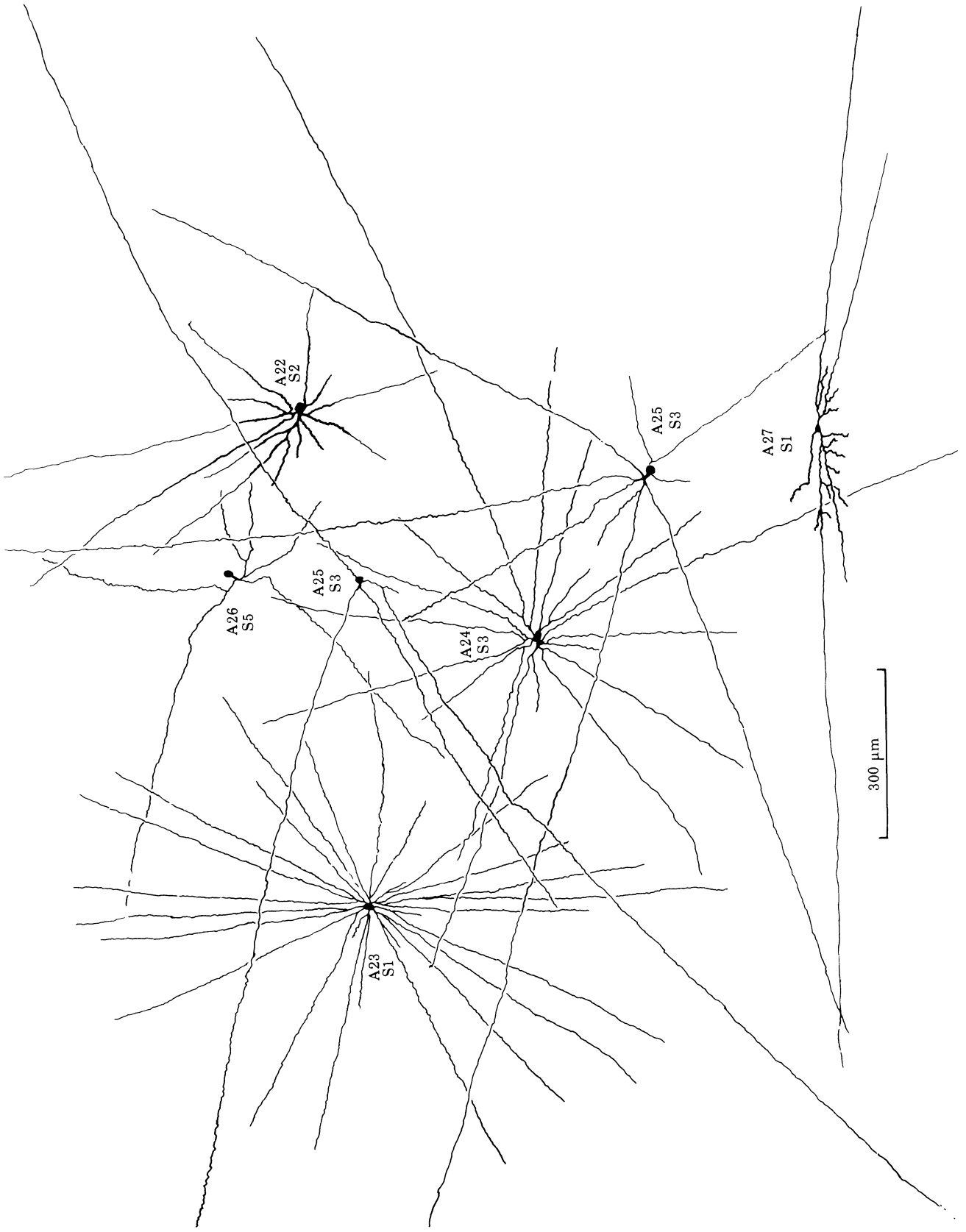

FIGURE 9. Camera lucida drawings of wide-field amcrine cells of the turtle retina. Cells A22–A26 are essentially stellate and monostratified. A27 is oriented parallel to the l.v.s. while the others have circular dendritic trees. All cells except A27 from the peripheral retina (7 mm from l.v.s.). A22–A24 and A27 are illustrated on plates 1 and 3.

l.v.s. (plate 1, figure 21). The cell body (9 μm × 11 μm) is flattened and the dendrites are profusely branched and characterized by bearing appendages and spines. Careful observation indicates that the very tips of the dendrites taper to the finest profiles that run for hundreds of micrometres before becoming unobservable among other Golgi-impregnated cell processes. The branches and fine tips are stratified very high in the i.p.l., in S1, below the amacrine cell bodies. The final field covered by such an amacrine cell is probably in excess of 2 mm and the orientation is exactly along the whole edge of the streak. Cajal's giant amacrine cell of lizard retina, fig. 2, pl. IV, bears a resemblance to A27 and is probably the same cell as fig. 4e, pl. III, (Cajal 1933).

Ganglion cells of the turtle retina

This Golgi study of turtle whole-mount retina has revealed 21 different morphological types of ganglion cells. The cells could be grouped according to size of cell body, size of dendritic fields, mono-, bi- or tristratification or diffuse branching patterns. Cell bodies of turtle ganglion cells appear to vary monotonically in size from small, with cell bodies approximately 11–12 μm in diameter, to large, with cell bodies 25 μm in diameter. The ganglion cells have smaller somal sizes when they are packed two or three deep in the l.v.s. region of the retina (plate 1, figure 18), but within 0.5 mm on either side of the steak their sizes increase substantially (plate 1, figure 19). However, this Golgi study cannot generate any meaningful quantitative data on cell body or dendritic field increases with eccentricity from the l.v.s. as the study is on too few cells scattered at random throughout the Golgi-impregnated material. In fact far peripheral cells in general do not seem to impregnate well. Thus, this study will not attempt to group the ganglion cells in turtle into any strict categories and the cells will be described by number, beginning with what appear to be the smallest in all respects and ending with the largest.

G1 (figure 10) has only been observed in or close to the l.v.s. in the present turtle material. It appears to be a small-field cell with a 55–70 μm dendritic tree and a small cell body (11 μm). The single apical dendrite breaks into compact overlapping branches at the S3/4 border. This ganglion cell type is essentially the same cell Cajal describes in lizard retina (figs 5C, 6D, F pl. III). Ganglion cell G2 is similarly small-field (40 μm) on the l.v.s., but appears to increase in size (70 μm) within a short distance from the streak (figure 10). This ganglion cell type, in contrast to G1, has a broadly stratified dendritic tree. The whole dendritic arbor is composed of a mass of fine short dendrites and appendages that stretch from S1 under the amacrine cells to S4 of the i.p.l. G2 bears some resemblance to Cajal's (1933) cell fig. 6E, pl. III.

Three diffuse ganglion cell types have been seen in turtle retina, one of which is a small-bodied, small-field type here designated G3 (figure 10). Its 15 μm cell body gives rise to two or three dendrites that branch as they pass up through all strata of the i.p.l. The dendrites appear to be particularly fine and beaded, occupying a field 150 μm in diameter.

Ganglion cells G4, G6 and G7 are all small-field compact bistratified cells, each of which stratifies at a different level of the i.p.l. G5 is a small-field tristratified cell. In general, in these ganglion cell types, the first layer of dendrites, stratifying close to the cell body, is more profusely branched, and the upper layers, closer to the amacrine cells, appear more delicate and lace-like (dotted profiles, G4–G7, figure 10). G4 has a 12 μm cell body and dendritic branches in S1 and S3, spreading over a 80–100 μm field (plate 4, figures 38–40). The dendritic field of G6 is larger (150 μm) than that of G4, particularly considering that the cell illustrated in

figure 10 (G6) lies on the very edge of the l.v.s. G7, on the other hand, appears to have a very elongate dendritic tree running orthogonally to the l.v.s. However, by 1 mm eccentricity (figure 11; plate 4, figures 41, 42) the dendritic tree is more oval in shape but still orthogonal in orientation. Somal dimensions of G7 cells reach 15 μm, and their dendritic branching pattern is coarser and wider-spread than the compact filigree patterns of G4 and G6.

The tristratified, small-field cell G5 (figure 10) has a small cell body (12 μm) and very narrow dendritic tree (45–50 μm) that branches at three levels in the i.p.l.: in S2, on the S3/4 border and S4/5 border. The G5 cell illustrated (figure 10) is the only clear example seen in this Golgi-impregnated turtle retina: however, Cajal also saw such a tristratified cell in the lizard retina (fig. 5B, pl. III).

The monostratified cells with 15 μm cell body sizes are G8 and G9 respectively. They differ primarily in the strata at which their dendrites ramify: S3 for G8 and the S2/3 border for G9. G9 has a larger dendritic field and its dendrites are quite beaded (plate 1, figure 22) compared with the delicate spidery dendrites of G8 (figure 11; plate 1, figures 24, 25). The branching pattern of G8 suggests that it is the equivalent of cell fig. 5A, pl. III, of Cajal's (1933) lizard material. G10 also has a 15 μm cell body but it is distinguished from G8 and G9 by its bistratified dendritic tree. The two major dendrites spread just above the ganglion cell bodies in S5 and fine wavy dendrites spring up from the main branches to spread in a loose network in S3 of the i.p.l. The cell is also notably oriented orthogonal to the l.v.s. Only a few examples of G10 have been seen.

There is a large tristratified ganglion cell in the turtle retina (G11, figure 11). This cell contrasts with the small tristratified cell G5 in being a much sturdier, larger cell. A 17 μm × 9 μm cell body gives rise to three major dendrites that run in S5 before breaking into branches that rise to ramify on the S2/3 border (heavy dotted profiles, G11, figure 11). Another network of dendrites (fine dotted lines, G11, figure 11) ultimately spreads in S1 under the amacrine cell bodies. Three other examples of G11 were seen in the turtle retina close to the cell illustrated.

The remaining ganglion cells that have been seen in this Golgi study, G12–G21, appear to have considerably larger cell bodies than the preceding cells (see above). Thus G12–G21 have cell body dimensions of 20–28 μm, with larger sizes predominating for cells located in peripheral retina. Most of these cells have large dendritic tree spans as well. G12 ganglion cells have only been observed on the edge of the l.v.s. (figure 12; plate 1, figure 20). They have profusely branched dendritic fields (300–350 μm) characterized by their bearing many spines and appendages. The dendrites are broadly stratified in S1 and S2 and oriented parallel to the visual streak. In all the examples observed, G12 cell bodies were displaced to the amacrine cell layer. Axons were clearly impregnated on most of them (G12, figure 12). G13 is a large, diffusely branching ganglion cell. The large (25 μm) cell body gives rise to four major dendrites that branch dichotomously into irregular overlapping coarse dendrites which spread over a 330 μm field. Although G13 (figure 12) lies in more peripheral retina (4 mm from l.v.s.) than G3, the other diffuse ganglion cell (0.8 mm), its much coarser dendrites and irregular branching pattern, in addition to its larger size, identify it as a different type. In fact, Cajal (1933) shows a very similar cell to G13 in fig. 6A, pl. III, of lizard material.

Cell G14 is a ganglion cell with a very characteristic bistratified dendritic tree. This cell does not appear to have been described by Cajal in reptilian retina. The large (25 μm) cell body produces characteristic thick dendrites that branch profusely, with a series of curving secondary dendrites in S3. A second layer of similar curving wavy dendrites pass up to branch

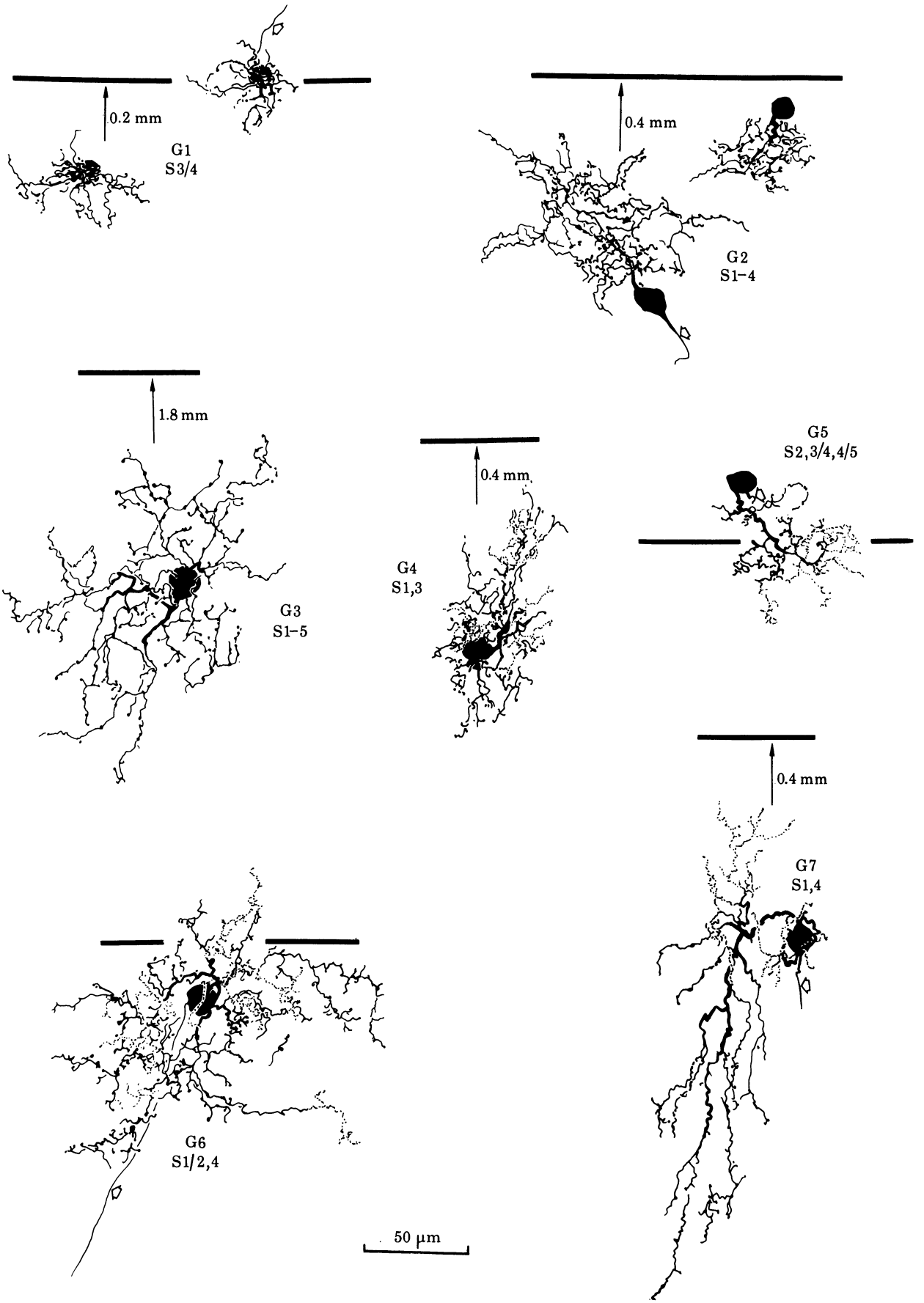

FIGURE 10. Camera lucida drawings of the small ganglion cell types of the turtle retina. G1 is a monostratified cell, G4, G6 and G7 are bistratified, G5 is tristratified and G2 and G3 are partially or completely diffuse cells. The top tier of dendrites of multistratified cells are denoted by dotted profiles. G4 is illustrated on plate 4. Axons are arrowed on this and all following drawings of ganglion cells.

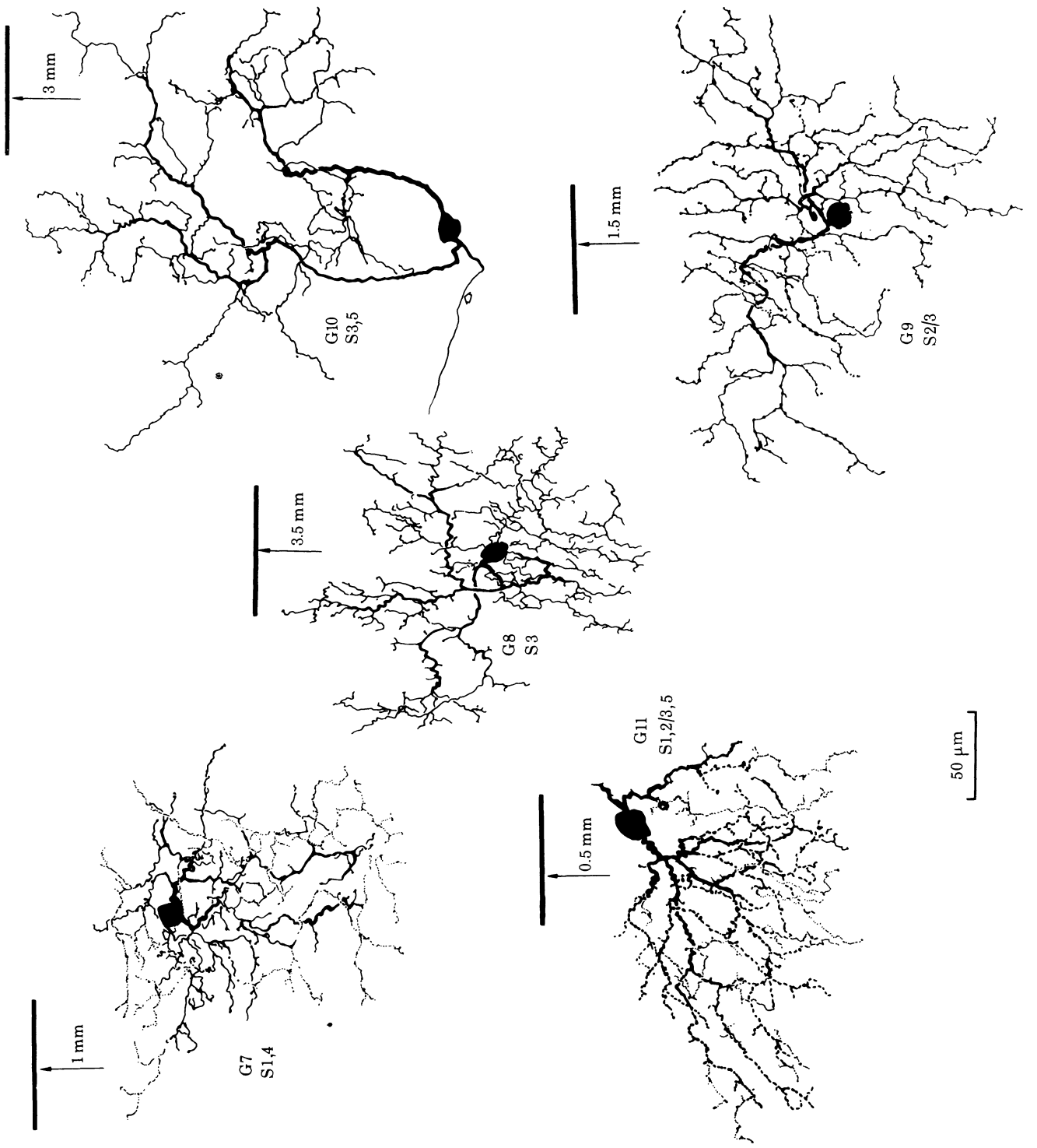

FIGURE 11. Camera lucida drawings of medium-size ganglion cells of the turtle retina. G8 and G9 are monostratified, G7 and G10 are bistratified, while G11 is a tristratified cell. On G7 the top tier of dendrites are shown as dotted profiles. On G11, the dendrites in S5 are shown as solid lines, on the S2/3 border are large dotted lines and in S1 are fine dotted lines. G7–G9 are illustrated on plates 1 and 4.

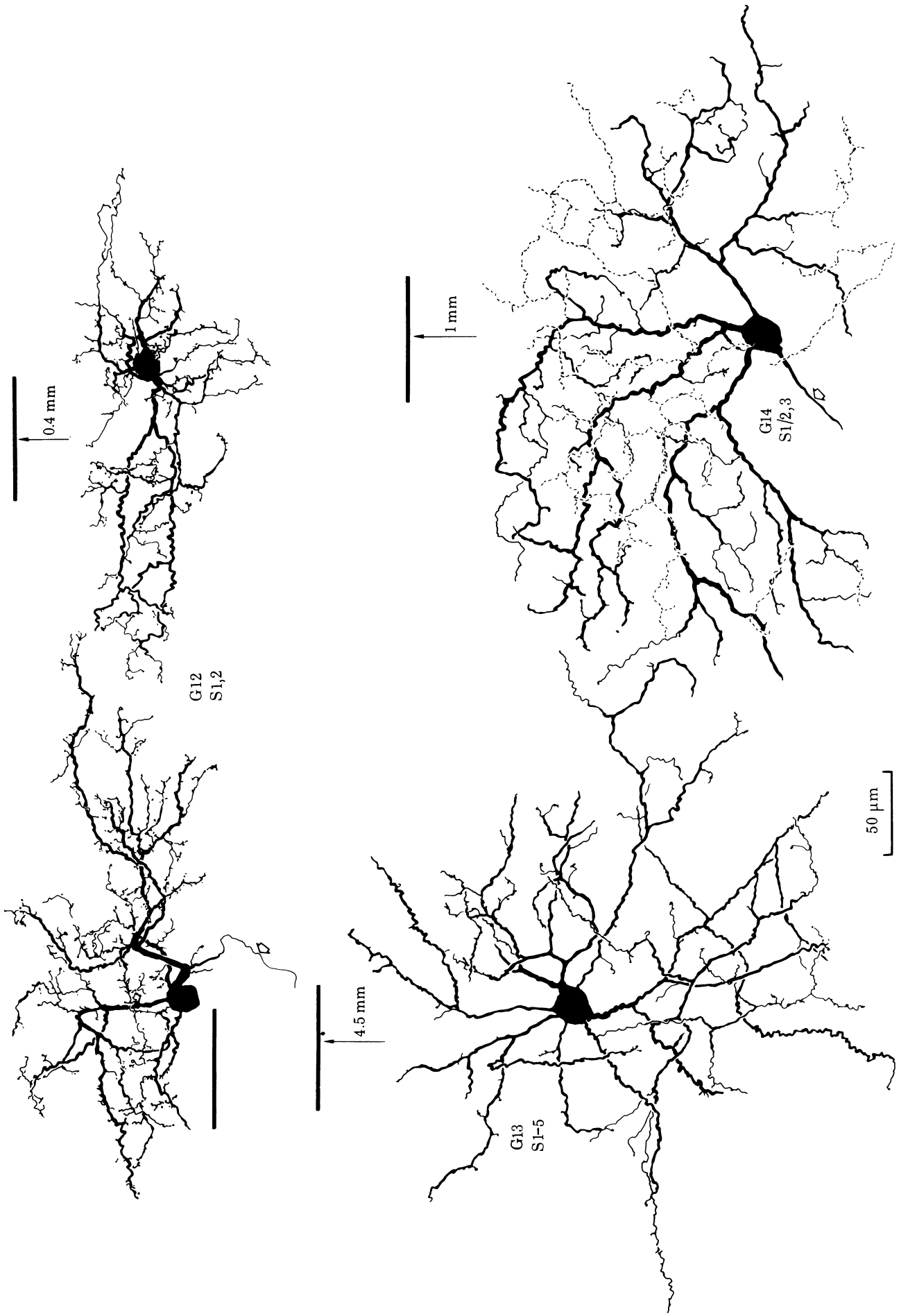

FIGURE 12. Camera lucida drawings of medium-size ganglion cells of the turtle retina. G12 cells are broadly stratified and oriented along the l.v.s. and have cell bodies displaced to the i.n.l. G13 is diffusely branched while G14 is a bistratified cell, with the top tier of dendrites denoted by dotted lines. G12 is illustrated on plate 1, and G14 on plate 5.

absolutely on a plane at the S1 border of the i.p.l. The large size (400 μm) and dominant morphology of this ganglion cell's dendritic field make such cells unmistakable in Golgi-impregnated turtle retina (figure 12; plate 5, figure 48).

Ganglion cells G15 and G16 are further large-field, bistratified cells, distinguished from each other and from G14 primarily by their branching patterns. Thus, G15 (figure 13) has a 19 μm flattened cell body, and a layer of thick angular dendrites branching in S4 of the i.p.l. From the secondary dendrites in the proximity of the cell body, coarse dendrites ascend to branch in similar irregular dichotomous fashion high in the i.p.l. under the amacrine cell bodies in S1. The ganglion cell has an elongated dendritic field oriented parallel to the l.v.s. Each layer of dendrites covers a 400 μm diameter elliptical field, but, interestingly, the lower layer of dendrites is displaced to the left of the cell body (figure 13; plate 4, figure 43) and the upper layer to the right (figure 13; plate 4, figure 44). In a vertical section one might get the impression that the cell has two layers of dendrites arborizing in opposite directions. G16, on the other hand, is a symmetrical but oriented ganglion cell with a large sparsely branched dendritic tree. The primary dendrites ramify in a band in S4 and are strongly oriented along the direction of the l.v.s., while the secondary branches rise gracefully to branch in a curving wavy fashion on the S1/2 border of the i.p.l. (figure 13). The upper dendritic tree spreads over an elliptical field measuring 970 μm in the long axis (figure 13). Cajal (1933) illustrated a cell in fig. 5 D, pl. III, that bears some resemblance to the bistratified ganglion cell G16.

The large tristratified ganglion cell of the reptilian retina described originally by Cajal (1933) and illustrated in two examples on his pl. III, figs 6C and H, is seen in the turtle retina and here is named G17. Only two well impregnated examples of such cells were seen in this Golgi study and both cells were oriented with the long axis of their dendritic tree orthogonal to the l.v.s. (figure 14). The large cell body (25 μm × 20 μm) produces five major dendrites that branch at the S3/4 border into a wavy array of secondary dendrites. The secondary branches give rise to a plexus of fine dendrites bearing appendages that lie on a plane at the S2/3 border of the i.p.l. Major dendrites also arise from the primary branches and from the ends of the branches on the S3/4 border to branch on a third prominent tier (dotted profiles, figure 14) on the S1/2 border. The whole dendritic tree of such a ganglion cell covers a 550 μm × 360 μm area.

G18 is a very distinctive ganglion cell type (figure 14; plate 5, figure 45). A group of five such cells were seen close to the l.v.s. in one Golgi-impregnated retina, and all but two of these had their cell bodies displaced to the amacrine cell layer of the i.n.l. The 19 μm × 22 μm, round cell body gives rise to large heavy distinctly varicose dendrites that ramify under the amacrine cell bodies in S1. The morphology is clearly that of the Dogiel (1895) cell of bird retinas, and is almost certainly the cell fig. 5e, pl. III, in Cajal's (1933) description of the lizard retina. Cajal gave this cell type the name 'nervous spongioblast'.

A third diffusely branching ganglion cell type in addition to G3 and G13 is seen in turtle retina. G19 (figure 15; plate 5, figure 47) is characterized by a large (625 μm) dendritic spread of particularly fine long tapering dendrites that pass gracefully up through all strata of the i.p.l. The cell body is large and flattened (22 μm × 16 μm) with large-calibre (4 μm) major dendrites emerging from each side. The branching pattern is of a tufted type (Ramon-Moliner 1962). G19 could be Cajal's cell fig. 6 B, pl. III, in lizard retina.

Cells G20 and G21 are the largest-field, radiate ganglion cells of the turtle retina. G20 stratifies on the S1/2 border while G21 stratifies in the vitread portion of the i.p.l. in S4

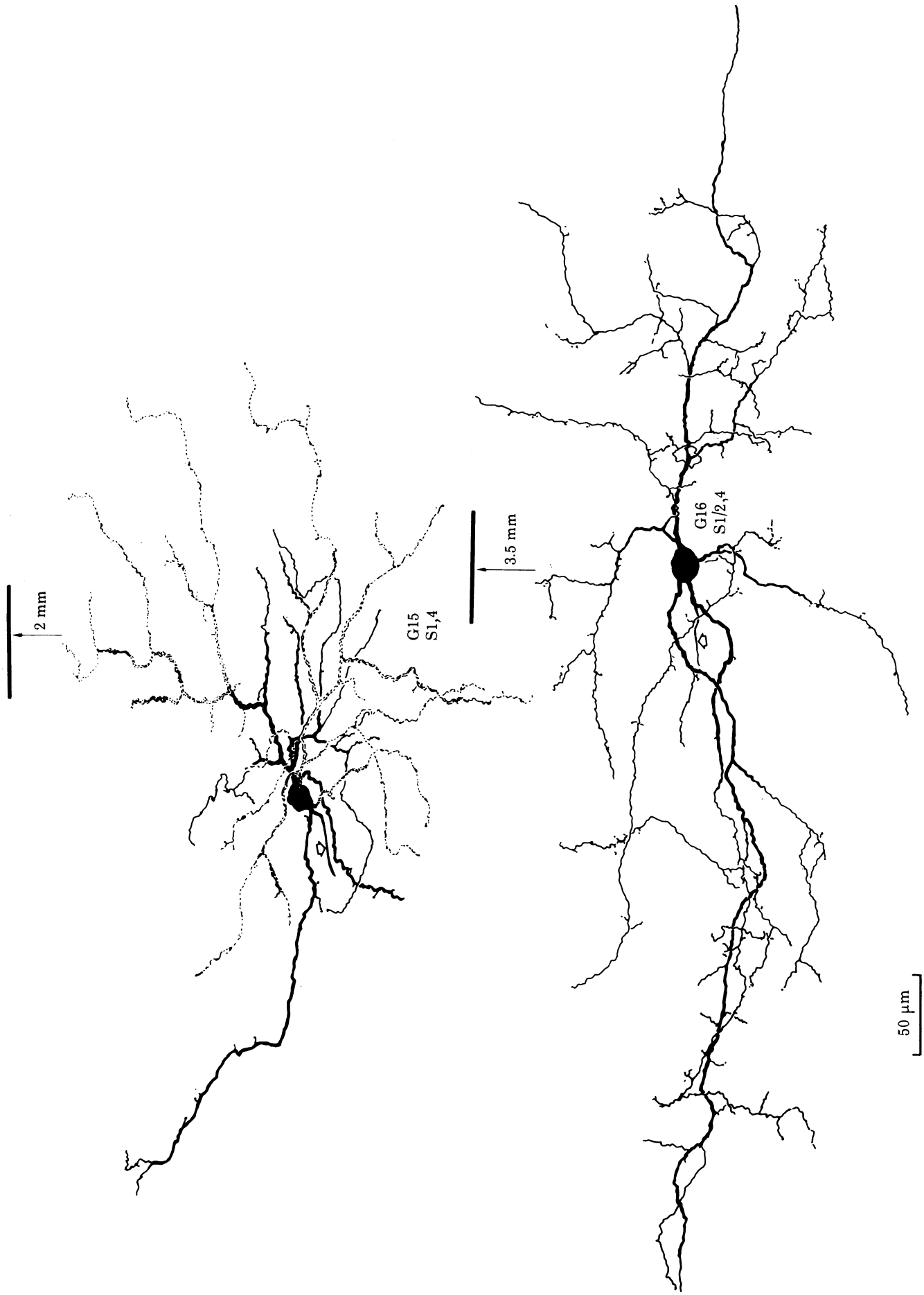

FIGURE 13. Camera lucida drawings of large bistratified ganglion cells of the turtle retina. G15 has two planes of arborization of sturdy dendrites, with the top tier represented as dotted profiles. G16 has fine dendrites rising to the distal strata of the i.p.l. G15 is also illustrated on plate 4.

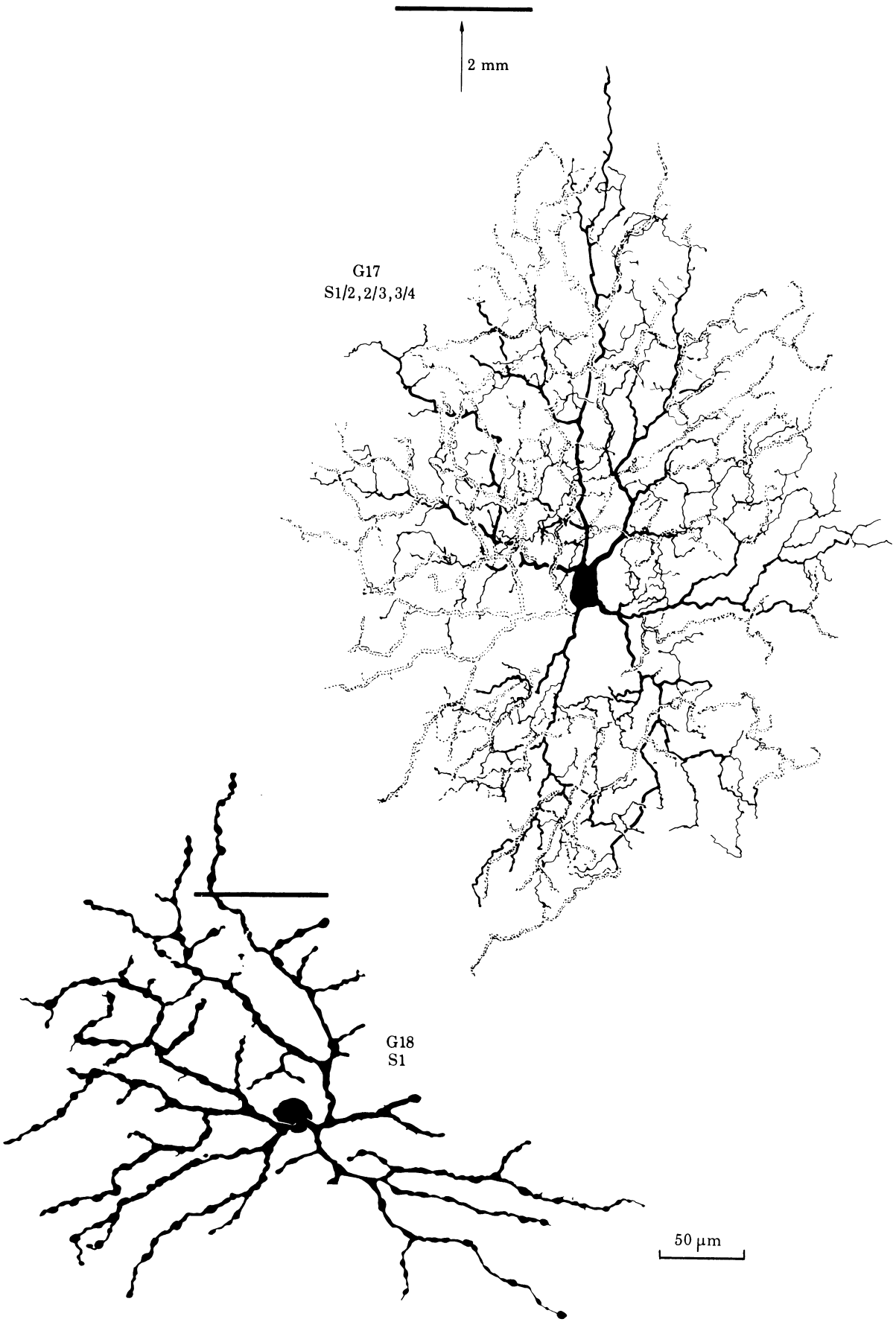

FIGURE 14. Camera lucida drawings of two large ganglion cells of the turtle retina. G17 is a large tristratified cell The heavy lines denote the proximal dendritic layer, the finer profiles are dendrites at intermediate levels and the dotted profiles are dendrites lying most distal in the i.p.l. G18 is a Dogiel cell with its cell body displaced to the i.n.l. G18 is illustrated on plate 5.

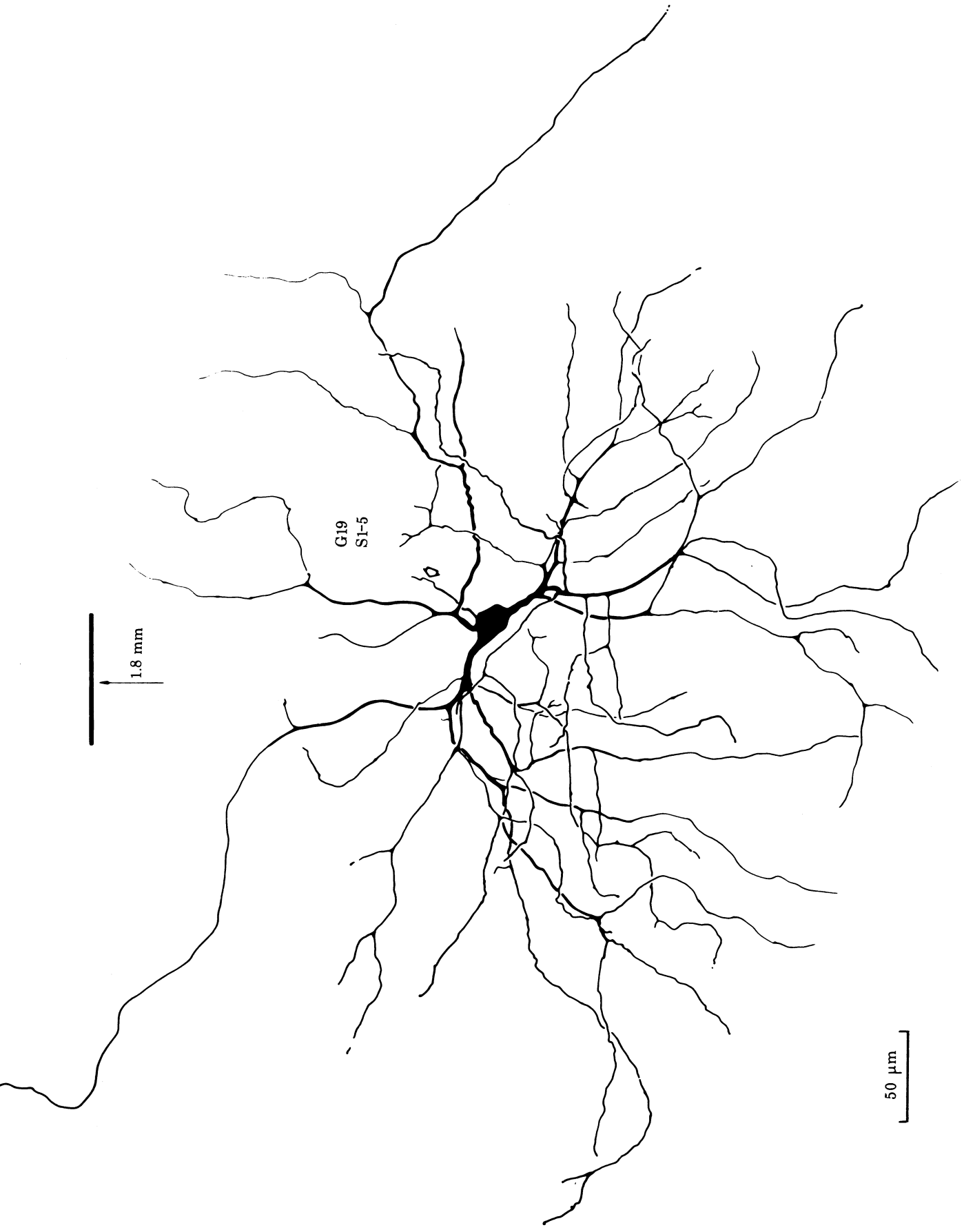

FIGURE 15. Camera lucida drawing of a large diffuse ganglion cell type (G19) in the retina of the turtle. It is also illustrated on plate 5.

(figures 16, 17). Although of similar large-body and large-field morphology, these cells are not mirror image pairs branching in two different regions of the i.p.l. as are certain ganglion cells of cat retina (Kolb *et al.* 1981). The branching pattern of G20 and G21 of turtle retina is entirely different. G20 (figure 16) increases in dendritic field size with eccentricity yet the cells maintain an orientation relative to the streak. The large cell body (25 μm × 27 μm) gives rise to three or four major dendrites that subdivide into a field of large-calibre curving dendrites covering 500–850 μm (plate 5, figure 46). The example from retina close to the l.v.s. (G20 above, figure 16) has a cell body displaced to the amacrine cell layer and the large axon (arrowed) arises from a primary dendrite. Other examples of G20 did not appear to be so displaced. It is possible that G20 is the equivalent cell to fig. 6I of pl. III in Cajal's (1933) description of lizard material, although his example appears to be smaller-bodied than the cell of this study.

G21 is the final type of large ganglion cell seen in turtle retina. No examples have been seen close to l.v.s., but presumably they occur there with dendritic field sizes similar to G20 of figure 16. G21 typically has a 28 μm cell body giving rise to four major dendrites that branch sparingly with long coarse secondary dendrites (figure 17). The dendritic tree does not branch above S4 of the i.p.l. and has a 850 μm span. The axons of G21 cells seem to be of particularly large diameter. Curiously, this cell type, which stained rather commonly in my turtle material, was not seen by Cajal (1933) in lizard retina.

Discussion

Cajal's (1933) opinion 'it is in reptiles that amacrine and ganglion cells have reached their highest degree of evolution and perfection' has been confirmed in this Golgi study of the turtle retina. There appears to be a plethora of complexly stratified neurons contributing dendrites of varied morphologies to the neuropil of the inner plexiform layer (i.p.l.). Thus, all but three cells that Cajal (1933) described in the lizard have been seen, but an extra 23 neurons of the i.p.l. have been added to his description. At least nine different bipolar cell types are described, all exhibiting Landolt clubs and most of them having bi- or tristratified axon terminals. There are at least 27 types of amacrine cell distinguishable on the basis of morphological criteria such as stratification, dendritic morphology and dendritic field size. Furthermore, 21 different morphological types of ganglion cell have been observed, distinguished according to similar criteria. Finally, there is a further complication of morphology superimposed on the intricacy of stratification of the many neurons in the turtle retina. Most of the cells appear to have a specific orientation relative to the linear visual streak.

Stratification of neurons of the i.p.l. in turtle retina

Tables 1 and 2 summarize the stratification of the various neurons in the i.p.l. of the turtle retina as described by this Golgi study. Most of the neurons appear to be monostratified with dendrites branching on a single plane in one of the five strata or at the border between strata of the i.p.l. (table 1). Yet most of the bipolar cells have bistratified axon terminals and several ganglion cell types also have dendritic trees branching at two levels (table 1). Tristratified and diffuse cells are also present, particularly among the amacrine and ganglion cells. Table 2 indicates the strata in which the various cell types branch; there appears to be a fairly even distribution of neural processes throughout the five strata of the i.p.l.

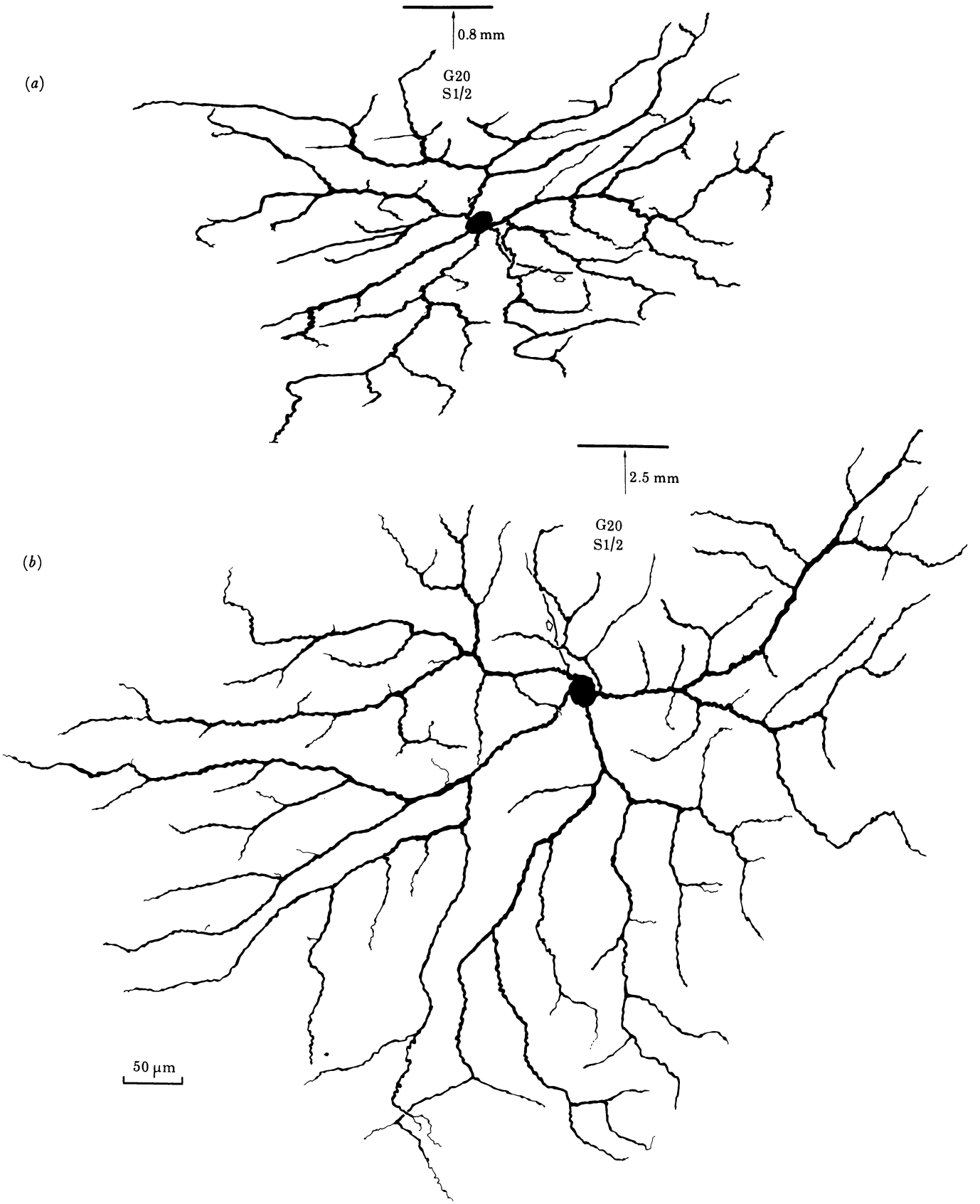

FIGURE 16. Camera lucida drawings of (*a*) a central and (*b*) a peripheral example of G20, which is one of the largest ganglion cell types found in the turtle retina. Cell (*a*) lies close to the l.v.s. and has a smaller more oriented dendritic tree than the more peripheral cell (*b*). G20 is also illustrated on plate 5.

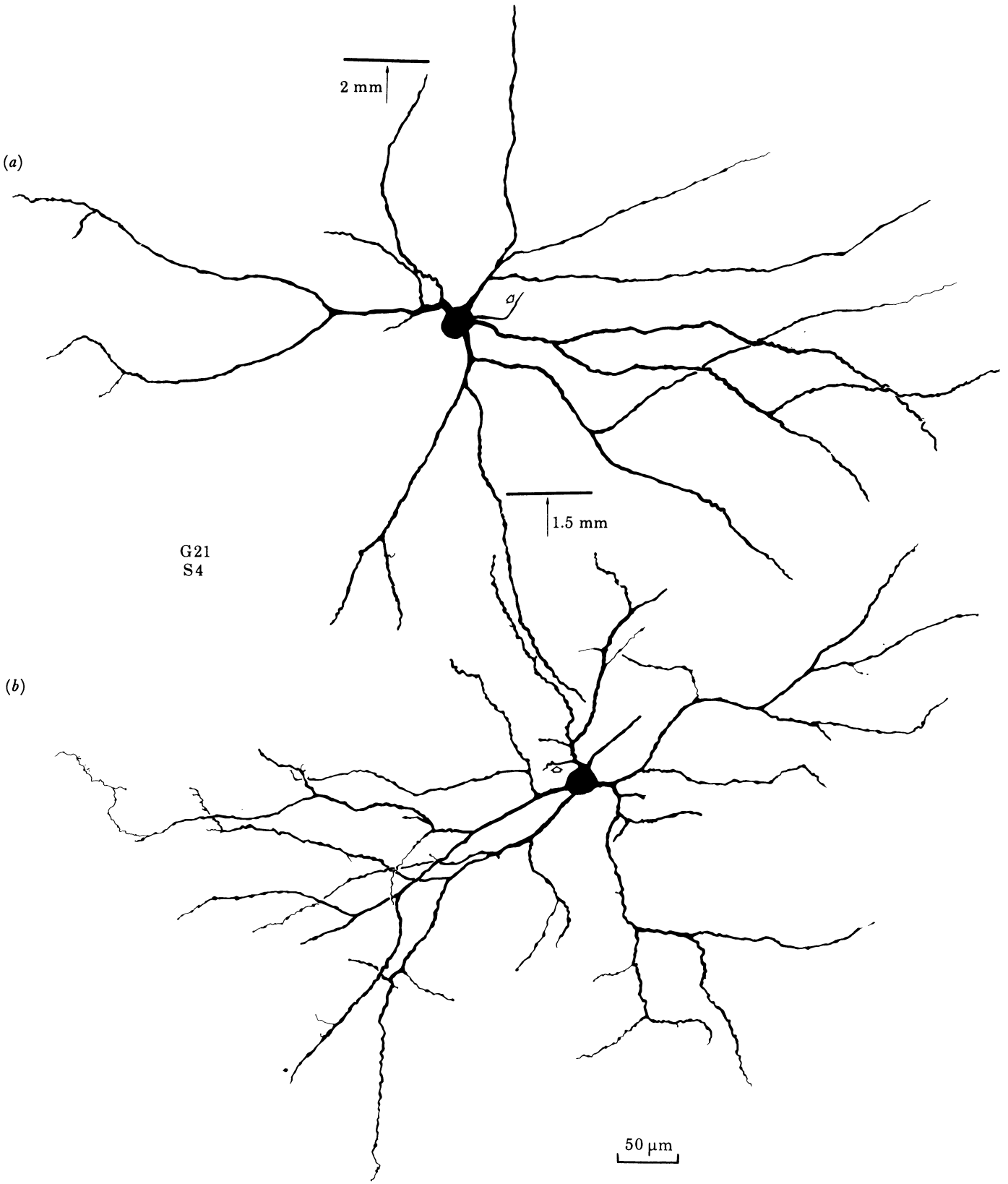

FIGURE 17. Camera lucida drawings of two large G21 ganglion cells of the turtle retina. The body of cell (*a*) is displaced to the i.n.l.

The division of the i.p.l. into five strata or 'plexuses' was proposed by Cajal (1933) for all vertebrate retinas. He considered these strata to be the granular concentric stripes of the i.p.l. visible by histological techniques, which are formed 'by the processes of spongioblasts (amacrine cells) and ganglion cells'. It is still not clear what forms the boundaries between the bands or strata, and whether the strata are of uniform thickness. Nevertheless, the S1–S5 scheme serves as a useful paradigm for classifying cells. A cautionary note must be interjected here, for in the retina of the turtle the i.p.l. is particularly thick (90 μm in the l.v.s., 62 μm in the peripheral

TABLE 1. THE STRATIFICATION CHARACTERISTICS OF THE BIPOLAR AXONS AND AMACRINE AND GANGLION CELL DENDRITES IN THE INNER PLEXIFORM LAYER OF THE TURTLE RETINA

stratification	bipolar	amacrine	ganglion
mono.	B1, B5	A2, A3, A7–A9, A13, A16–A27	G1, G8, G9, G15, G16, G18, G20, G21
bi.	B4, B6, B8, B9	A11, A14, A15	G4, G6, G7, G10, G14
tri.	B3, B7	A5, A12	G5, G11, G17
broad	B2	A4, A10	G2, G12
diffuse	—	A1, A6	G3, G13, G19

TABLE 2. THE SPECIFIC STRATUM OR STRATA IN WHICH THE BIPOLAR AXONS AND AMACRINE AND GANGLION CELL DENDRITES BRANCH

stratum	bipolar	amacrine	ganglion
S1	B4, B5, B9	A1, A5, A6, A7, A8, A12 A14, A17, A18, A19, A23, A27	G2, G3, G4, G7, G11 G12, G13, G15, G18, G19
		A15	G6, G14, G16, G17, G20
S2	B3, B8	A1, A2, A3, A6, A11, A13	G2, G3, G5, G12, G13 G19
	B4	A22, A24	G9, G11, G17
S3	B3, B6, B7	A1, A4, A5, A6, A10, A12 A14, A20	G2, G3, G4, G8, G10 G13, G14, G19
		A9, A25	G1, G5, G17
S4	B2, B3, B7	A1, A4, A6, A10, A21	G2, G3, G6, G7, G13 G15, G16, G19, G21
	B9	A15	G5
S5	B1, B2, B6 B7, B8	A1, A5, A6, A10, A11 A12, A16, A26	G3, G10, G11, G13 G19

retina; plate 1, figures 18, 19) and consequently each stratum is very broad (18 μm in the l.v.s., 12 μm in peripheral retina). This means that each stratum is wide enough that two cell types branching within a particular stratum might not lie close enough to interact. So, although table 2 shows the strata in which the various neurons branch, it is not possible, at this stage, to state unequivocally that the cells within each strata are intereacting functionally. Future investigations may in fact show that division of the turtle i.p.l. into five strata is inadequate, and that there may be even more functional strata.

So far the significance of dividing the i.p.l. into strata has been linked only to ON-centre and OFF-centre activity of bipolar and ganglion cells (Nelson *et al.* 1978; Famiglietti *et al.* 1977; Marc *et al.* 1979). The boundary between neuropil subserving the OFF and ON pathways varies somewhat between species. Thus, in cat the boundary divides the i.p.l. into a distal third

(below the amacrine cells (S1 and S2)) and a proximal two-thirds stretching to the ganglion cells (S3–S5), yet in fish retina, the boundary, to judge from ganglion cell recordings (Famiglietti *et al.* 1977) lies approximately halfway through the thickness of the i.p.l. In cat retina, the boundary between OFF and ON strata is determined by bipolar axon terminals and ganglion cell dendrites. However, in cat, the bipolar axons are monostratified or distribute vertically through a number of strata. The situation might be different in the turtle retina, where most of the bipolar cells are multistratified with respect to their axon terminals. Marchiafava & Weiler (1980) have made intracellular recordings from and stained bipolar cells of the turtle retina. Although their experiments did not address the question of ON-centre and OFF-centre response types and stratification, their centre-hyperpolarizing bipolar is clearly B4 of this study with both branches of its axon in distal i.p.l. (the S1, S2/3 border region of neuropil). Their centre-depolarizing bipolar is probably B6 with axon branches in proximal i.p.l. (S3 and S5). These findings together with their ganglion cell data (Marchiafava & Weiler 1980) suggest a division of the turtle i.p.l. into OFF-centre and ON-centre regions at a position a little above the halfway point, nearer to the amacrine cells than to the ganglion cell bodies: probably in the middle of S3.

Orientation of dendritic fields relative to the linear visual streak in the turtle retina

It has become evident from this study that the majority of neurons in the turtle retina have dendritic trees oriented parallel, and sometimes orthogonal, to the l.v.s. Cells having circular non-oriented dendritic trees are a minority in turtle retina.

Most of the cells exhibit an elongated morphology of their dendritic trees with the long axis between 1.3 and 1.6 times the short axis. The morphology of these cell types probably results from their development in a retina with a linear visual streak. Although almost nothing is known of the development of the turtle retina, it is reasonable to assume that cells are added peripherally, as in the goldfish (Johns 1977; Johns & Easter 1977), relative to the initially organized streak region (a streak is present in hatchling turtles with eyes only one-tenth of the size of adult eyes) (R. A. Normann, personal communication). The radial growth of the retina and the stretching that must occur to maintain a streak region of smaller, highly concentrated cells could result in stretched elliptical dendritic trees for all cell types. On the other hand, the occurrence of cells with dendritic trees oriented orthogonal to the streak, such as A21, G7 and

---

DESCRIPTION OF PLATE 1

FIGURE 18. Vertical section of the visual streak region of the turtle retina. The section was $\frac{1}{2}$ μm thick and stained with methylene blue. (Magn. × 400.)

FIGURE 19. Vertical section of a peripheral region of the same turtle retina. The section was $\frac{1}{2}$ μm thick and stained with methylene blue. Abbreviations: ph., photoreceptors; o.p.l., outer plexiform layer; i.n.l., inner nuclear layer; i.p.l., inner plexiform layer; g., ganglion cell layer. (Magn. × 400.)

FIGURE 20. Light micrograph of Golgi-impregnated G12 ganglion cells lying along the edge of the l.v.s. (Magn. × 400.)

FIGURE 21. Several A27 amacrine cells and one A19 amacrine cell lying along the edge of the l.v.s. (Magn. × 400.)

FIGURE 22. The monostratified dendritic tree of ganglion cell G9. The cell body is out of focus in the centre of the dendritic field. (Magn. × 400.)

FIGURE 23. Dendritic tree of a monostratified A7 cell with its cell body visible but out of the plane of focus. (Magn. × 400.)

FIGURES 24 AND 25. A bipolar amacrine A16 seen at two planes of focus; close to the cell body (figure 24) and at the dendritic arborization in S5 (figure 25). A ganglion cell G8 is also seen at both levels of focus. (Magn. × 400.)

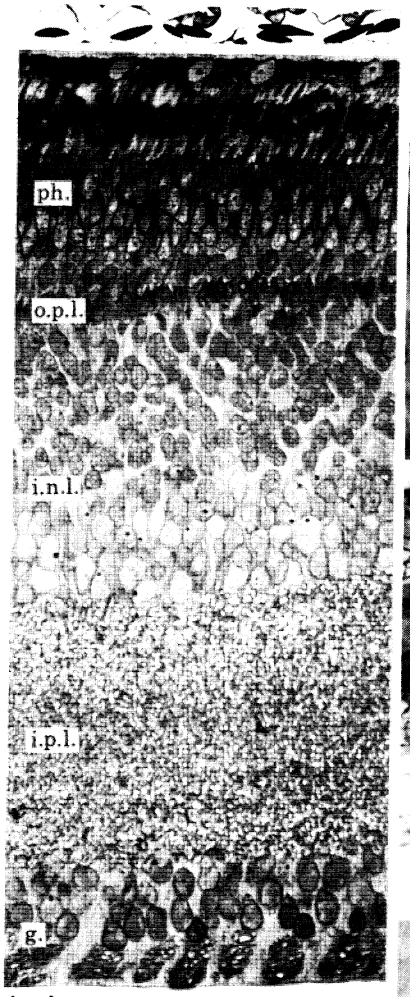

'18'

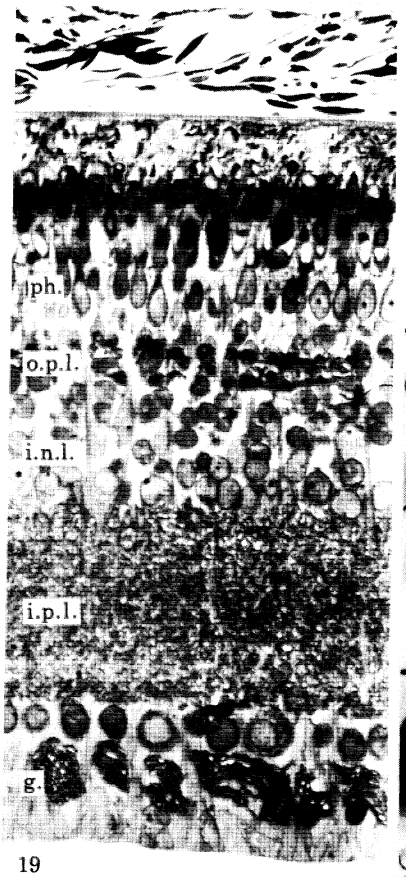

19

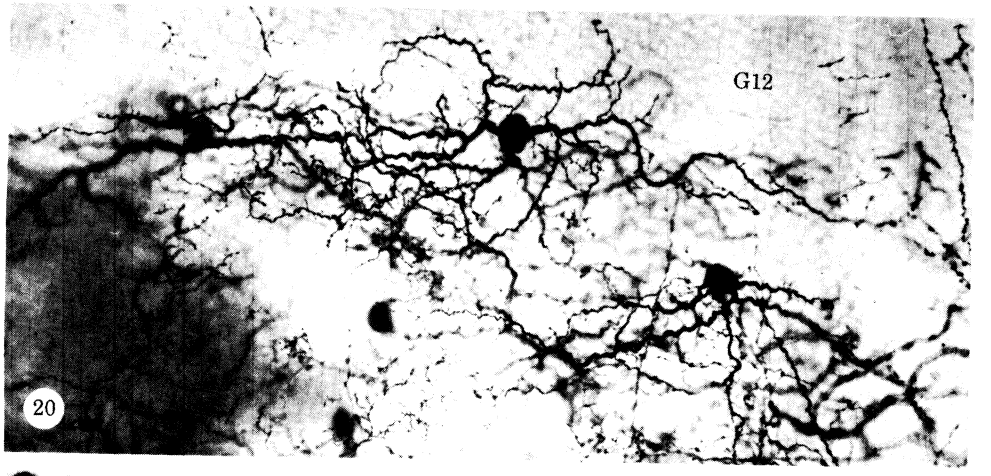

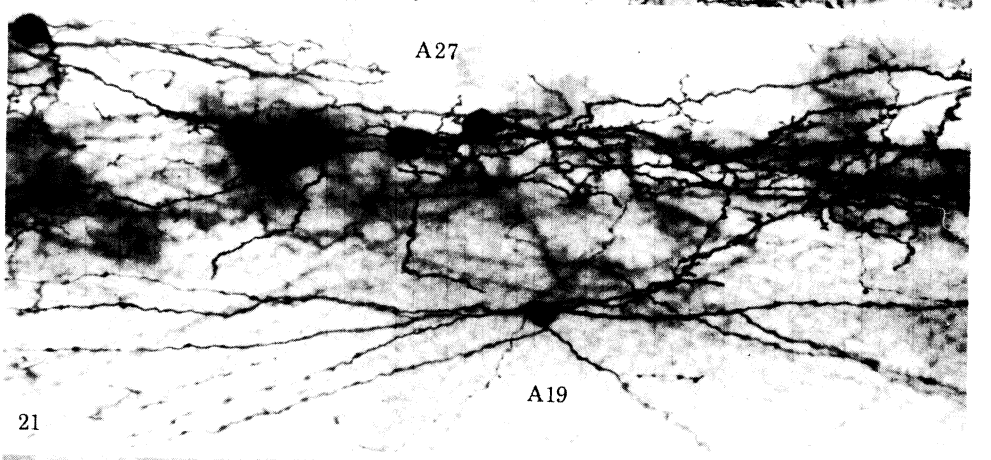

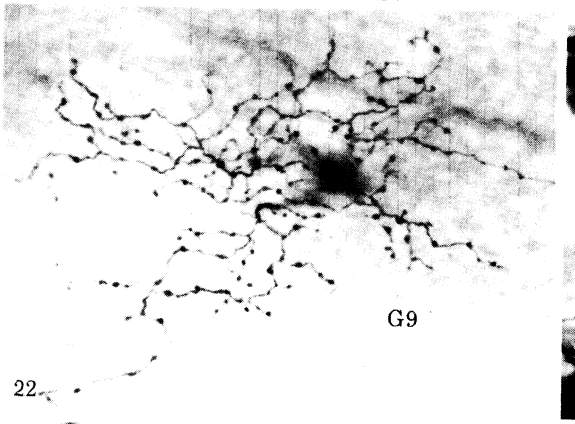

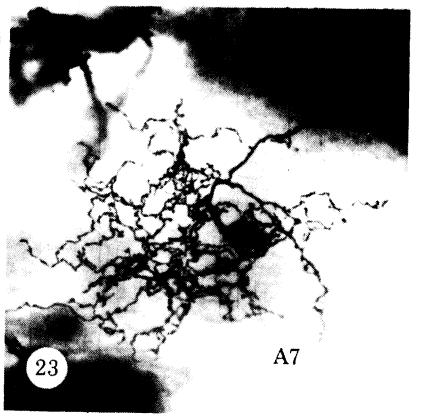

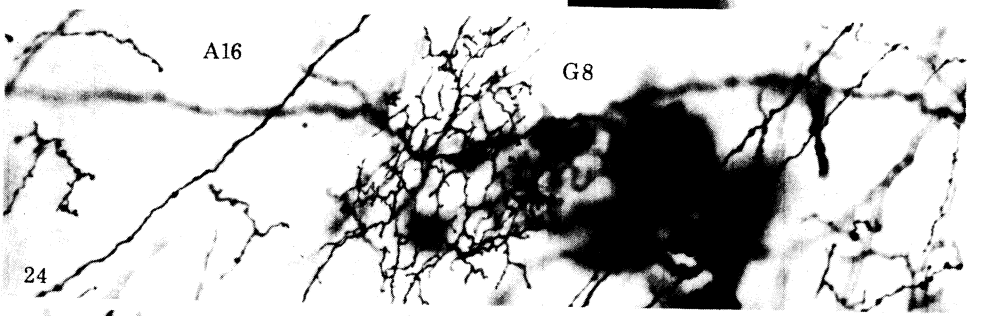

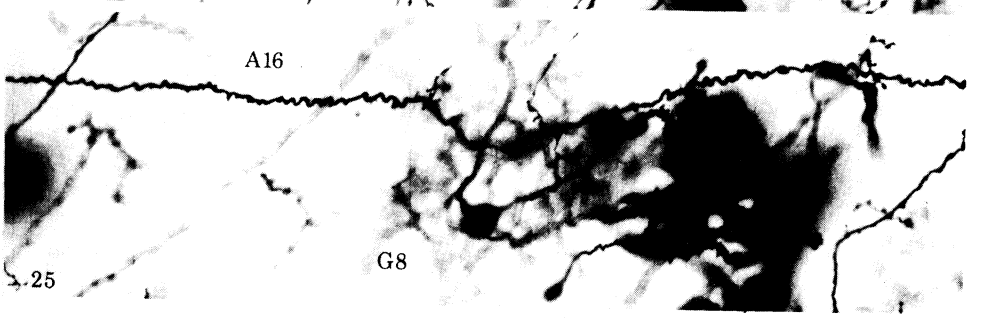

(*Facing p.* 384)


B3
B6
26

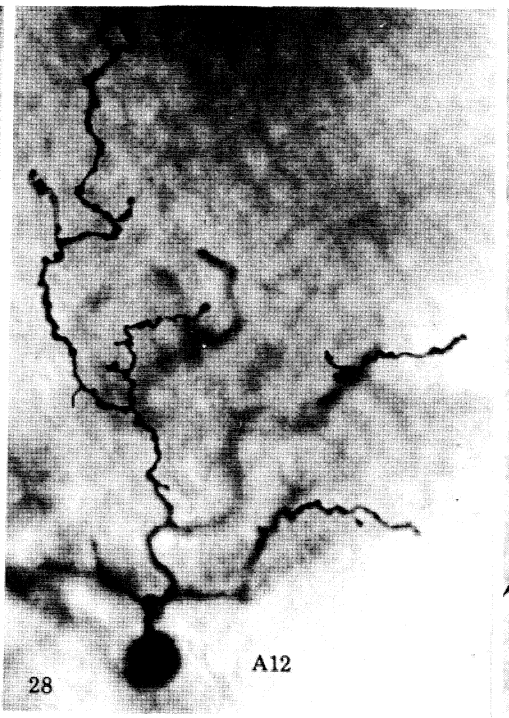
A12
28


A4
31

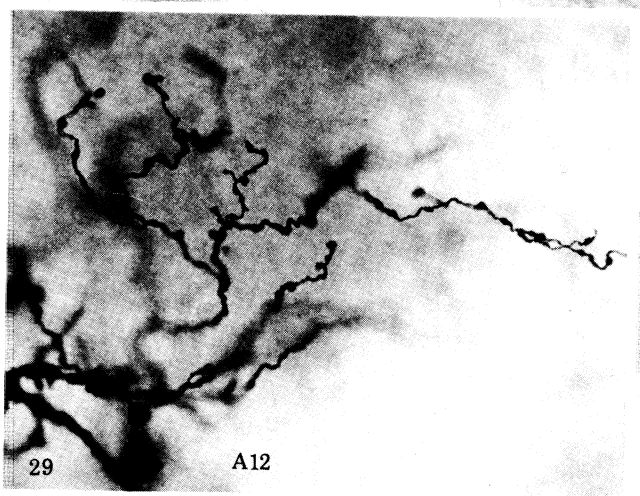
A12
29

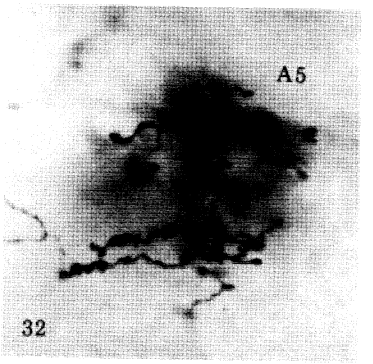
A5
32

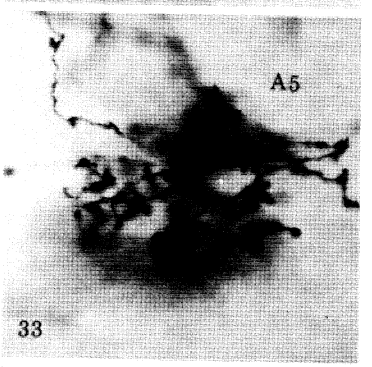
A5
33


A2
27

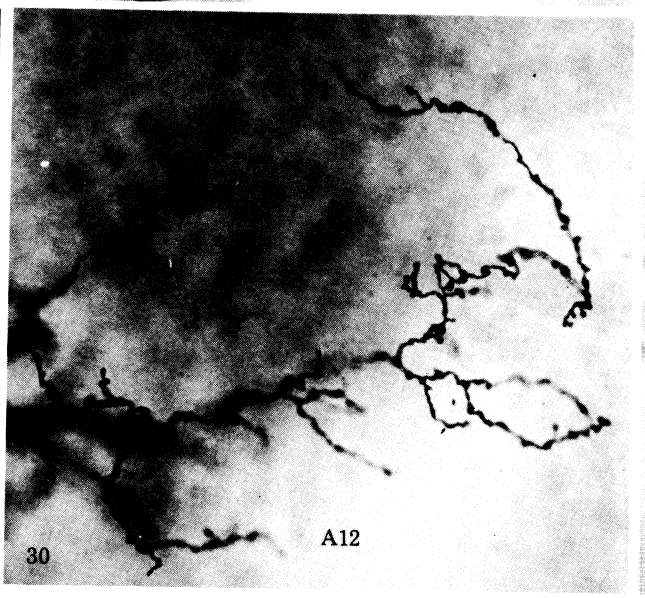
A12
30

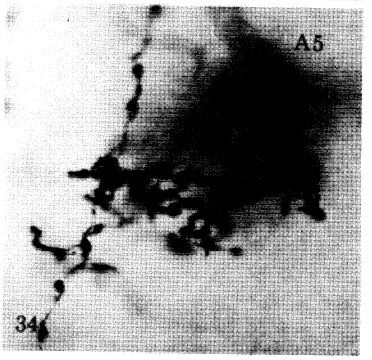
A5
34

Description of plate 2

Figure 26. Two bipolar cells photographed at three planes of focus to show the dendritic arbors, the cell bodies and the axon terminations. B3 has axonal branches in S2, S3 and S4, while B6 has branches in S3 and S5. (Magn. × 1000.)

Figure 27. Dendrites of an A2 amacrine branch on a plane in S2. Cell body out of focus. (Magn. × 1200.)

Figures 28–30. Three views of the tristratified amacrine cell A12: top tier of dendrites and cell body (figure 28), dendritic tier in S3 (figure 29) and dendritic tier in S5 (figure 30). (Magn. × 1000.)

Figure 31. Dendritic tree of A4 amacrine branching in S3 and S4. Cell body out of plane of focus. (Magn. × 1200.)

Figures 32–34. Three views of the tristratified narrow-field amacrine cell A5: dendrites in S1 (figure 32), S3 (figure 33) and S5 (figure 34). (Magn. × 1200.)

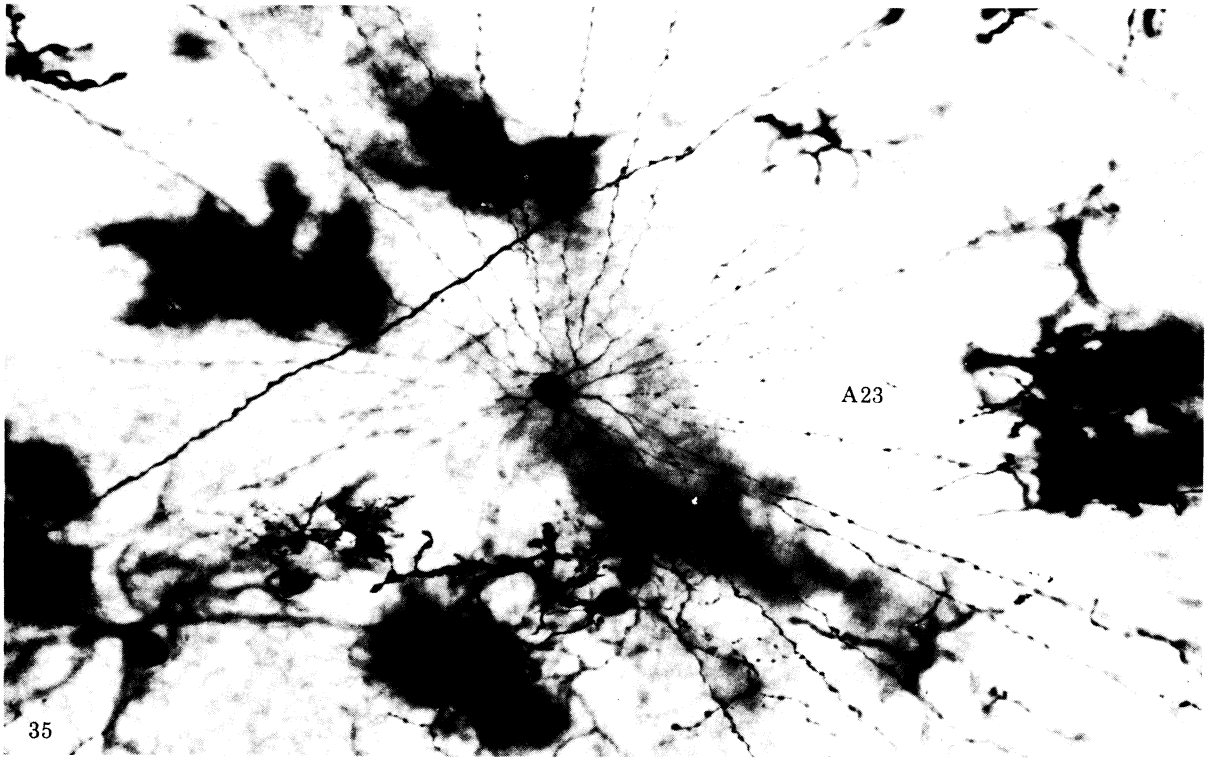
A23
35

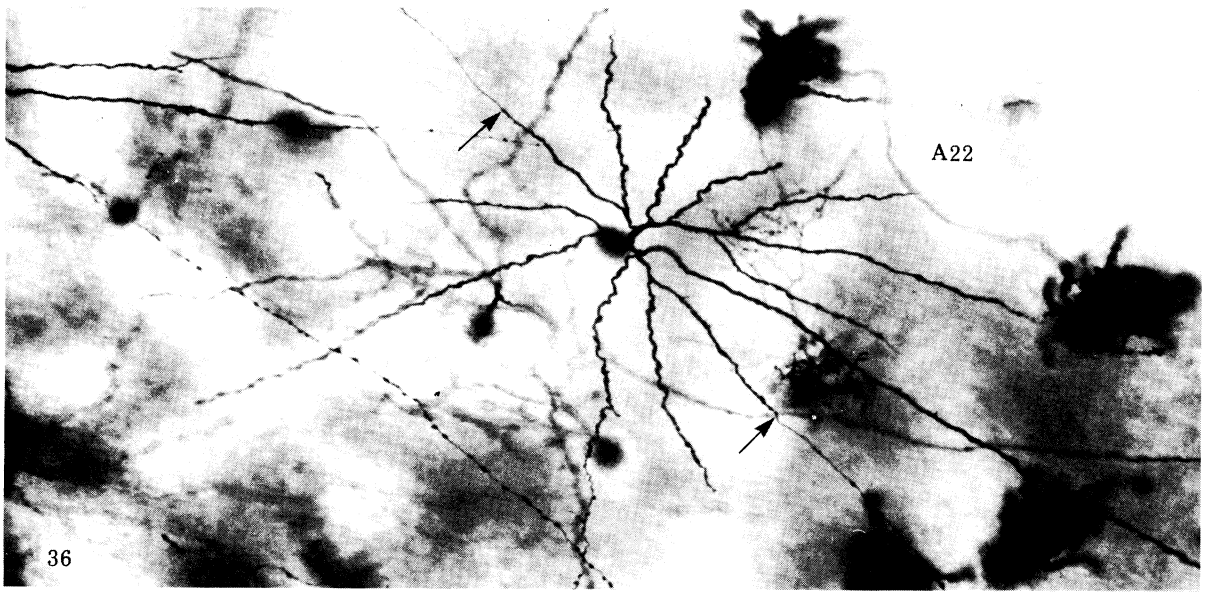
A22
36

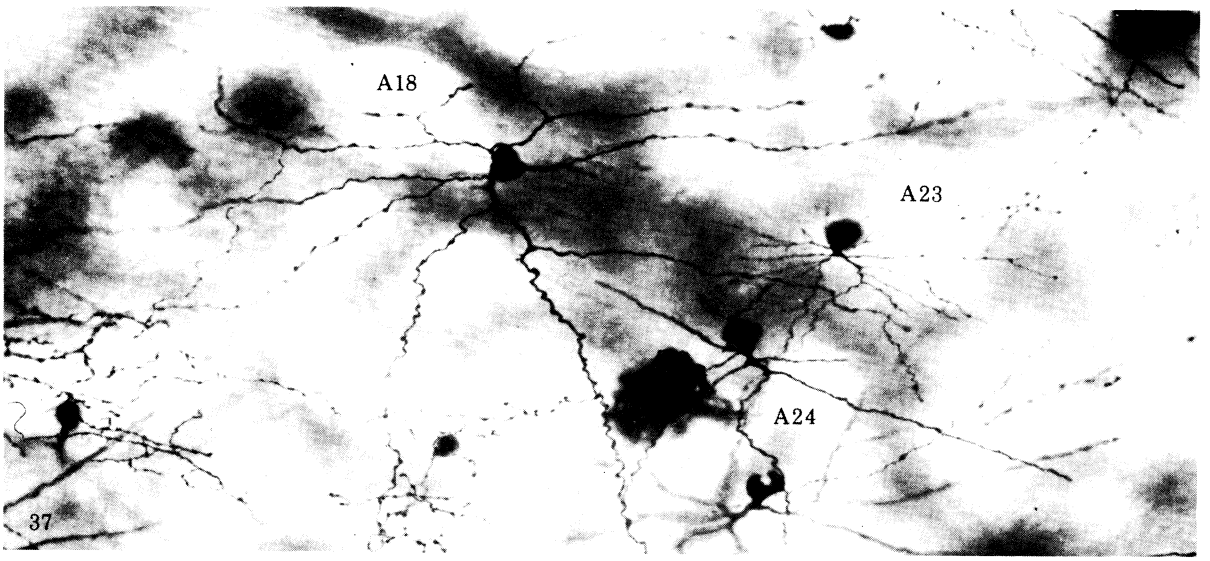
A18
A23
A24
37

Description of plate 3

Figure 35. Light micrograph of the stellate wide-field amacrine cell A23 branching on a plane in S1. Cell body is in focus. (Magn. × 500.)

Figure 36. A22 stellate large amacrine of the turtle retina. The thick major dendrites taper to fine profiles (arrowed) and travel for hundreds of micrometres. (Magn. × 500.)

Figure 37. Wide-field amacrine cell A18 branches in S1. Less completely impregnated (A23) or other amacrine cells out of the plane of focus (A24) are also seen. (Magn. × 500.)

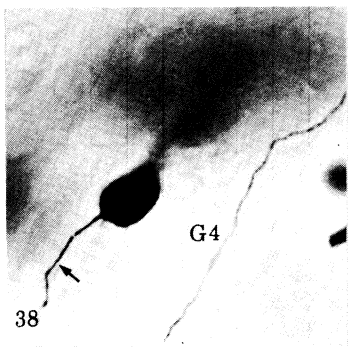

38

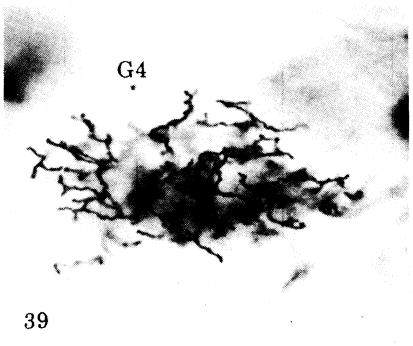

39

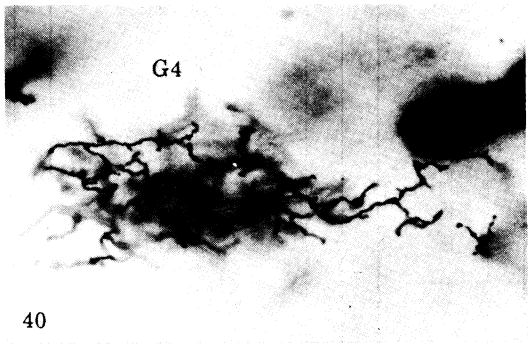

40

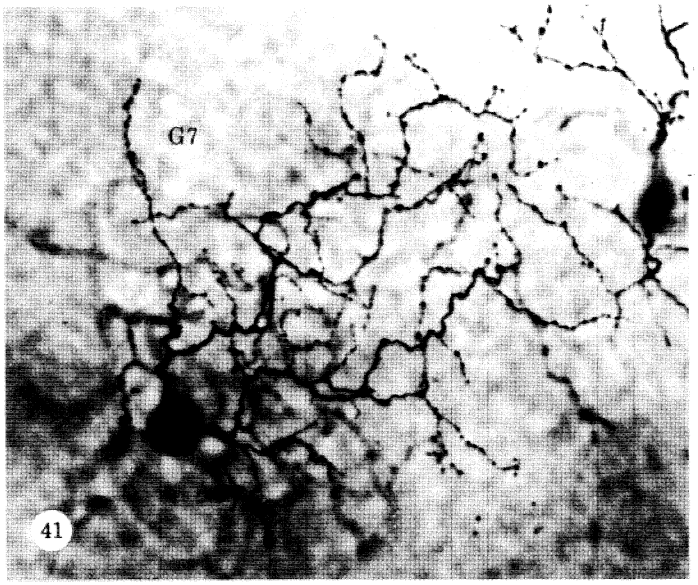

41

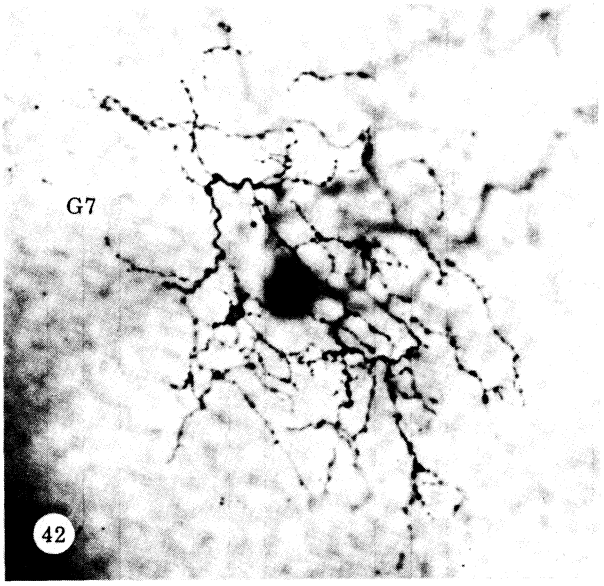

42

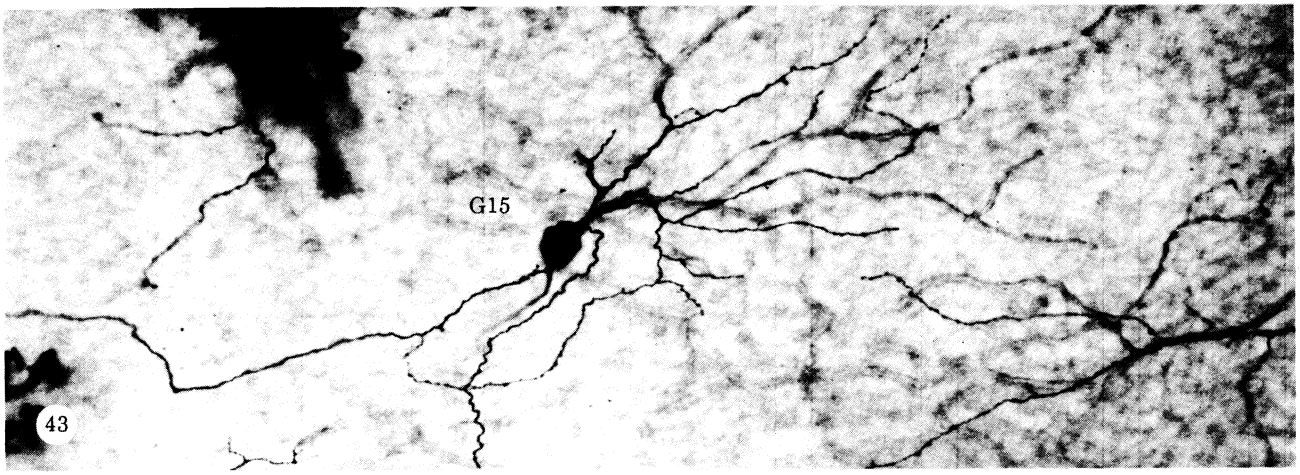

43

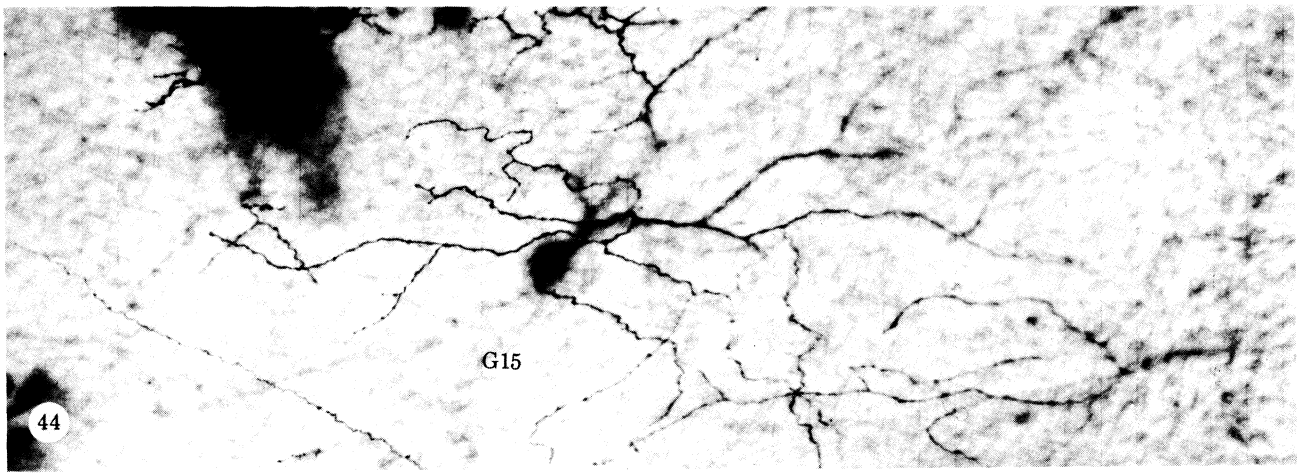

44

Description of plate 4

Figures 38–40. Bistratified small ganglion cell G4 of the turtle retina as seen in three planes of focus: cell body and axon (arrowed) (figure 38), first tier of dendrites in S3 (figure 39) and the second tier of dendrites in S1 (figure 40). (Magn. × 750.)

Figures 41 and 42. Two views of the bistratified small ganglion cell G7. The dendrites in the tier closer to the cell body in S4 (figure 41) branch at 90° to the tier in S1 (figure 42). (Magn. × 750.)

Figures 43 and 44. Two views of a bistratified large ganglion cell G15 taken at the level of the proximal layer of dendrites and cell body (figure 43) and at the distal layer in S1 (figure 44). (Magn. × 500.)

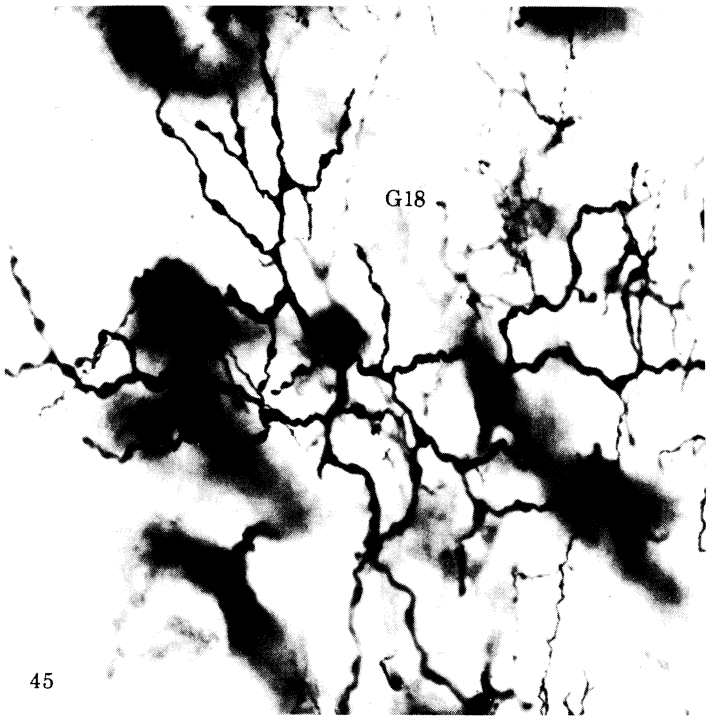
G18
45

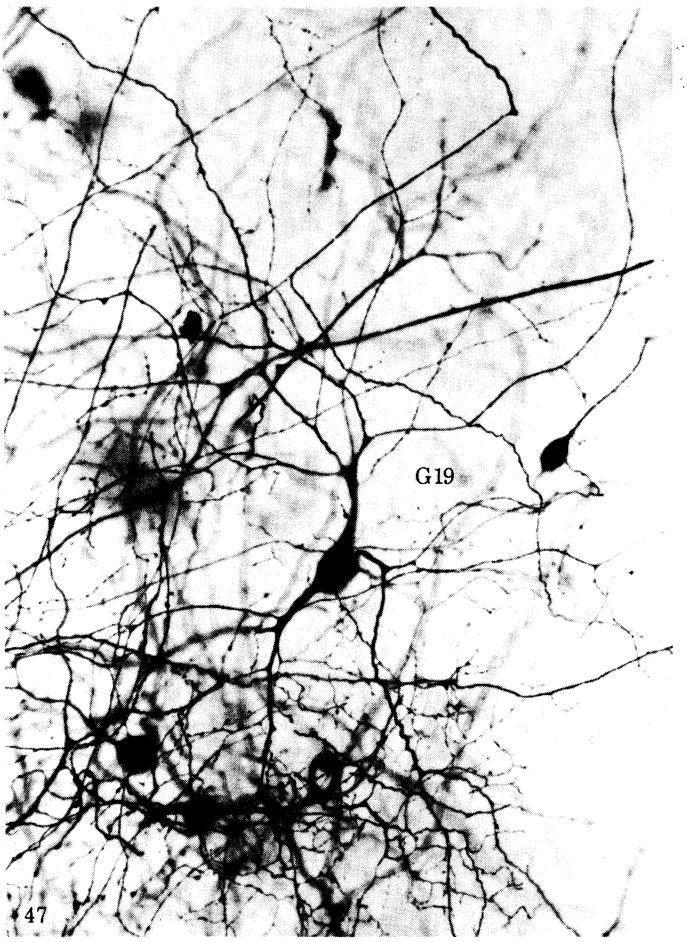
G19
47

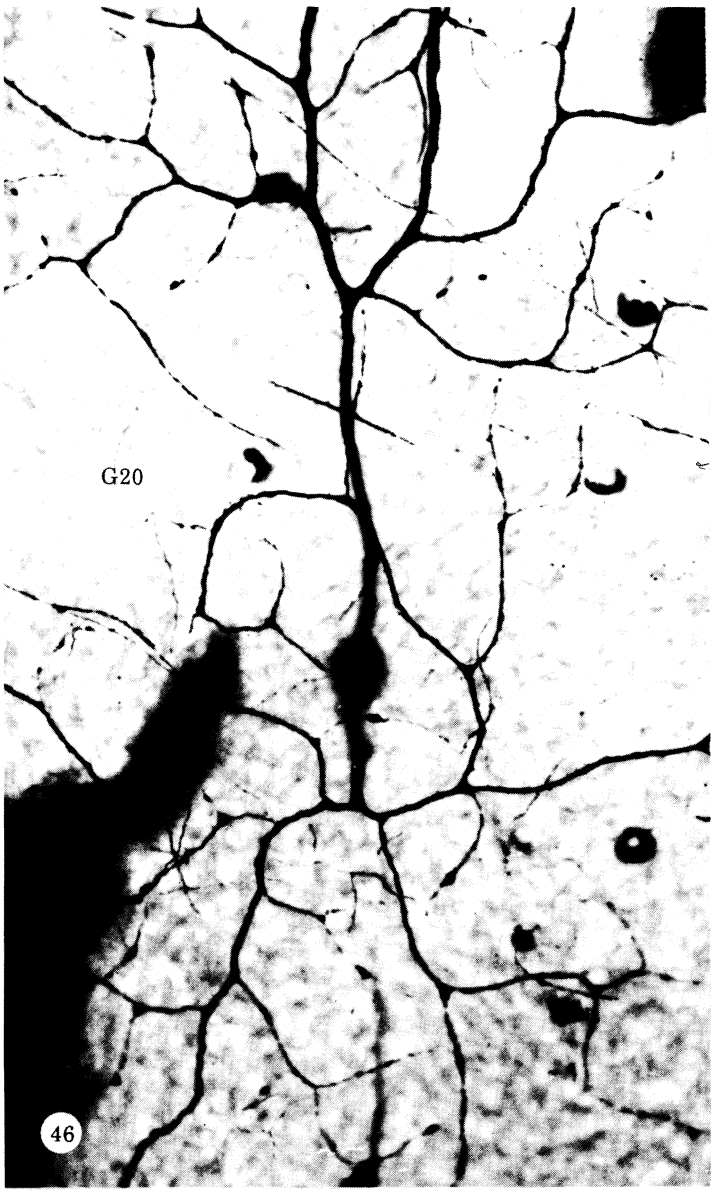
G20
46

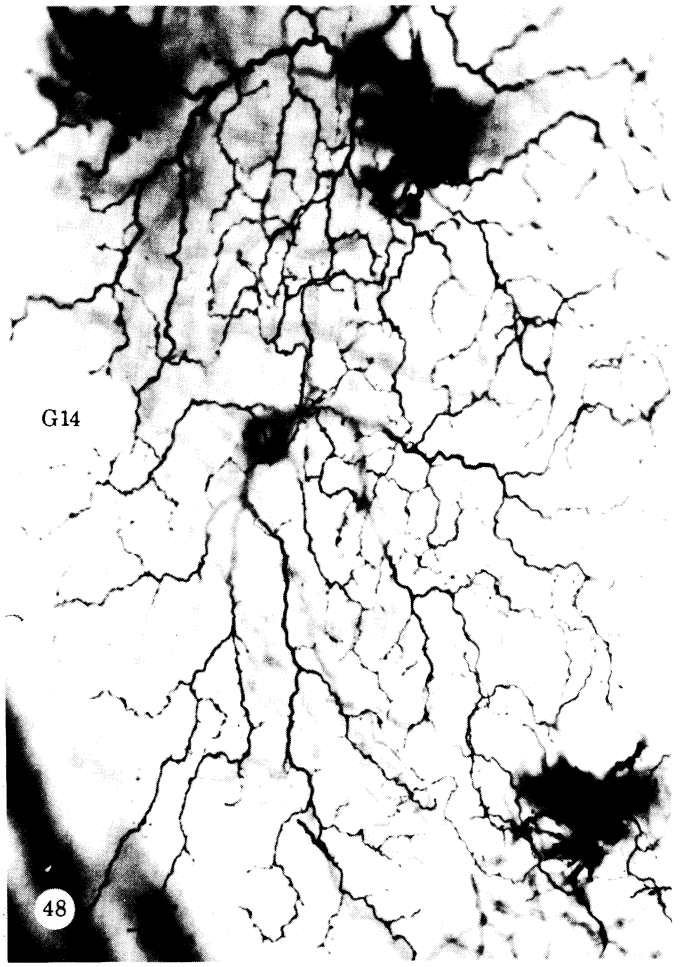
G14
48

G17, or of cells that have a completely bipolar dendritic spread parallel to the edge of the streak, such as A14 and A16, would seem to require special developmental cues.

It is still not clear exactly what function a linear visual streak subserves. Almost all vertebrates, including most mammals, have an extension of the area centralis along the horizontal meridian where ganglion cell concentration is highest (Hughes 1977). This suggests that there is a fundamental importance in maintaining a retinal specialization along the horizontal visual axis. Two current theories are popular concerning the function of the visual streak. The 'terrain' hypothesis of Hughes (1977) suggests that the streak is important for species that live in areas where the field of view is unobscured by nearby vegetation and the horizontal meridian forms a reference point. The other theory (Brown 1969) states that the streak is a *linear area centralis* subserving high resolution vision; however, the streak of turtle probably has the highest photoreceptor to ganglion cell convergence (Peterson & Ulinski 1979), contrary to what is normally considered ideal for high acuity vision. Both theories have problems and we clearly need more experimental data to substantiate either of them. However, one striking correlation can be made between species with streak-bearing retinas and ganglion cell physiology: all the vertebrate retinas that have dramatic linear visual streaks and have been studied by physiological recordings of ganglion cells (rabbit, ground squirrel and turtle) show a large proportion of orientation and directionally selective units.

In the linear visual streak of the turtle retina, horizontal cell axon terminals have an elongated shape and are oriented parallel to the streak (Normann *et al.* 1979; Normann & Kolb 1981). The receptive fields of these cells are correspondingly elongated and oriented (Normann *et al.* 1979; Normann & Kolb 1981). Thus, it is possible that the architecture of the linear visual streak imposes oriented receptive field properties on the neurons even at the first synaptic level, and these receptive field characteristics are then elaborated at other sites of neuronal interaction through to the ganglion cell level. Certainly all the oriented ganglion cell receptive fields of the rabbit retina are recorded in or near the streak (Levick 1967) and there is a suggestion that a similar situation exists in turtle (J. E. Fulbrook, personal communication). Thus, the available physiology suggests that the visual streak organization provides the morphological basis and the underlying neural circuitry responsible for orientation and directional selectivity. In contrast, animals without linear visual streaks in their retinas may reserve the information processing necessary for these features of visual integration for the visual cortex.

Correlation of the morphological data with electrophysiological recordings

(i) *Bipolar cells*

A great deal of attention has been focused on the photoreceptors and horizontal cells of the turtle retina and relatively little on the neurons of the proximal retina. Only a few bipolar cell

---

DESCRIPTION OF PLATE 5

FIGURE 45. Light micrograph of a Golgi-impregnated large ganglion cell G18. The cell body is displaced to the i.n.l. The cell is probably the Dogiel cell. It lies on the edge of the l.v.s. (Magn. × 500.)

FIGURE 46. The largest-field type of ganglion cells in the turtle retina is G20. The cell is from far peripheral retina (8 mm). (Magn. × 500.)

FIGURE 47. G19 cell has a diffusely spreading dendritic tree of fine tapering dendrites. (Magn. × 500.)

FIGURE 48. A medium-sized bistratified ganglion cell G14. The plane of focus is at the level of the major dendrites in S3. Finer dendrites pass up to the S1/2 border (not in focus). The cell lies 1 mm from the l.v.s. (Magn. × 500.)

recordings have been made and the accompanying morphological characterizations of the cells typically have not included the stratification of the axon terminal in the i.p.l., a characteristic that is the basis for identifying bipolar cell types in this Golgi study. Thus, although Yazulla (1976) has described the greatest variety of bipolar types (five different types dependent on centre sign and chromatic characteristics), unfortunately none of them can be matched to the bipolar cells shown here. The commonest bipolar type recorded by Yazulla and others is centre-depolarizing, surround-hyperpolarizing to red light. The second commonest is the centre-hyperpolarizing, surround-depolarizing bipolar cell. The Marchiafava & Weiler (1980) stained examples of these two common bipolar types appear to be equivalent to B4 and B6.

The Richter & Simon (1975) data on the red-sensitive hyperpolarizing bipolar cells suggest that they can be further subdivided into those that receive antagonistic surrounds from H1 axon terminals (L1 units) and others that receive surrounds from H1 cell bodies (L2 units based upon physiological criteria). B5 described in this Golgi study is clearly a candidate for a centre-hyperpolarizing bipolar by virtue of its monostratified axon terminating in S1. It could be the Richter & Simon (1975) second bipolar type. Bipolar cells with multistratified axons penetrating to the S3–S5 regions of the i.p.l., such as B3 and B7–B9, have not yet been recorded from. Their responses to light stimulation could be either ON-centre or OFF-centre if we can draw from our experiences with the cat retina (Nelson *et al.* 1976; Nelson 1980). Sophisticated chromatic types or even double-opponent types of bipolar cell such as have been described in the goldfish (Kaneko & Tachibana 1981) can also be expected.

(ii) *Amacrine cells*

A large ON–OFF amacrine cell with a body 12–14 μm in diameter and large-diameter dendrites stratifying at the S2/S3 border has been recorded from and stained by intracellular dye injection in the turtle (Schwartz 1973; Marchiafava & Weiler 1980; Jensen & DeVoe 1980). This type of amacrine cell is almost certainly A22 of the present Golgi study.

Such transient ON–OFF amacrine cells are recorded fairly commonly in retinas of cold-blooded vertebrates (Werblin & Dowling 1969; Kaneko 1970; Werblin & Copenhagen 1974; Miller & Dacheux 1976; Naka 1976; Famiglietti *et al.* 1977; Murakami & Shimoda 1977; Frumkes & Miller 1979). However, in contrast to the turtle retina, the ON–OFF amacrine cells of the carp and goldfish retinas have been identified as large bistratified amacrines (Murakami & Shimoda 1977; Famiglietti *et al.* 1977). It has been proposed that the ON–OFF inputs to these amacrine cells are provided by bipolar cells of different centre sign ending in the two sublaminae and having synaptic input onto the two separate dendritic trees of the bistratified amacrine (Famiglietti *et al.* 1977). However, this attractively simple explanation cannot be true for the turtle amacrine cell, for it is monostratified. The major input to the ON–OFF cell of the turtle is also thought to be from different bipolar types (Schwartz 1973; Marchiafava & Torre 1978). It is probable that the ON–OFF cell of turtle (A22) is receiving bipolar input of different centre sign to its monostratified dendritic tree by way of multistratified bipolar cells. There are two bistratified varieties that have one portion of their axon branching in the vicinity of the A22 cells' dendritic tree (i.e. B4 and B8; see table 2).

Recent investigations in catfish (Davis & Naka 1980; Chan & Naka 1976) have split the ON–OFF amacrine cells or C-neurons into two types, the slow and fast transient cells. Extrapolating to other species, it is possible that in turtle retina there are several varieties of amacrine cells that respond in similar ON–OFF manner, but other differentiating physiological properties

have not yet been elucidated. In fact, Marchiafava (1982) has recently described another variety of ON–OFF transient amacrine cell in the turtle retina. Its morphology suggests that it is A20 of this Golgi study. This adds further evidence that transient amacrine cells in the turtle retina are primarily monostratified types (Marchiafava 1982).

Amacrine cells responding in a sustained fashion to light stimulation have been recorded from in several vertebrate retinas (Toyoda *et al.* 1972; Kaneko 1973; Naka 1976) and appear to be prevalent in mammalian retinas (Nelson *et al.* 1976; Nelson & Kolb 1978; Kolb & Nelson 1981). In turtle retina, preliminary evidence (Marchiafava 1982) suggests that sustained amacrine cells have diffuse or multistratified dendritic trees. One sustained cell of Marchiafava (1982) is probably the tristratified cell A12 of this study. In this respect, it is interesting to note that the sustained amacrine cells of the cat retina (Nelson & Kolb 1978; Kolb & Nelson 1981) also have diffuse dendritic trees or broadly bistratified dendritic trees permeating all strata of the i.p.l.

It is reasonable to assume that orientation-specific amacrine cells (Naka 1980) and colour-opponent amacrine cells (Kaneko 1973) will also be found in turtle retina in due course, given the extraordinarily diverse population of amacrine cells present in this species' retina. Furthermore, recent findings suggest that different morphological types of amacrine cell contain specific neurotransmitters and peptides (Ehinger & Falck 1971; Lam 1972; Voaden *et al.* 1977; Ehinger 1977; Marc *et al.* 1978; Masland & Mills 1979; Pourcho 1979, 1980, 1981; Brecha *et al.* 1979; Karten & Brecha 1980; Brandon *et al.* 1980; Yamada *et al.* 1980; Vaughn *et al.* 1981; Eldred & Karten 1981). The multifarious amacrine cells of the turtle retina will probably prove to have functional significance by virtue of their different branching patterns and consequent neurocircuitry and different chemical interactions upon other amacrine, bipolar and ganglion cells.

(iii) *Ganglion cells*

The commonest ganglion cell types described in the turtle retina are ON–OFF, direction-selective, motion-sensitive and orientation-sensitive (Schwartz 1973; Fulbrook 1979; Jensen & DeVoe 1980; Bowling 1980). From the Schwartz (1973) and Jensen & DeVoe (1981) intracellular stainings, it appears that two of the ON–OFF ganglion cell types correspond to G14 and G17. G14 has a large cell body and large bistratified dendritic tree branching on the S1/2 border and in S3 while G17 is the large tristratified ganglion cell with branches at the strata borders of S1/2, S3/4 and S4/5. It is possible that the G17 is a direction-selective cell (Jensen & DeVoe 1981) and it is particularly noteworthy that the G17 cells of this Golgi study exhibited dendritic trees oriented orthogonal to the l.v.s.

Two further ON–OFF ganglion cells which are non-directional have been described by Marchiafava & Weiler (1980). The procion-injected cells are probably G13 and G5 of this Golgi study. An interesting correlation can also be made between the large-field OFF-centre A-type ganglion cell described by these authors and G20 of the present study. This ganglion cell is the largest-bodied, largest-field cell seen in turtle retina. It branches in S2 in the presumed OFF-centre sublamina of the turtle i.p.l. in a position to receive input from the OFF-centre bipolar cells. In an attempt to compare turtle and cat retinal ganglion cells, Marchiafava & Weiler (1980) suggest that their type A and B ganglion cells are the equivalent of the alpha and beta cells of Boycott & Wässle (1974) or the Y and X cells of Enroth-Cugell & Robson (1966). Clearly this is a misinterpretation for although G20 is a large ganglion cell type, super-

ficially similar in morphology to an alpha cell in cat, the physiology of turtle type A ganglion cells is very sustained and probably mostly bipolar-driven, more like that of X cells of the cat retina.

The available data suggest that most turtle ganglion cells receive input from both rod and cone systems (Bowling 1980) and that the dominant cone input is from the long-wavelength cones. Colour-opponent (Fulbrook 1979) or double-opponent ganglion cells (Bowling 1980) have been demonstrated, with the red- and green-wavelength cones being most represented. The blue cone system does not appear to be easily detected at the ganglion cell level, to judge by the paucity of physiological data. Marchiafava & Wagner (1981) have recorded a single example of a ganglion cell that is ON-centre to blue light of wavelength 489 nm and has an OFF surround to stimulation by blue light of wavelength 434 nm. The truncated sketch of the stained blue ganglion cell in Marchiafava & Wagner (1981) suggests that it might be G21 of this study. Clearly more evidence is needed before making precise identifications of physiologically recorded ganglion cells with the Golgi-impregnated cells of the turtle retina. It is probable that in the retina of the turtle many colour-coded and colour-specific ganglion cell types are still to be discovered.

How does the turtle retina compare with other vertebrate retinas?

More numerous cell types, particularly among the amacrine varieties, have been seen in this Golgi study of turtle retina than in any other retina so far investigated, including the avian retina (Cajal 1933; Mariani 1978) and frog retina (Cajal 1933; Maturana *et al.* 1960). However, more detailed morphological studies beyond those of Cajal (1933) are still needed to make meaningful comparisons of cell types and morphological architecture among various vertebrate retinas. Only generalizations can be made at the present.

(i) *Bipolar cells*

The bipolar cells of the pigeon retina are strikingly similar to those of turtle retina (Mariani 1978), with many bi- and tristratified types bearing Landolt clubs characterizing both species. The bipolar cells of frog (Cajal 1933) and a teleost retina (Rudd) (Scholes 1975) are also commonly multistratified. On the other hand, mammalian species appear to have mostly unistratified bipolar cells (Cajal 1933; Polyak 1941; Boycott & Dowling 1969; Boycott & Kolb 1973*b*; Kolb *et al.* 1981). However, there is a single type of bistratified cone bipolar cell in cat retina (Kolb *et al.* 1981), which stratifies in similar manner to B8 of turtle retina. Furthermore, ground squirrel (West 1976) apparently has a bistratified bipolar cell with both axon branches in the distal i.p.l., possibly the equivalent of B4 of the present study in turtle.

In mammals such as cat and primate (Polyak 1941) the bipolar cells in general have axon terminals that are vertically oriented and stretch through two or three strata of the i.p.l., rather than branching horizontally in a strictly stratified fashion, as in turtle. The vertical tortuosity of the mammalian bipolar cells is almost certainly related to the occurrence of paramorphic pairs of broadly stratified alpha and beta ganglion cells of central retina in the cat and midget and parasol ganglion cells in the primate (Polyak 1941). Such ganglion cells subserve parallel OFF-centre and ON-centre channels for the X and Y pathways (Famiglietti & Kolb 1976). The turtle retina, on the other hand, may not have developed X and Y channels. The circuitry for sophisticated receptive field types in the turtle may be occurring at the retinal level, obviating

the need to develop parallel X and Y channels carrying information to the visual cortex for later receptive field construction.

(ii) *Amacrine cells*

The amacrine cells of turtle, bird and frog retina are very similar. It looks as though the simple stellate type of amacrine cell, with long, essentially unbranched dendrites emerging from the cell body like spokes of a wheel or from a 'magnificent star' (Cajal 1933), are particularly well developed in turtle and bird. Boycott & Dowling (1969) show such cells in pigeon retina, stained with the reduced-silver method, arranged in four distinct bands in the i.p.l. The pigeon cells are strikingly similar in stratification to A23–A26, respectively, of the turtle retina (see figure 9; plate 3, figures 35, 37). Such symmetrical stellate cells have not been seen in cat retina (Kolb *et al.* 1981). On the other hand, monostratified amacrine cells with irregular dichotomous branching patterns are found in all vertebrate retinas. It is interesting that the highly anisotropic amacrine cell varieties seen in turtle retina (A16 and A21) have also been seen in another streak-bearing retina, namely that of the rabbit (personal observation). It is tempting to suggest that such cell types are associated only with species where the linear visual streak is well developed and orientation- and direction-selective ganglion cells are more commonly found.

Narrow-field, densely branched amacrine cells are relatively uncommon in turtle, frog and bird retinas compared with mammalian retinas where such narrow-field cells predominate. Furthermore, it is almost certain that the highly specialized narrow-field bistratified amacrine cells AII and A8 (Famiglietti & Kolb 1975; Kolb *et al.* 1981) and the large-field diffuse amacrine cells named A17 in cat retina (Kolb *et al.* 1981; Kolb & Nelson 1981) are not seen in retinas other than mammalian. This is probably because these cells in mammalian retinas are highly specialized for the rod-driven pathways through the retina. The development of AII, A8 and A17 in mammalian species alone, may parallel the development of segregated rod bipolar pathways in these species as compared to submammalian species, for all submammalian species so far investigated, including the turtle, appear to have mixed rod–cone bipolar cells and no purely rod bipolar cells (fish (Scholes 1975; Stell *et al.* 1977; Ishida *et al.* 1980); salamander (Lasansky 1973); turtle (Dacheux 1980)).

(iii) *Ganglion cells*

Half of the ganglion cell types seen in the turtle are also seen in the cat (Kolb *et al.* 1981) and ground squirrel (West 1976). However, it is clear that the three ganglion cell types so well described and emphasized in cat retina to the extent that generalizations have been made to other vertebrate retinas, namely the alpha, beta and gamma cells of Boycott & Wässle (1974), are probably not present in the retina of the turtle.

There are two bistratified ganglion cell types in cat retina, which correspond to two bistratified ganglion cells in turtle, namely G6 and G14, and ground squirrel appears to have ganglion cells comparable to G6, G14 and G15 of turtle (West 1976). A cell equivalent to the small monostratified G1 of turtle retina is also seen in frog retina (Cajal 1933) and poses an interesting question of a mammalian equivalent. This ganglion cell has the smallest dendritic tree of the ganglion cells of submammalian species, and in appearance has some similarities with a central beta cell in cat, but as it does not occur in *a* and *b* varieties (it is only a *b* variety, branching in proximal i.p.l.) it cannot be regarded a beta or X type ganglion cell. Cell types such as G1

are found in both ground squirrel and cat (G9, ground squirrel; G12, cat). Electron microscope analysis of the Golgi-impregnated ground squirrel G9 indicates that this cell type receives mainly amacrine cell input (West 1976). Thus, it may *not* be a ganglion cell to subserve acuity as is thought to be the major function of the small field beta cell of the cat retina, which is clearly bipolar-dominated (Kolb 1979; Stevens *et al.* 1980).

The largest ganglion cells of turtle retina (G20 and G21) have cell bodies of diameter 25 μm and dendritic trees covering 500–800 μm of retina. These cells are almost certainly not paramorphic pairs of a single class because they have distinctly different branching patterns. For this reason they cannot be considered the equivalents of alpha cells of the cat. However, such cells have counterparts in ground squirrel (West 1976: G14) and in cat retina (Kolb *et al.* 1981: G19 and G21). In cat retina these large ganglion cells are thought to be delta cells (Boycott & Wässle 1974) and epsilon cells (Levinthal *et al.* 1980; Stone & Clarke 1980). Epsilon cells are known to have distinct physiological properties and projection sites that distinguish them from Y cells.

There is one large ganglion cell that appears to be unique to birds and reptiles. This is the displaced ganglion cell of Dogiel (1895), which this study has indicated either can be displaced or can occur in the normal position in the ganglion cell layer in the turtle. This ganglion cell (G18) has a unique morphology and stratification in the distal i.p.l. In pigeons these Dogiel cells have been shown to project exclusively to the nucleus of the basal optic root (Karten *et al.* 1977) and are thought to be involved in oculomotor reflexes. Their occurrence and projection sites are similar in the turtle (Reiner 1981). Ganglion cells equivalent to G18 or the Dogiel cell have not yet been seen in a mammalian retina.

What conclusions can one draw from this comparison of Golgi-impregnated *Pseudemys* turtle retina with Golgi studies on other vertebrate retinas? It appears that, as Cajal (1933) concluded, there are many similarities of retinal structure among the various vertebrate retinas. Most of the cell types are common to all species including mammals but their relative numbers and involvement in neuronal networks vary between species, probably as a result of the different emphasis put on particular functional pathways in the different species.

I thank Dr Larry Stensaas for reading the manuscript, and Dr Richard A. Normann and Jill Jones for help at various stages of the research for this paper. This work was supported in part by grant EY03323.

References

Baylor, D. A. & Fuortes, M. G. F. 1970 Electrical responses of single cones in the retina of the turtle. *J. Physiol., Lond.* **207**, 77–92.

Baylor, D. A., Fuortes, M. G. F. & O'Bryan, P. M. 1971 Receptive fields of cones in the retina of the turtle. *J. Physiol., Lond.* **214**, 265–294.

Baylor, D. A. & Hodgkin, A. L. 1973 Detection and resolution of visual stimuli by turtle photoreceptors. *J. Physiol., Lond.* **234**, 163–198.

Bowling, D. B. 1980 Light responses of ganglion cells in the retina of the turtle. *J. Physiol., Lond.* **299**, 173–196.

Boycott, B. B. & Dowling, J. E. 1969 Organization of the primate retina: light microscopy. *Phil. Trans. R. Soc. Lond.* B **255**, 14–176.

Boycott, B. B. & Kolb, H. 1973*a* The horizontal cells of the rhesus monkey retina. *J. comp. Neurol.* **148**, 115–140.

Boycott, B. B. & Kolb, H. 1973*b* The connexions between bipolar cells and photoreceptors in the retina of the domestic cat. *J. comp. Neurol.* **148**, 91–114.

Boycott, B. B. & Wässle, H. 1974 The morphological types of ganglion cells of the domestic cat's retina. *J. Physiol., Lond.* **240**, 397–419.

Brandon, C., Lam, D. M. K., Su, Y. Y. & Wu, J.-Y. 1980 Immunocytochemical localization of GABA neurons in the rabbit and frog retina. *Brain Res. Bull.* **5** (suppl. 2), 21–29.

Brecha, N., Karten, H. J. & Laverack, C. 1979 Enkephalin-containing amacrine cells in the avian retina: immunohistochemical localization. *Proc. natn. Acad. Sci. U.S.A.* **76**, 3010–3014.

Brown, K. T. 1969 A linear area centralis extending across the turtle retina and stabilized to the horizon by non-visual cues. *Vision Res.* **9**, 1053–1062.

Cajal, S. R. y. 1933 *Die Retina der Wirbeltiere.* Wiesbaden: Bergmann. (Transl. S. A. Thorpe & M. Glickstein (1972). *The structure of the retina.* Springfield: Thomas.)

Chan, R. Y. & Naka, K.-I. 1976 The amacrine cell. *Vision Res.* **16**, 1119–1129.

Colonnier, M. 1964 The tangential organization of the visual cortex. *J. Anat.* **98**, 327–344.

Dacheux, R. F. 1980 Connections between small bipolar cells and photoreceptors in the turtle retina. *Invest. Ophthal. vis. Sci., Ass. Res. Vision Ophthal. Suppl.*, p. 70.

Davis, G. W. & Naka, K.-I. 1980 Spatial organization of catfish retinal neurons. I. Single- and random-bar stimulation. *J. Neurophysiol.* **43**, 807–831.

Dogiel, A. S. 1895 Die Retina der Vogel. *Arch. mikrosk. Anat. EntwMech.* **44**, 622–648.

Ehinger, B. 1977 Glial and neuronal uptake of GABA, glutamic acid, glutamine and glutathione in the rabbit retina. *Expl Eye Res.* **25**, 221–234.

Ehinger, B. & Falck, B. 1971 Autoradiography of some suspected neurotransmitter substances: GABA, glycine, glutamic acid, histamine, dopamine and L-DOPA. *Brain Res.* **33**, 157–172.

Eldred, W. D. & Karten, H. J. 1981 Neuropeptide containing amacrine cells in the retina of the turtle, *Pseudemys scripta. Soc. Neurosci. Abstr.* **7**, 277.

Enroth-Cugell, C. & Robson, J. G. 1966 The contrast sensitivity of retinal ganglion cells of the cat. *J. Physiol., Lond.* **187**, 517–552.

Famiglietti, E. V., Kaneko, A. & Tachibana, M. 1977 Neuronal architecture of on and off pathways to ganglion cells in carp. *Science, N.Y.* **198**, 1267–1269.

Famiglietti, E. V. & Kolb, H. 1975 A bistratified amacrine cell and synaptic circuitry in the inner plexiform layer of the retina. *Brain Res.* **84**, 293–300.

Famiglietti, E. V. & Kolb, H. 1976 Structural basis for 'ON' and 'OFF'-center responses in retinal ganglion cells. *Science, N.Y.* **194**, 193–195.

Frumkes, T. E. & Miller, R. F. 1979 Pathways and polarities of synaptic interactions in the inner retina of the mudpuppy: II. Insight revealed by an analysis of latency and threshold. *Brain Res.* **161**, 13–24.

Fulbrook, J. E. 1979 Receptive field properties of retinal ganglion cells in the turtle (*Pseudemys scripta elegans*). Master's thesis, University of Delaware.

Fuortes, M. G. F. & Simon, E. J. 1974 Interactions leading to horizontal cell responses in the turtle retina. *J. Physiol., Lond.* **240**, 177–198.

Gallego, A. & Perez-Arroyo, M. 1976 Photoreceptors and horizontal cells of the turtle retina (*'Clemmys caspica'*). In The structure of the eye III (ed. Y. Mishima). *Jap. J. Ophthal.*, pp. 311–317.

Granda, A. M. & Haden, K. W. 1970 Retinal oil globule counts and distributions in two species of turtles: *Pseudemys scripta elegans* (Wied) and *Chelonia mydas mydas* (Linnaeus). *Vision Res.* **10**, 79–84.

Hughes, A. 1977 The topography of vision in mammals of contrasting life style: comparative optics and retinal organisation. *Handbook of sensory physiology*, vol. 7 (5) (ed. F. Crescitelli), pp. 613–756. New York: Springer-Verlag.

Ishida, A. T., Stell, W. K. & Lightfoot, D. O. 1980 Rod and cone inputs to bipolar cells in goldfish retina. *J. comp. Neurol.* **191**, 315–335.

Jensen, R. J. & DeVoe, R. D. 1980 Intracellular recordings from amacrine and directional ganglion cells. *Invest. Ophthal. vis. Sci., Ass. Res. Vision Ophthal. Suppl.*, p. 5.

Jensen, R. J. & DeVoe, R. D. 1981 Identification of specific ganglion cell types in the turtle retina. *Invest. Ophthal. vis. Sci., Ass. Res. Vision Ophthal. Suppl.*, p. 184.

Johns, P. R. 1977 Growth of the adult goldfish eye. III. Source of new retinal cells. *J. comp. Neurol.* **176**, 343–358.

Johns, P. R. & Easter, S. S. 1977 Growth of the adult goldfish eye. II. Increases in retinal cell number. *J. comp. Neurol.* **176**, 331–341.

Kaneko, A. 1970 Physiological and morphological identification of horizontal, bipolar and amacrine cells in goldfish retina. *J. Physiol., Lond.* **207**, 623–633.

Kaneko, A. 1973 Receptive field organization of bipolar and amacrine cells in the goldfish retina. *J. Physiol., Lond.* **235**, 133–153.

Kaneko, A. & Tachibana, M. 1981 Retinal bipolar cells with double colour-opponent receptive fields. *Nature, Lond.* **293**, 220–222.

Karten, H. J. & Brecha, N. 1980 Localization of substance P immunoreactivity in amacrine cells of the retina. *Nature, Lond.* **283**, 87–88.

Karten, H. J., Fite, K. V. & Brecha, N. 1977 Specific projection of displaced retinal ganglion cells upon the accessory optic system in the pigeon (*Columba livia*). *Proc. natn. Acad. Sci. U.S.A.* **74**, 1753–1756.

Kolb, H. 1979 The inner plexiform layer in the retina of the cat: Electron microscopic observations. *J. Neurocytol.* **8**, 295–329.

Kolb, H. & Nelson, R. 1981 Amacrine cells of the cat retina. Proceedings of a symposium on information processing in the retina (ed. A. Kafka-Lützow). *Vision Res.* **21**, 1625–1634.

Kolb, H., Nelson, R. & Mariani, A. 1981 Amacrine cells, bipolar cells and ganglion cells of the cat retina: a Golgi study. *Vision Res.* **21**, 1081–1114.

Lam, D. M. K. 1972 The biosynthesis and content of γ-aminobutyric acid in the goldfish retina. *J. Cell Biol.* **54**, 225–231.

Landolt, E. 1871 Beitrag zur Anatomie der Retina vom Frosch, Salamander und Triton. *Arch. mikrosk. Anat. EntwMech.* **7**, 81–100.

Lasansky, A. 1969 Basal junctions at synaptic endings of turtle visual cells. *J. Cell Biol.* **40**, 577–581.

Lasansky, A. 1971 Synaptic organization of cone cells in the turtle retina. *Phil. Trans. R. Soc. Lond.* B **262**, 365–381.

Lasansky, A. 1973 Organization of the outer synaptic layer in the retina of the larval tiger salamander. *Phil. Trans. R. Soc. Lond.* B **265**, 471–489.

Leeper, H. F. 1978*a* Horizontal cells of the turtle retina. I. Light microscopy of Golgi preparations. *J. comp. Neurol.* **82**, 777–794.

Leeper, H. F. 1978*b* Horizontal cells of the turtle retina. II. Analysis of interconnections between photoreceptor cells and horizontal cells by light microscopy. *J. comp. Neurol.* **182**, 795–810.

Levick, W. R. 1967 Receptive fields and trigger features of ganglion cells in the visual streak of the rabbit's retina. *J. Physiol., Lond.* **188**, 285–307.

Levinthal, A. G., Keens, J. & Tork, I. 1980 The afferent ganglion cells and cortical projections of the retinal recipient zone (RRZ) of the cat's 'pulvinar complex'. *J. comp. Neurol.* **194**, 535–554.

Liebman, P. A. & Granda, A. M. 1971 Microspectrophotometric measurements of visual pigments in two species of turtle, *Pseudemys scripta* and *Chelonia mydas*. *Vision Res.* **11**, 105–114.

Marc, R. E., Stell, W. K., Bok, D. & Lam, D. M. K. 1978 GABA-ergic pathways in the goldfish retina. *J. comp. Neurol.* **182**, 221–246.

Marchiafava, P. L. 1979 The responses of retinal ganglion cells to stationary and moving stimuli. *Vision Res.* **19**, 1203–1211.

Marchiafava, P. L. 1982 The organization of inputs to amacrine and ganglion cells in the turtle. Proceedings of the Fourth Taniguchi Foundation Symposium on Visual Science. *Vision Res.* (In the press.)

Marchiafava, P. L. & Torre, V. 1978 The responses of amacrine cells to light and intracellularly applied currents. *J. Physiol., Lond.* **276**, 83–102.

Marchiafava, P. L. & Wagner, H. H. 1981 Interactions leading to colour opponency in ganglion cells of the turtle retina. *Proc. R. Soc. Lond.* B **211**, 261–267.

Marchiafava, P. L. & Weiler, R. 1980 Intracellular analysis and structural correlates of the organization of inputs to ganglion cells in the retina of the turtle. *Proc. R. Soc. Lond.* B **208**, 103–113.

Mariani, A. P. 1978 Organization of the outer plexiform layer of the pigeon retina. Ph.D. thesis, Pennsylvania State University, Hershey, Pennsylvania.

Masland, R. H. & Mills, J. W. 1979 Autoradiographic identification of acetylcholine in the rabbit retina. *J. Cell Biol.* **83**, 159–178.

Maturana, H. R., Lettvin, J. Y., McCulloch, W. S. & Pitts, W. H. 1960 Anatomy and physiology of vision in the frog (*Rana pipiens*). *J. gen. Physiol.* **43** (suppl. 2, Mechanisms of vision), 129–171.

Miller, R. F. & Dacheux, R. F. 1976 Synaptic organization and ionic basis of on and off channels in mudpuppy retina. I. Intracellular analysis of chloride-sensitive electrogenic properties of receptors, horizontal, bipolar cells and amacrine cells. *J. gen. Physiol.* **67**, 639–659.

Murakami, M. & Shimoda, Y. 1977 Identification of amacrine and ganglion cells in the carp retina. *J. Physiol., Lond.* **264**, 801–818.

Naka, K.-I. 1976 Neuronal circuitry in the catfish retina. *Invest. Ophthal. vis. Sci.* **15**, 926–935.

Naka, K.-I. 1980 A class of catfish amacrine cells responds preferentially to objects which move vertically. *Vision Res.* **20**, 961–965.

Nelson, R. 1980 Functional stratification of cone bipolar cell axons in the cat retina. *Invest. Ophthal. vis. Sci., Ass. Res. Vision Ophthal. Suppl.*, p. 130.

Nelson, R., Famiglietti, E. V. & Kolb, H. 1978 Intracellular staining reveals different levels of stratification for ON- and OFF-center ganglion cells in cat retina. *J. Neurophysiol.* **41**, 472–483.

Nelson, R. & Kolb, H. 1978 Small field amacrines in the rod system of cat retina. *Invest. Ophthal. vis. Sci., Ass. Res. Vision Ophthal. Suppl.*, p. 110.

Nelson, R., Kolb, H., Famiglietti, E. V. & Gouras, P. 1976 Neural responses in rod and cone systems of the cat retina: intracellular records and procion stains. *Invest. Ophthal. vis. Sci.* **15**, 946–953.

Normann, R. A. & Kolb, H. 1981 Anatomy and physiology of the horizontal cells of the visual streak region of the turtle retina. Proceedings of a symposium on information processing in the retina (ed. A. Kafka-Lützow). *Vision Res.* **21**, 1585–1588.

Normann, R. A., Kolb, H., Hanani, M., Pasino, E. & Holub, R. 1979 Orientation of horizontal cell axon terminals in the streak of the turtle retina. *Nature, Lond.* **280**, 60–62.

Peterson, E. H. & Ulinski, P. S. 1979 Quantitative studies of retinal ganglion cells in a turtle, *Pseudemys scripta elegans*. I. Number and distribution of ganglion cells. *J. comp. Neurol.* **186**, 17–42.

Polyak, S. L. 1941 *The retina.* University of Chicago Press.

Pourcho, R. G. 1979 Localization of cholinergic synapses in mammalian retina with peroxidase-conjugated α-bungarotoxin. *Vision Res.* **19**, 287–292.

Pourcho, R. G. 1980 Uptake of [3H]glycine and [3H]GABA by amacrine cells in the cat retina. *Brain Res.* **198**, 333–346.

Pourcho, R. G. 1981 [3H]taurine-accumulating neurons in the cat retina. *Expl Eye Res.* **32**, 11–20.

Ramon-Moliner, E. 1962 An attempt at classifying nerve cells on the basis of their dendritic patterns. *J. comp. Neurol.* **119**, 211–227.

Reiner, A. 1981 A projection of displaced ganglion cells and giant ganglion cells to the accessory optic nuclei in turtle. *Brain Res.* **204**, 403–409.

Richter, A. & Simon, E. J. 1975 Properties of centre-hyperpolarizing, red-sensitive bipolar cells in the turtle retina. *J. Physiol., Lond.* **248**, 317–334.

Saito, T., Miller, W. H. & Tomita, T. 1974 C- and L-type horizontal cells in the turtle retina. *Vision Res.* **14**, 119–123.

Scholes, J. H. 1975 Colour receptors, and their synaptic connexions, in the retina of a cyprinid fish. *Phil. Trans. R. Soc. Lond.* B **270**, 8–118.

Schwartz, E. A. 1973 Organization of ON–OFF cells in the retina of the turtle. *J. Physiol., Lond.* **230**, 1–14.

Simon, E. J. 1973 Two luminosity horizontal cells in the retina of the turtle. *J. Physiol., Lond.* **230**, 199–211.

Stell, W. K., Ishida, A. T. & Lightfoot, D. O. 1977 Structural basis for On- and Off-center responses in retinal bipolar cells. *Science, N.Y.* **198**, 1269–1271.

Stevens, J. K., McGuire, B. A. & Sterling, P. 1980 Toward a functional architecture of the retina: serial reconstruction of adjacent ganglion cells. *Science, N.Y.* **207**, 317–319.

Stone, J. & Clarke, R. 1980 Correlation between soma size and dendritic morphology in cat retinal ganglion cells: evidence of further variation in the γ-cell class. *J. comp. Neurol.* **192**, 211–217.

Toyoda, J.-I., Hashimoto, H. & Ohtsu, K. 1972 Bipolar–amacrine transmission in the carp retina. *Vision Res.* **12**, 1–12.

Vaughn, J. E., Famiglietti, E. V., Barber, R. P., Saito, K., Roberts, E. & Ribak, C. E. 1981 GABAergic amacrine cells in rat retina: immunocytochemical identification and synaptic connectivity. *J. comp. Neurol.* **197**, 113–128.

Voaden, M. J., Lake, N., Marshall, J. & Marjaria, B. 1977 Studies on the distribution of taurine and other neuractive amino acids in the retina. *Expl Eye Res.* **25**, 249–257.

Werblin, F. S. & Copenhagen, D. R. 1974 Control of retinal sensitivity. III. Lateral interactions at the inner plexiform layer. *J. gen. Physiol.* **63**, 88–110.

Werblin, F. S. & Dowling, J. E. 1969 Organization of the retina of the mudpuppy, *Necturus maculosus*. II. Intracellular recordings. *J. Neurophysiol.* **32**, 339–355.

West, R. W. 1976 Light and electron microscopy of the ground squirrel retina: functional considerations. *J. comp. Neurol.* **168**, 355–378.

Yamada, T., Marshak, D., Basinger, S., Walsh, J., Morley, J. & Stell, W. 1980 Somatostatin-like immunoreactivity in the retina. *Proc. natn. Acad. Sci. U.S.A.* **77**, 1691–1695.

Yazulla, S. 1976 Cone inputs to bipolar cells in the turtle retina. *Vision Res.* **16**, 737–744.

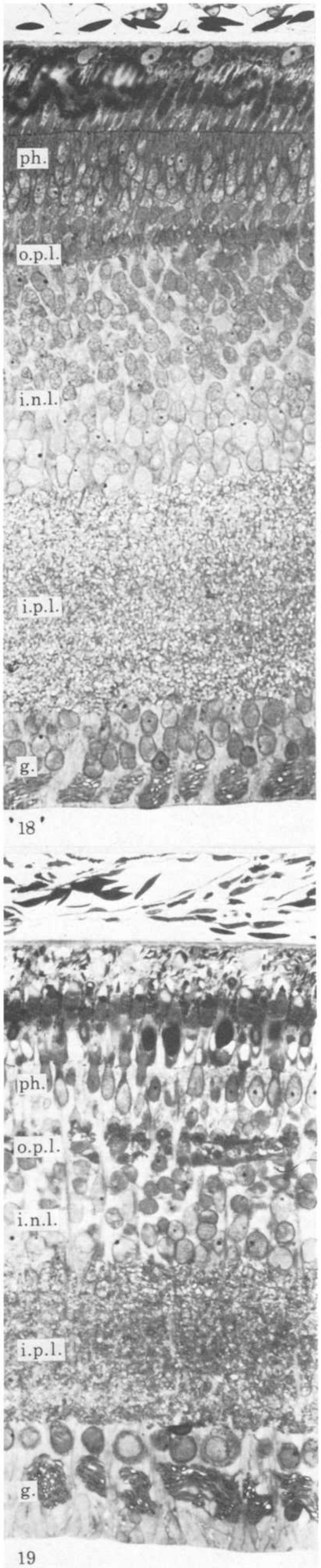
ph.
o.p.l.
i.n.l.
i.p.l.
g.

'18'

ph.
o.p.l.
i.n.l.
i.p.l.
g.

19

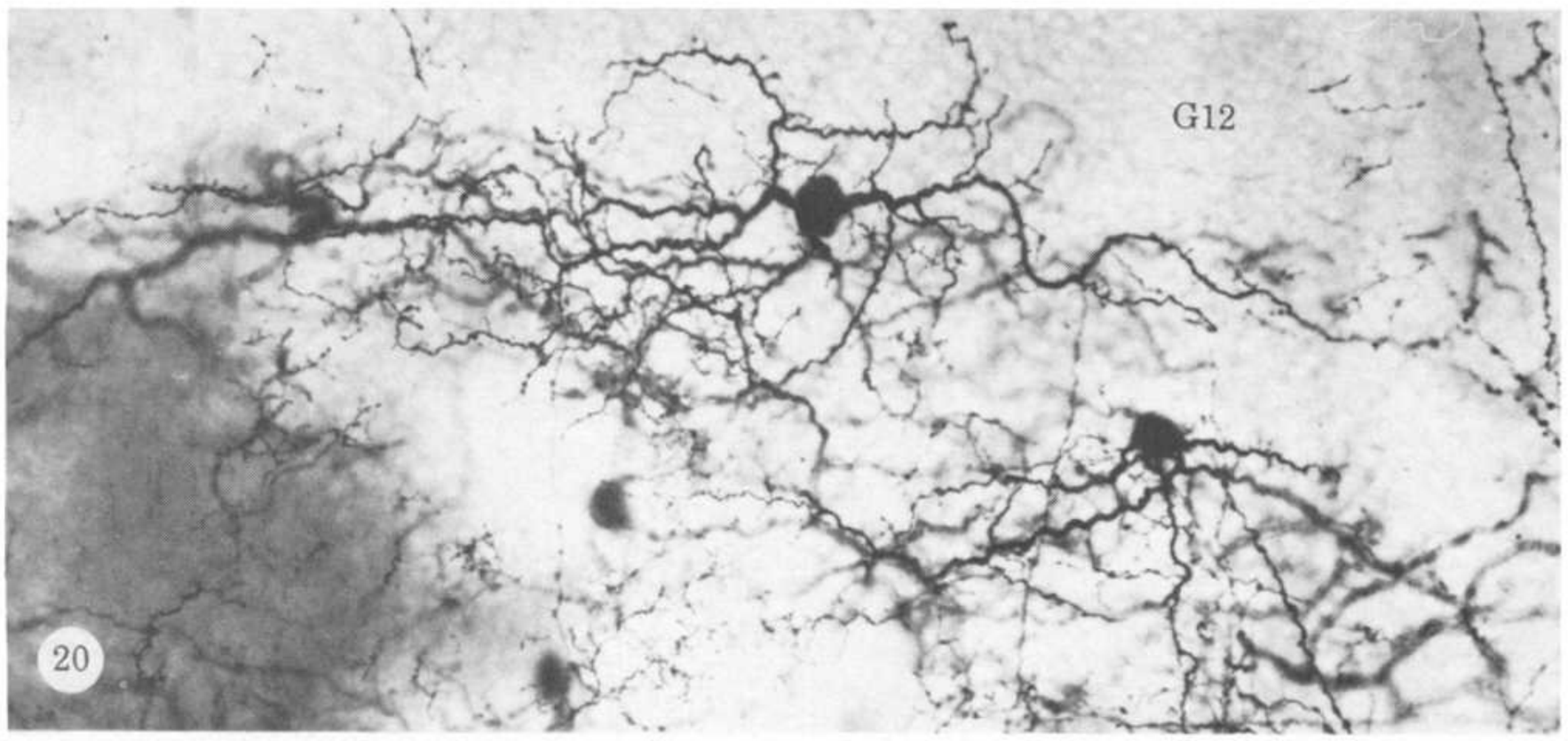
G12
20

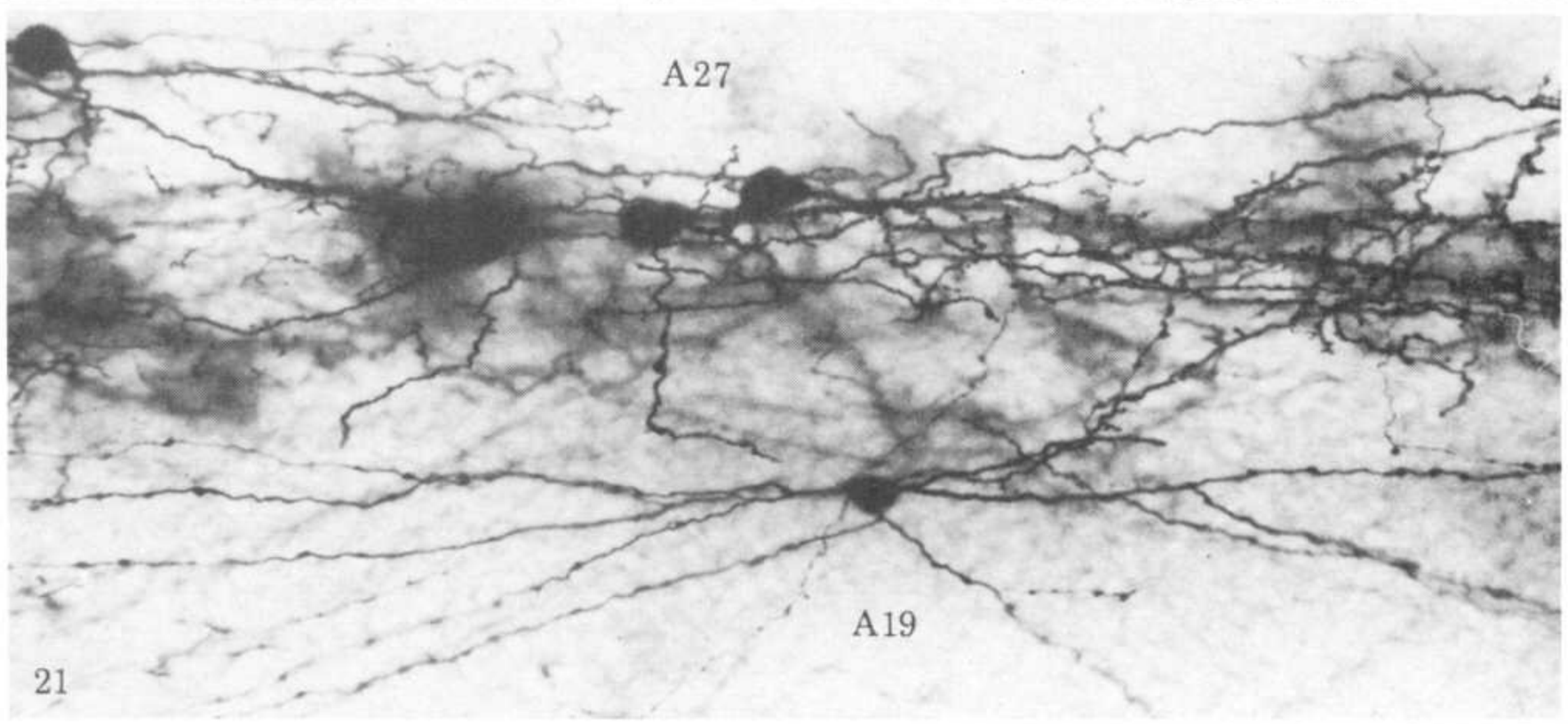
A27
A19
21

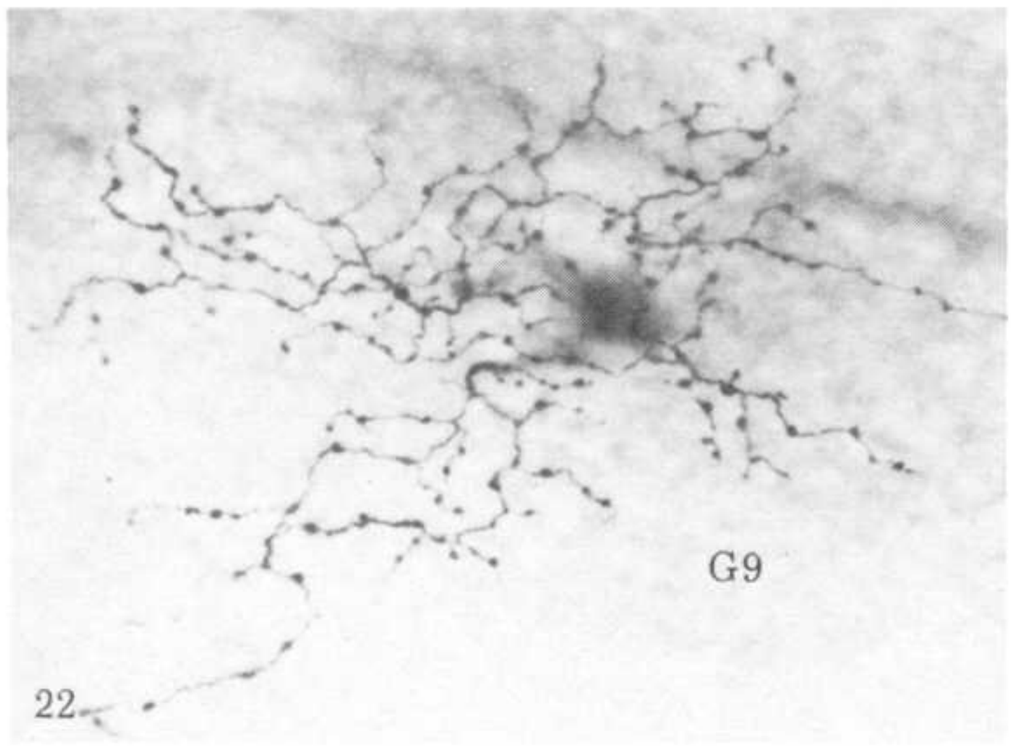
G9
22

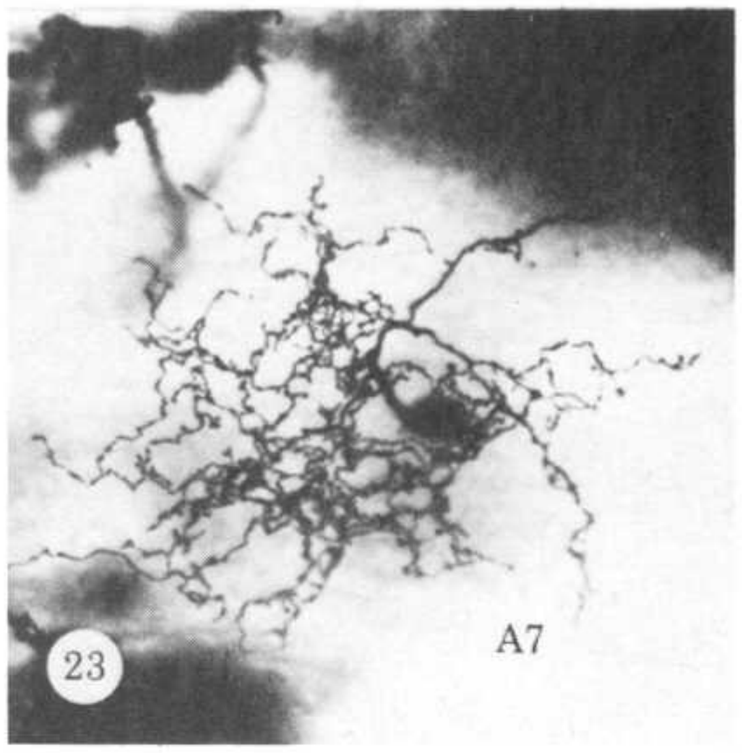
A7
23

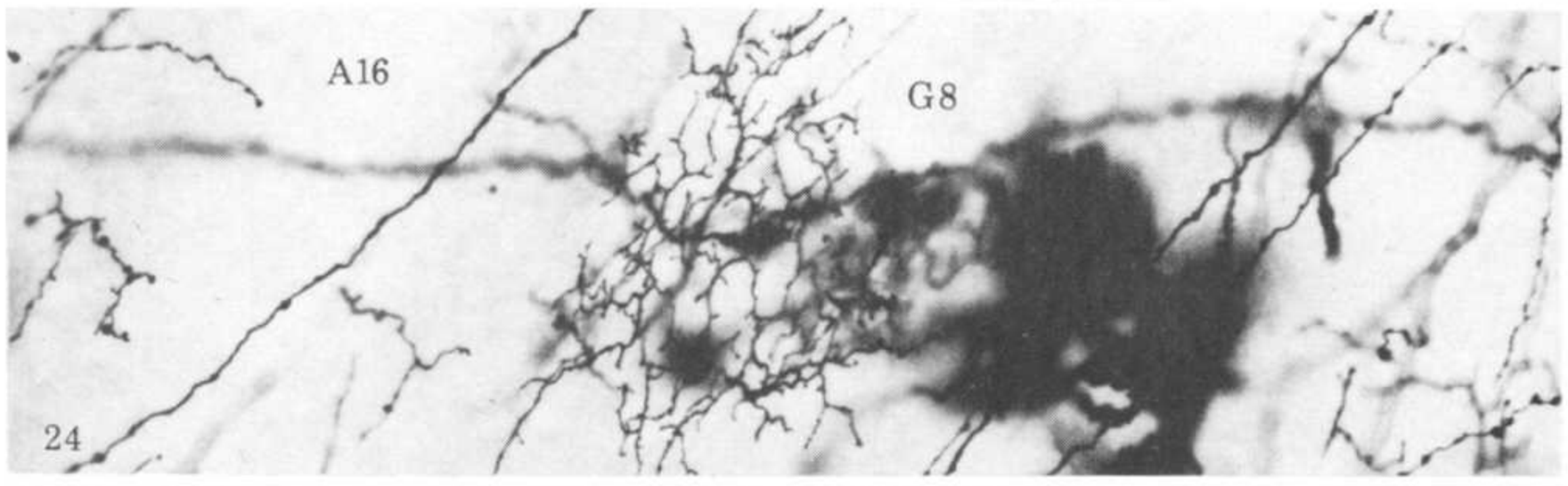
A16
G8
24

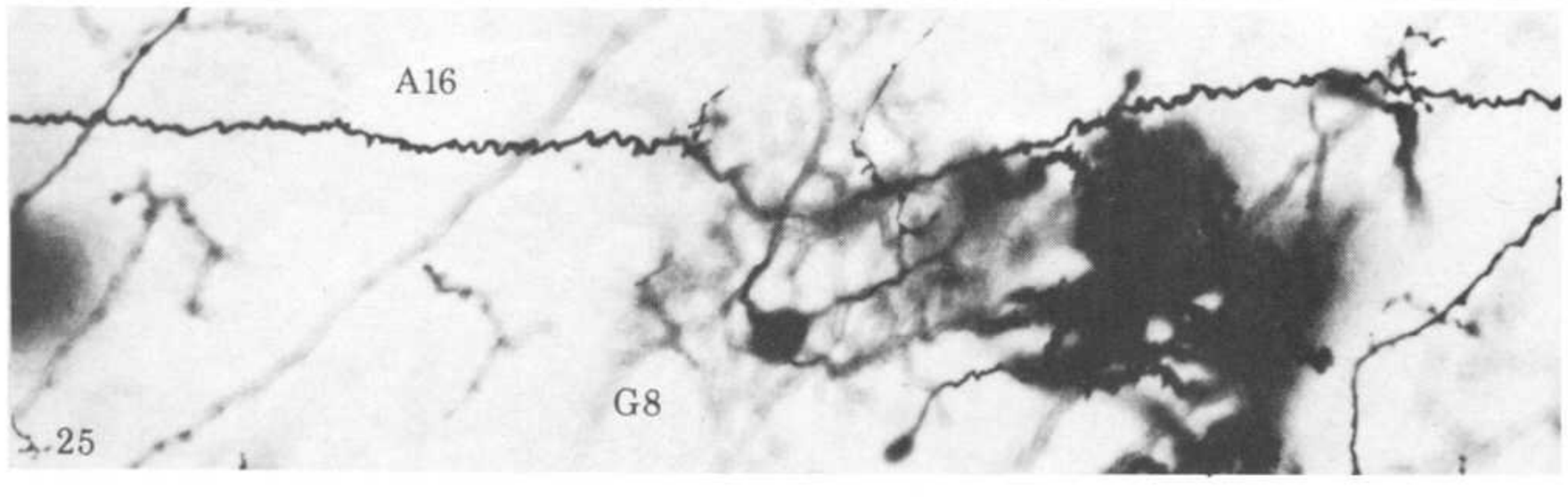
A16
G8
25

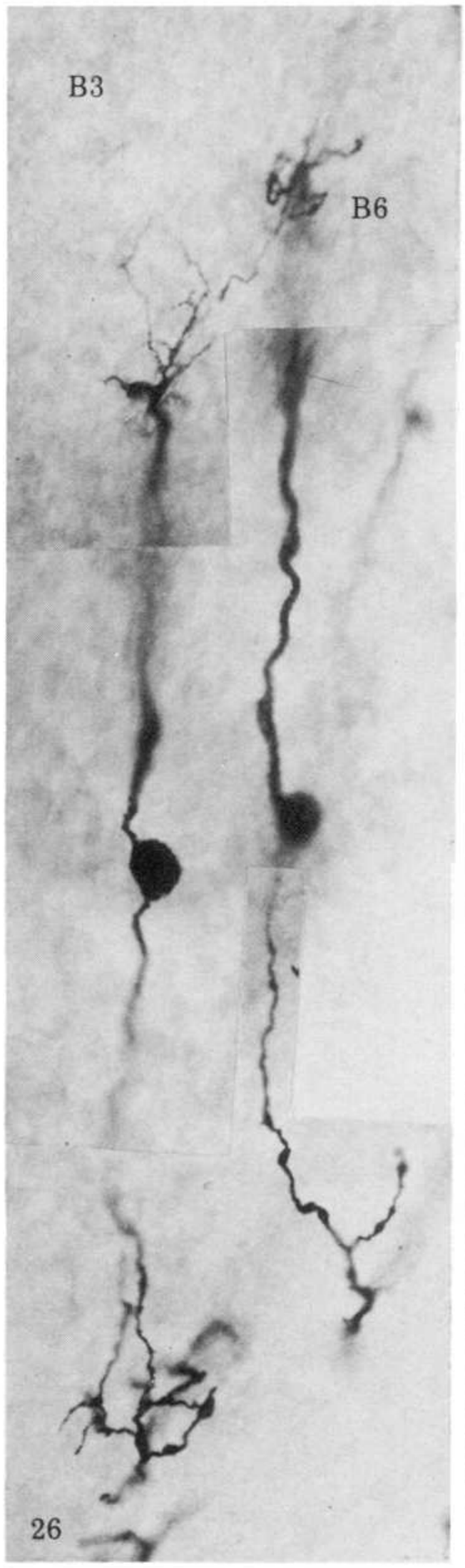

26

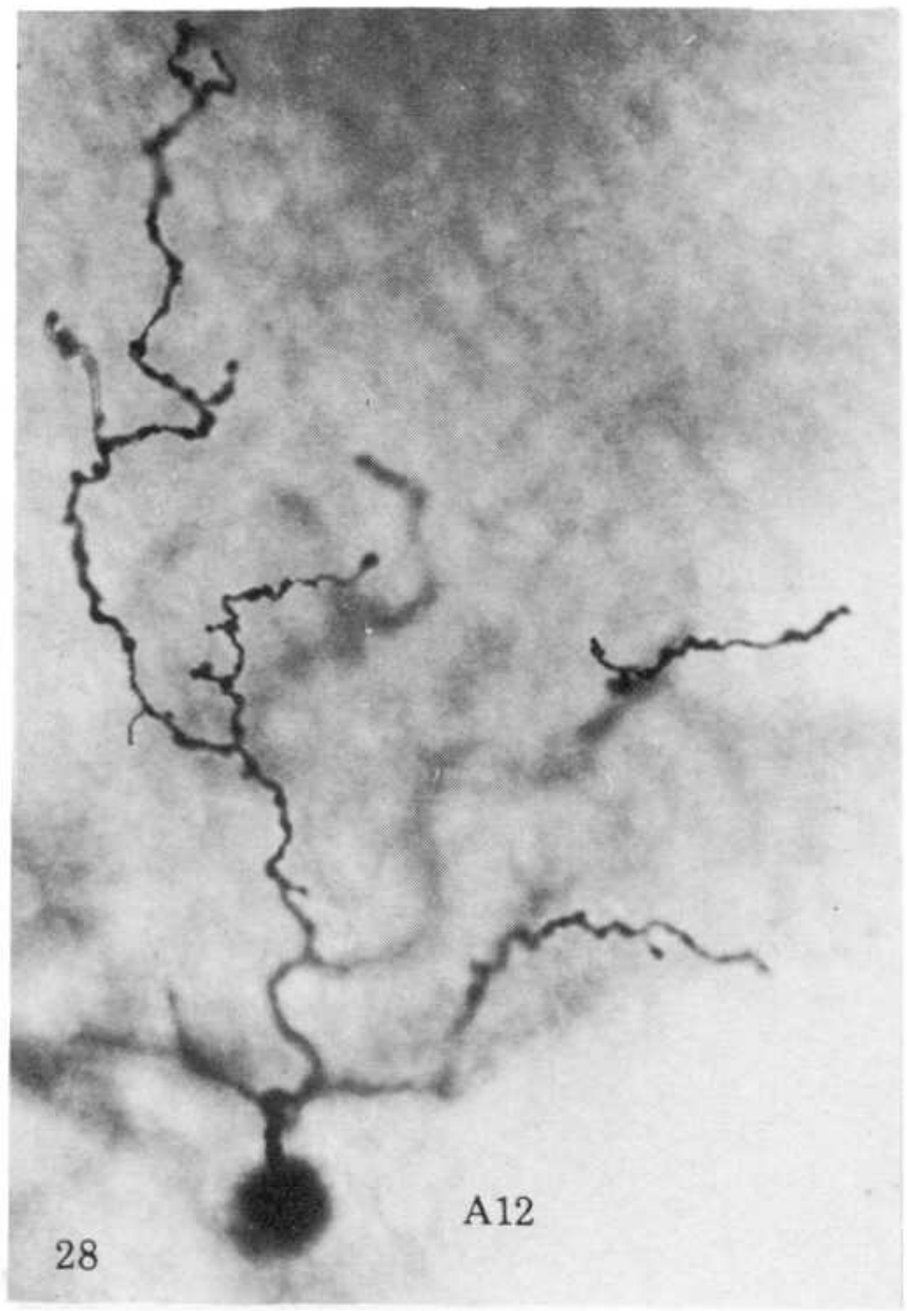

28

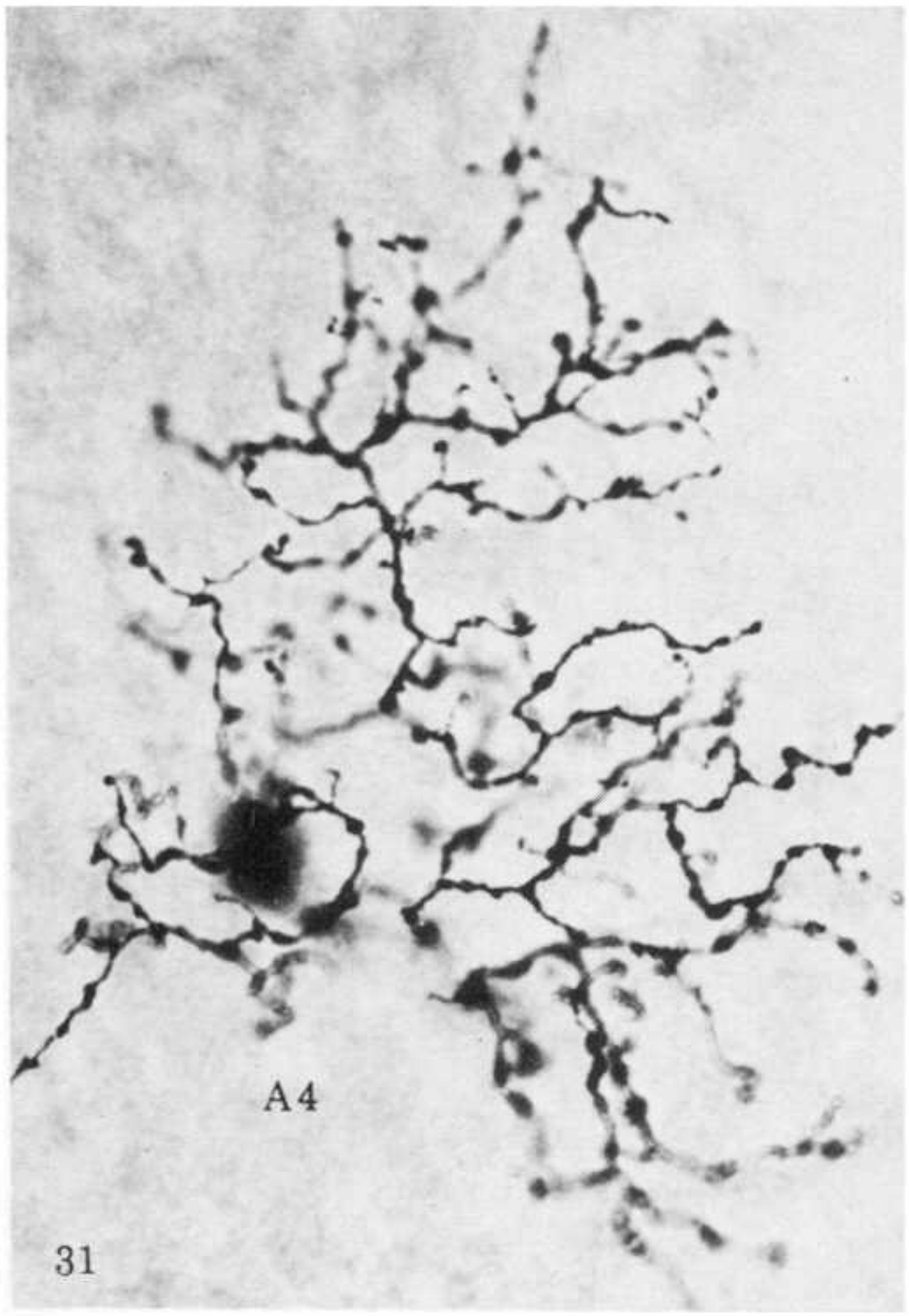

31

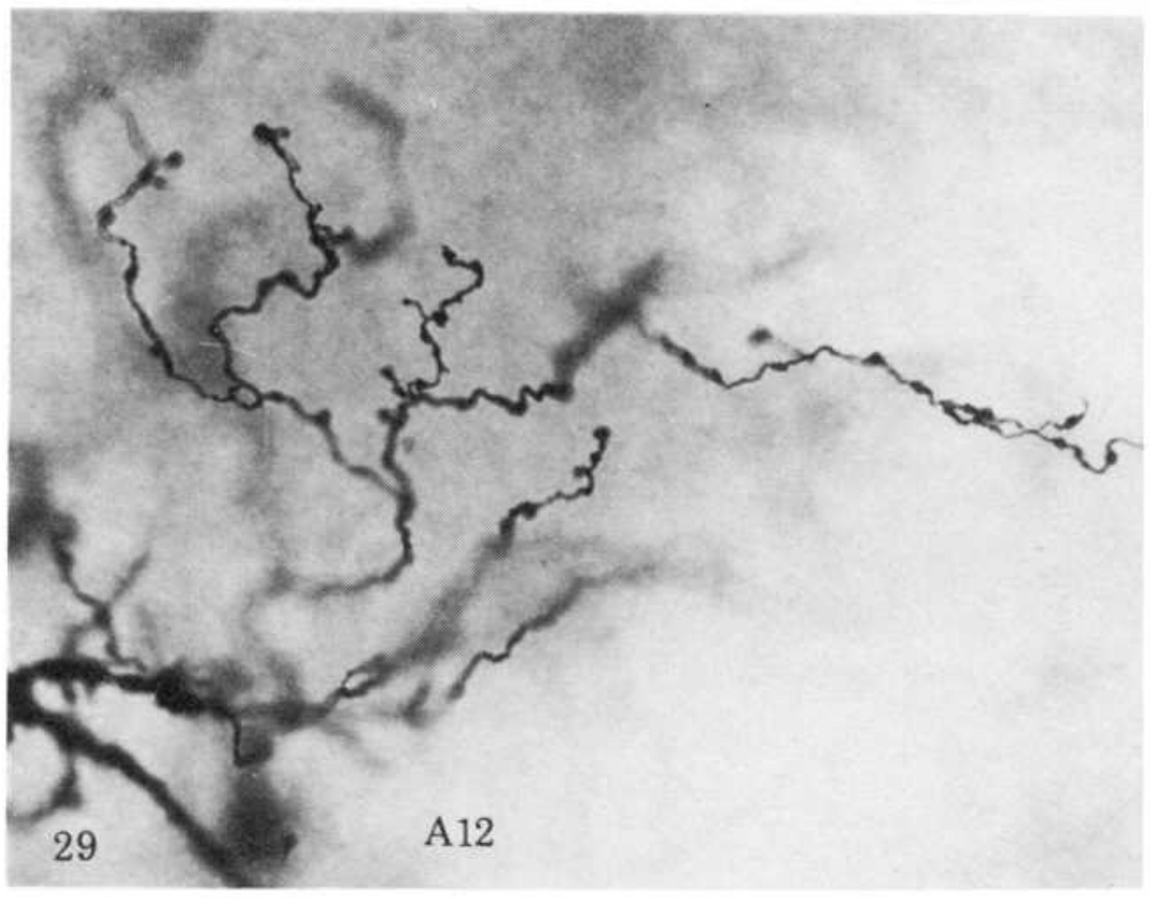

29

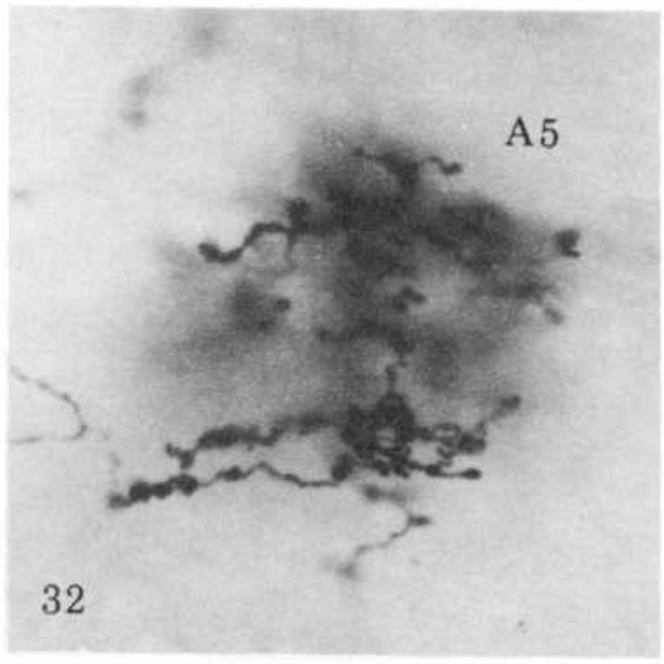

32

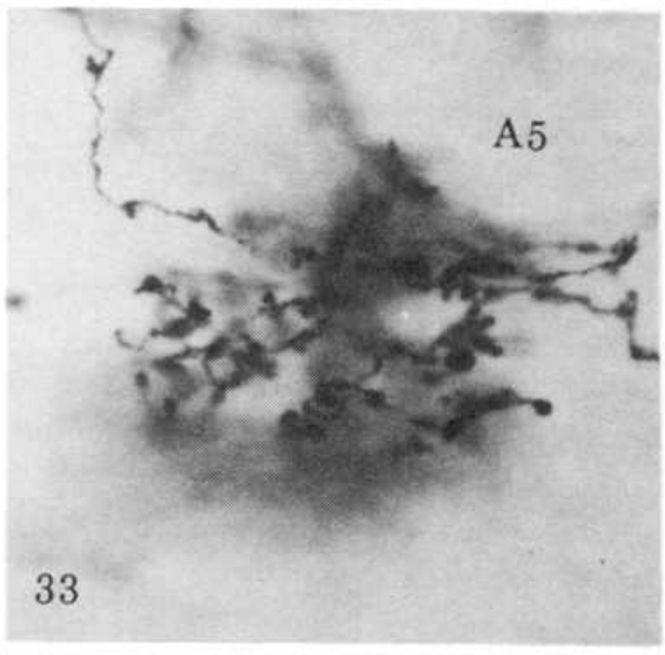

33

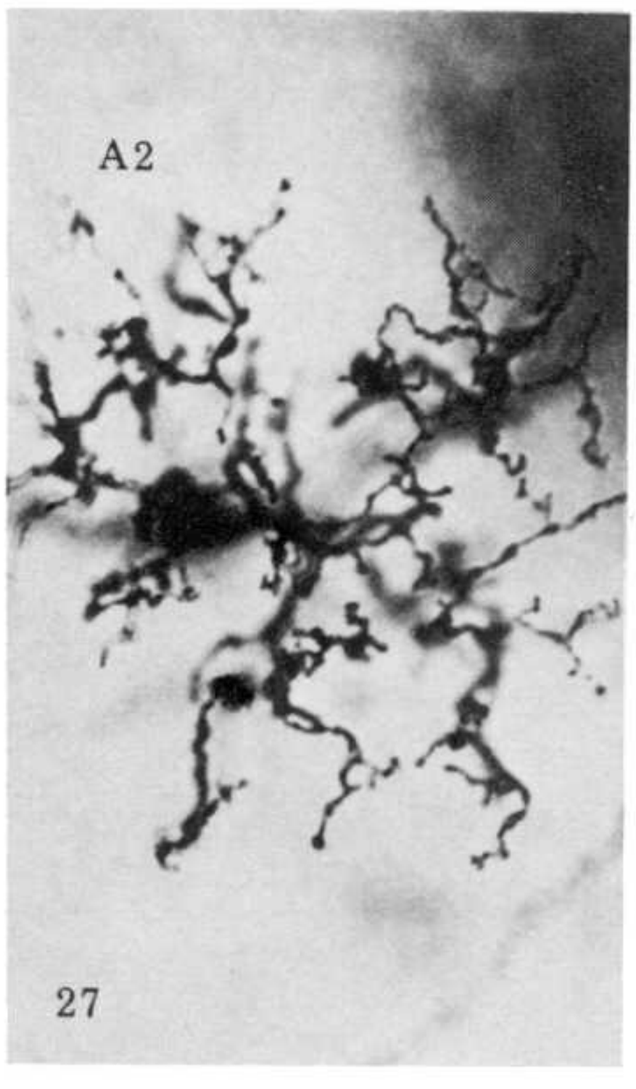

27

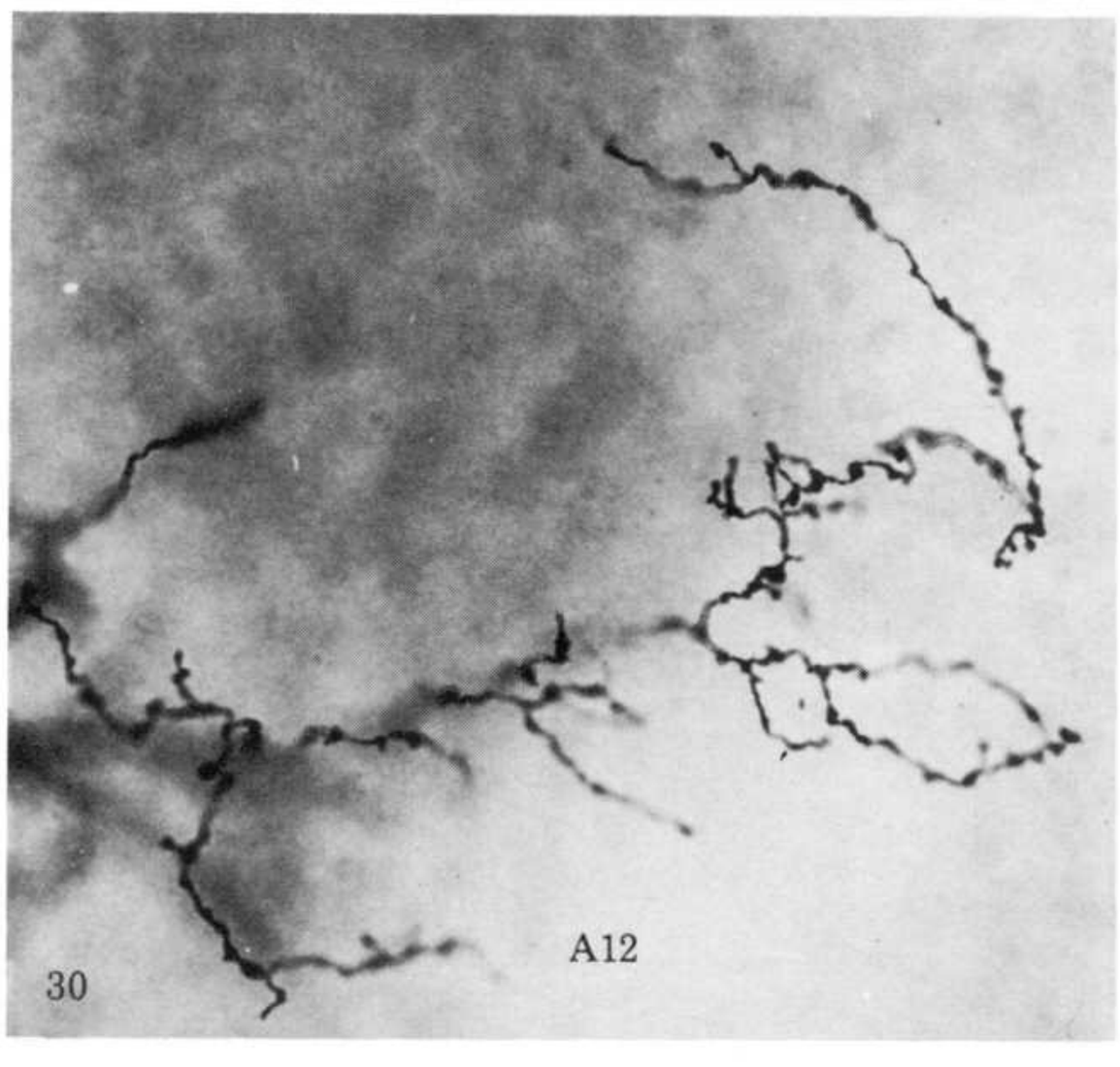

30

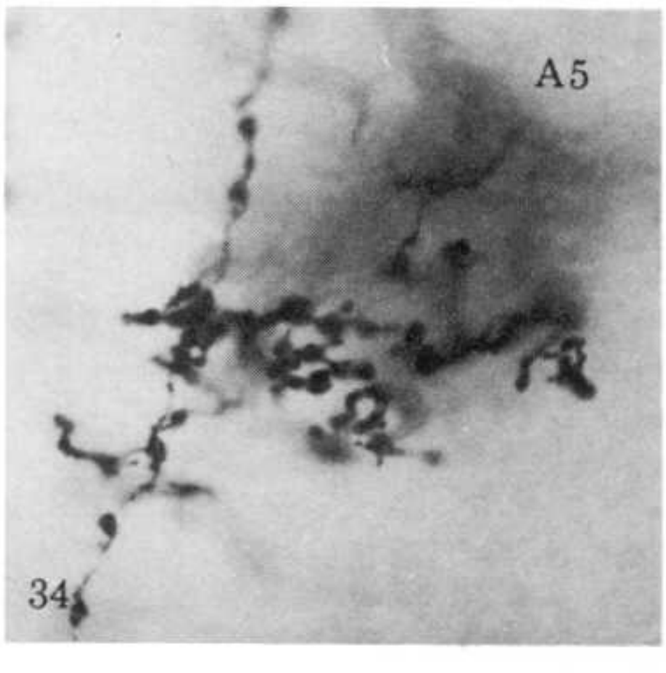

34

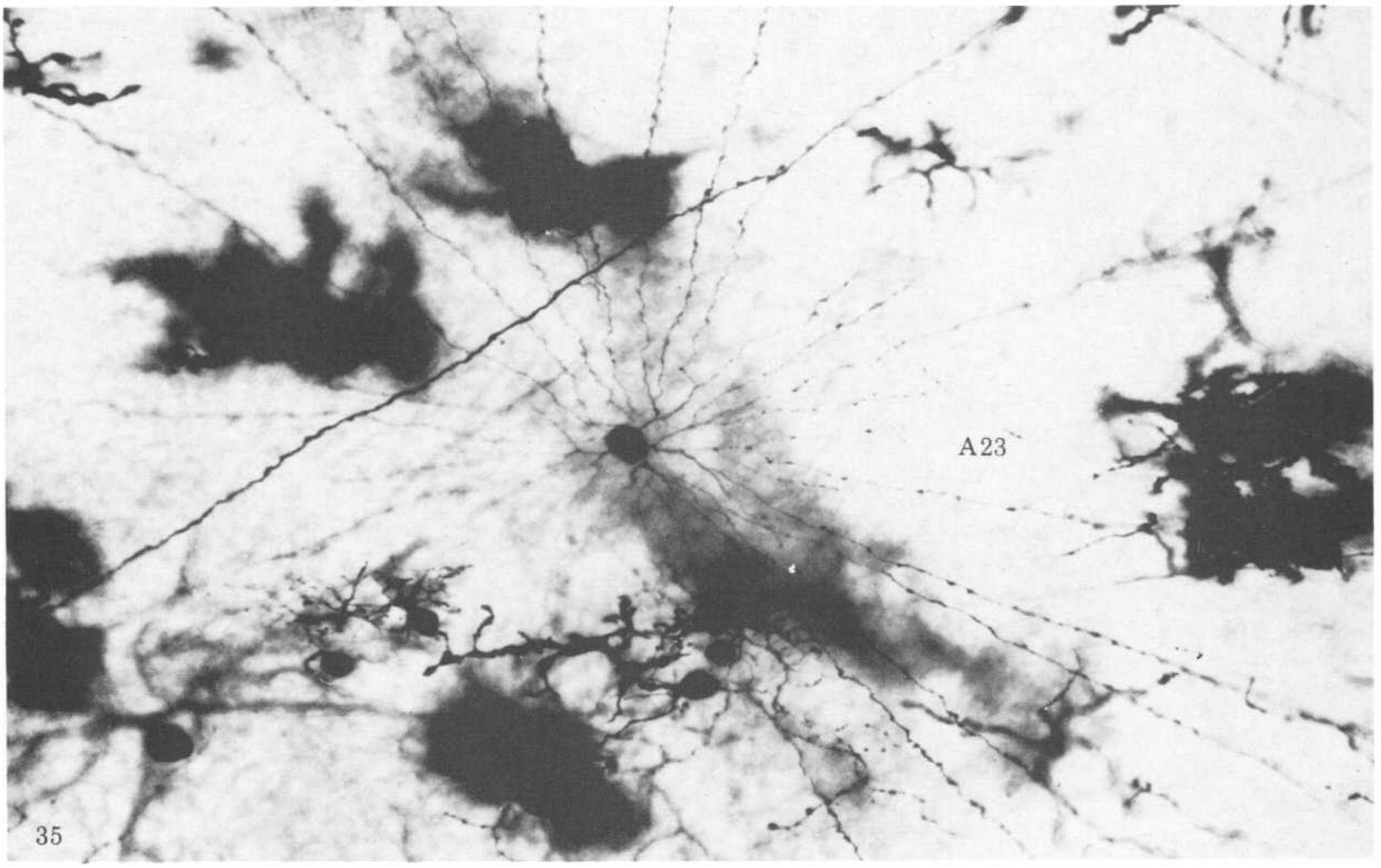
A23
35

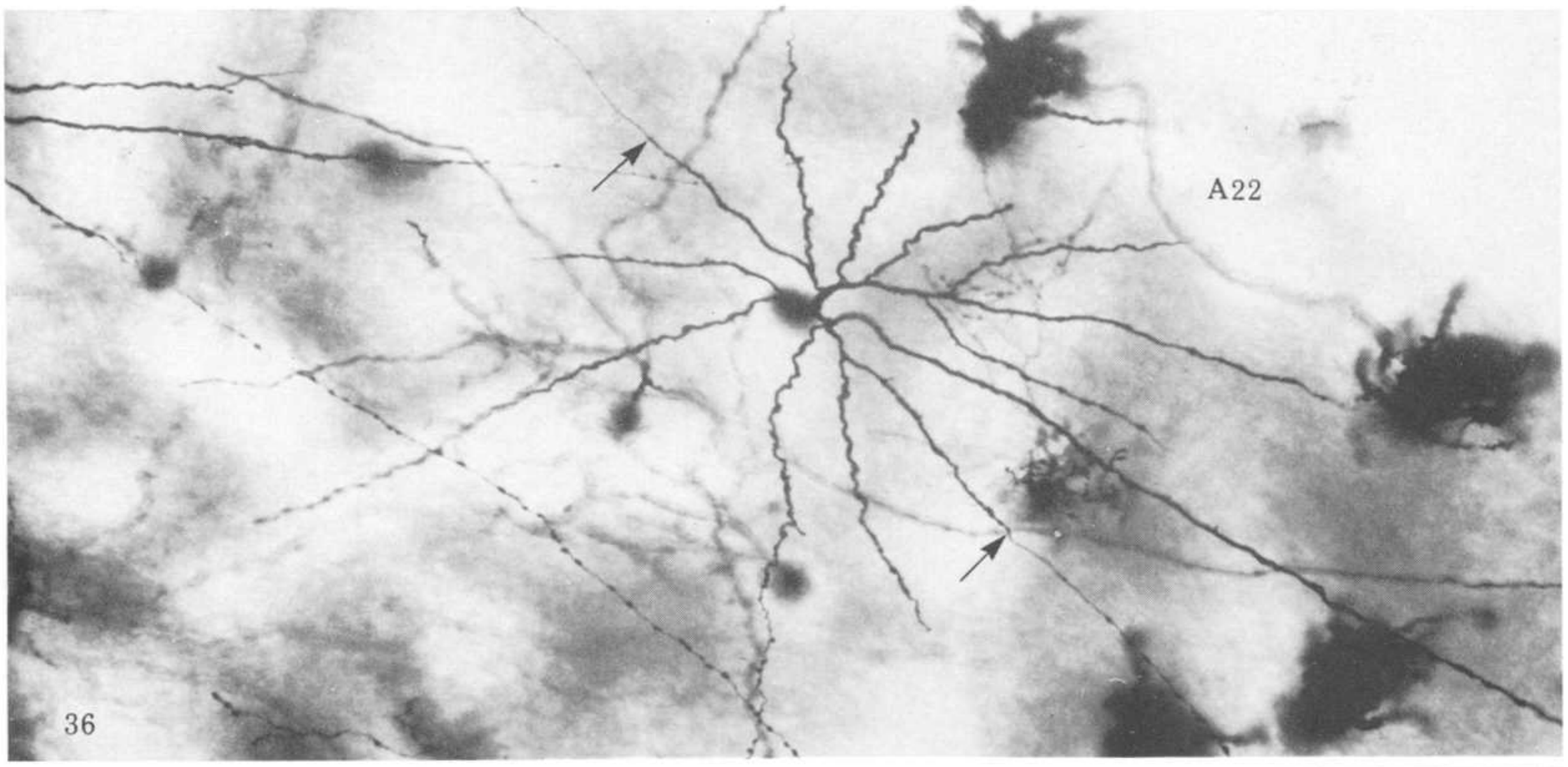
A22
36

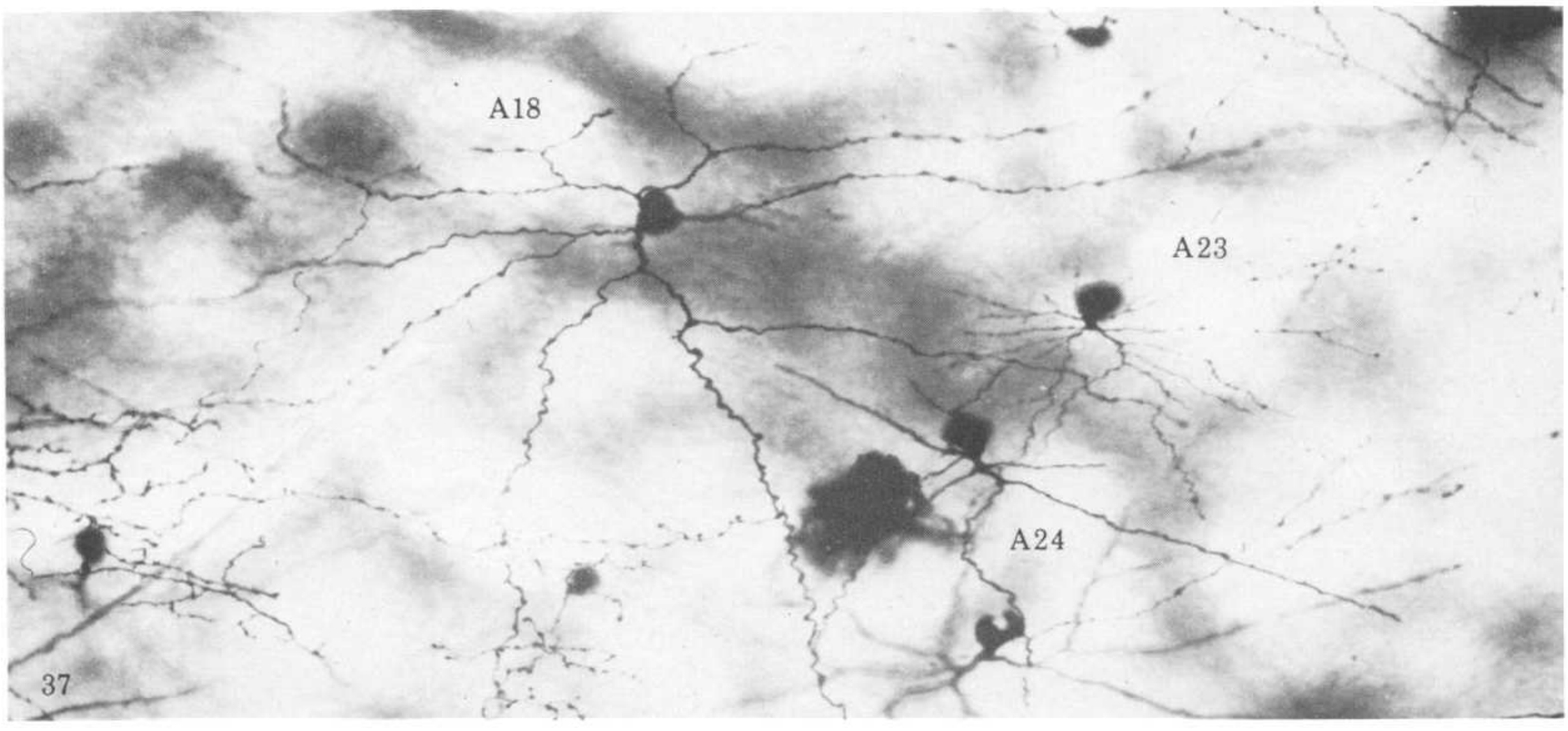
A18
A23
A24
37

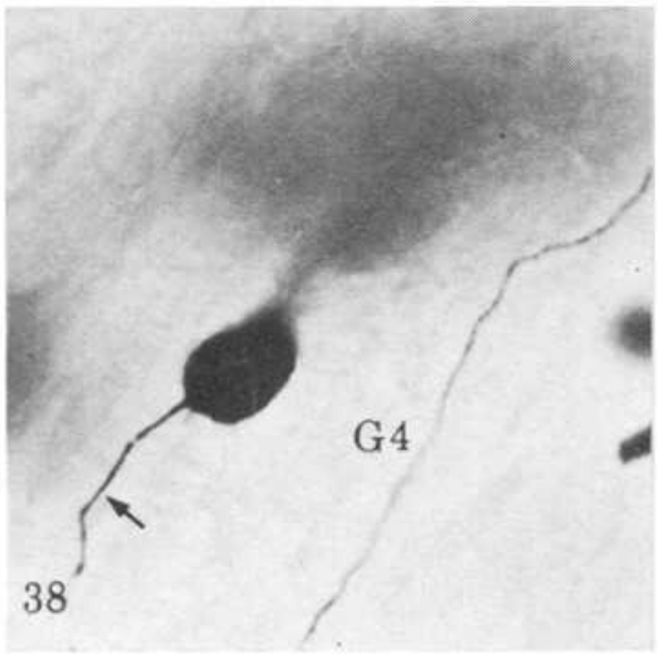

38

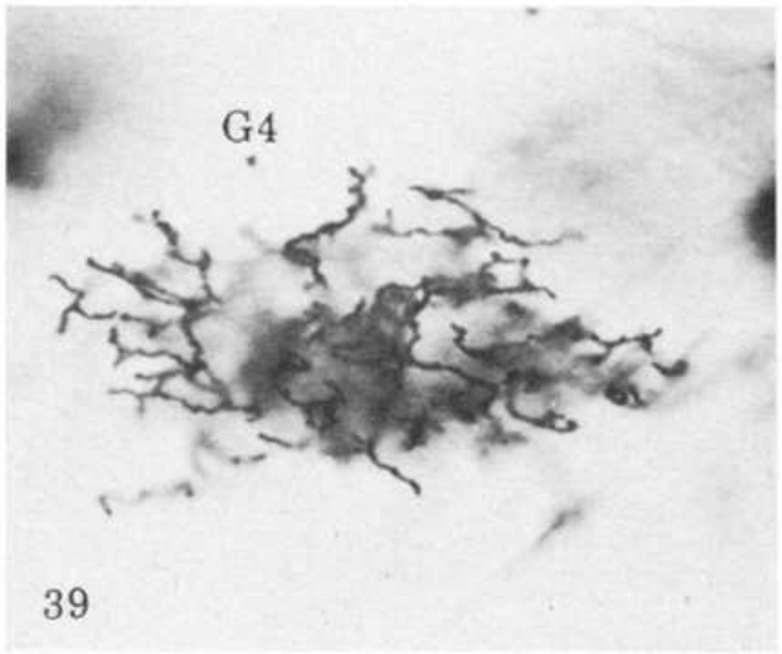

39

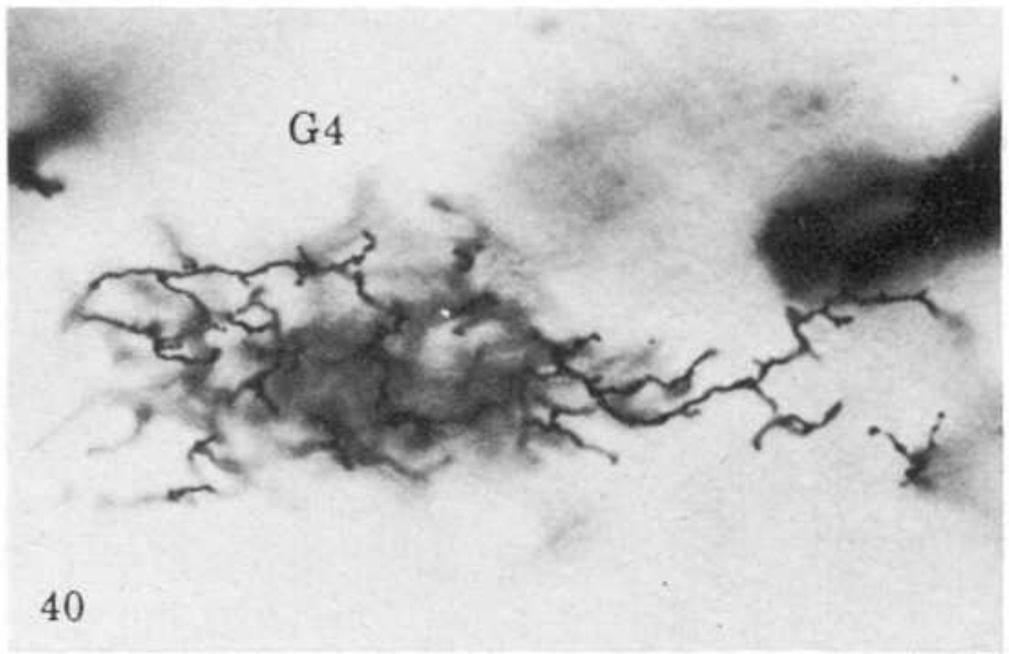

40

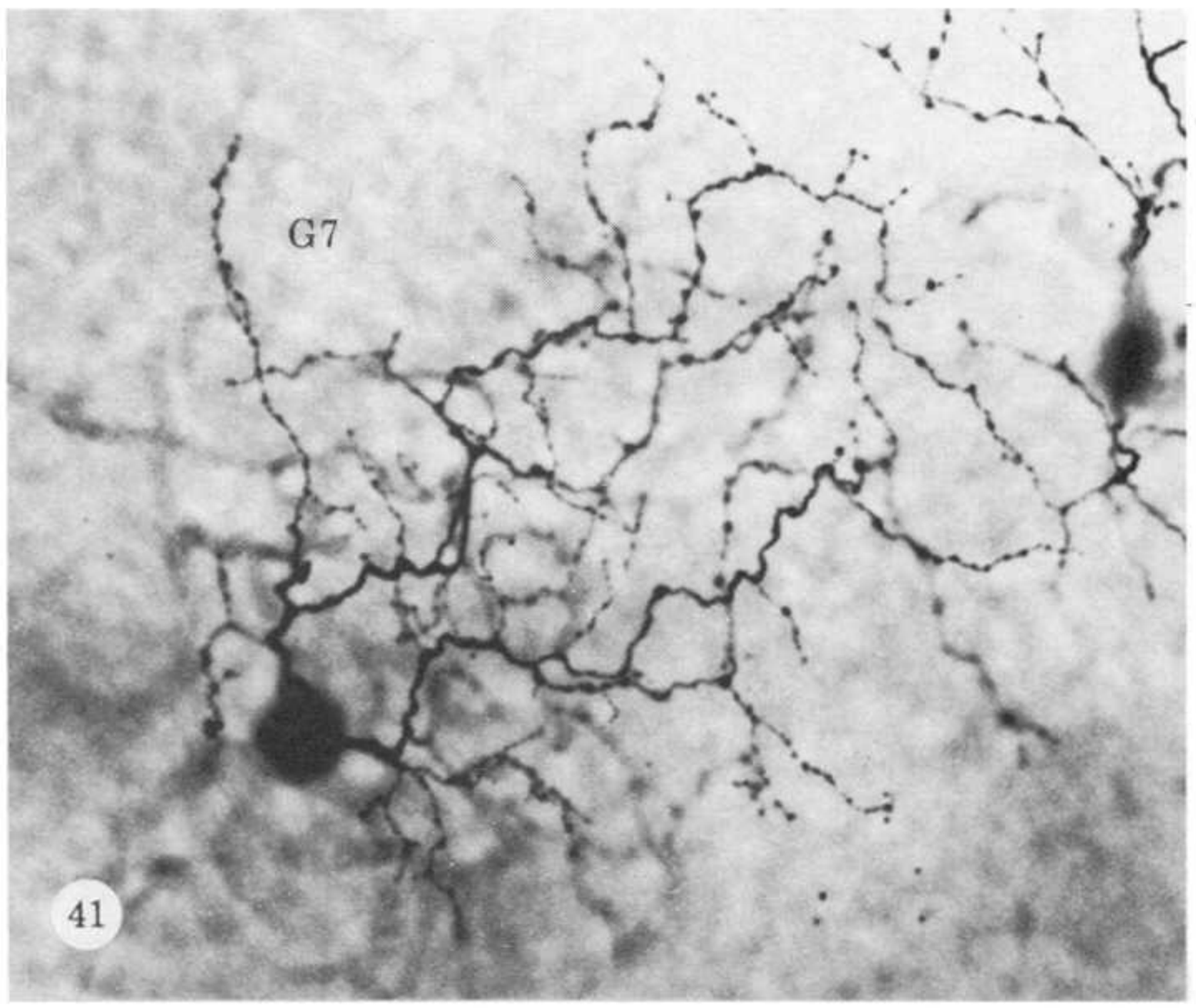

41

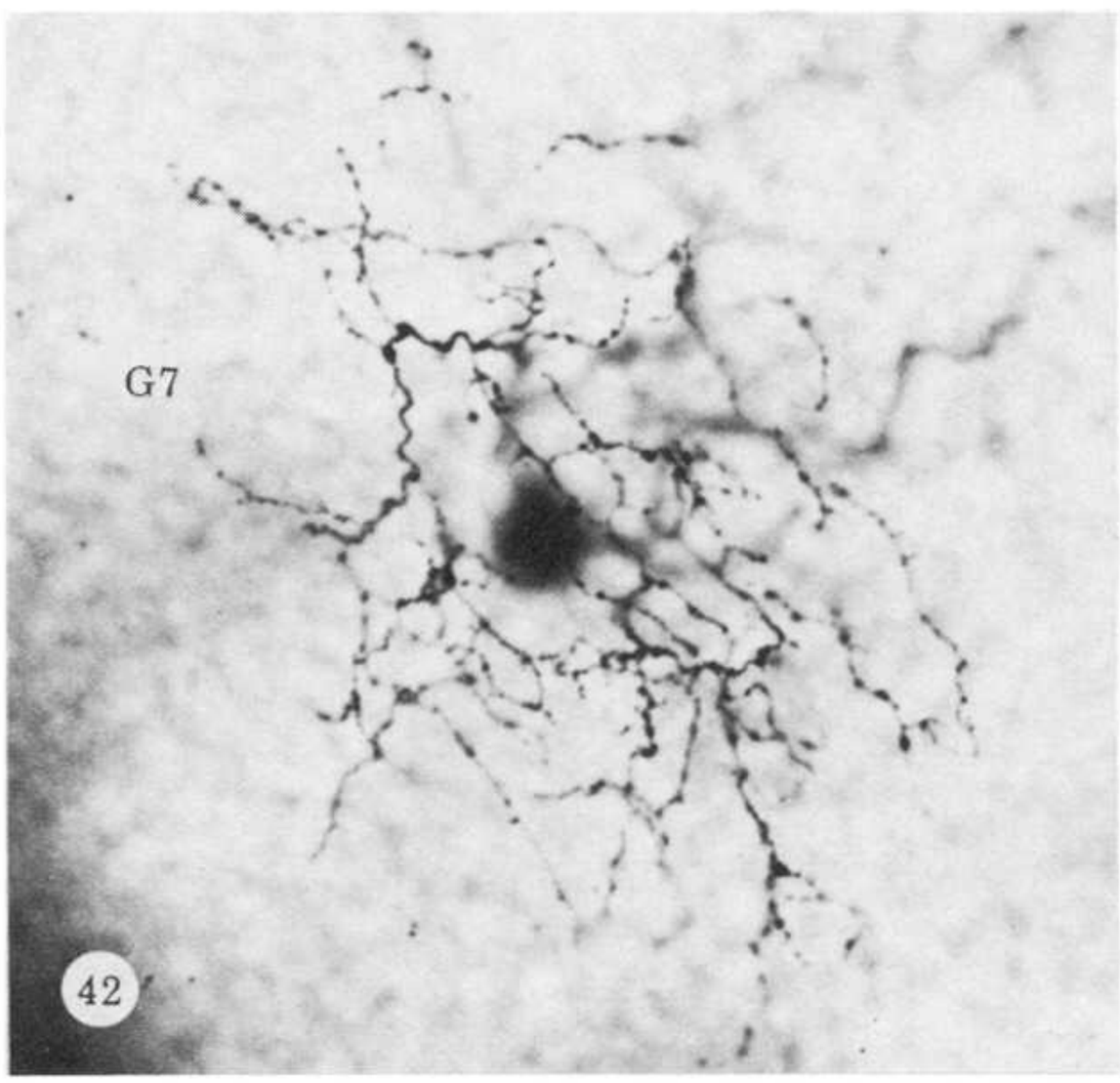

42

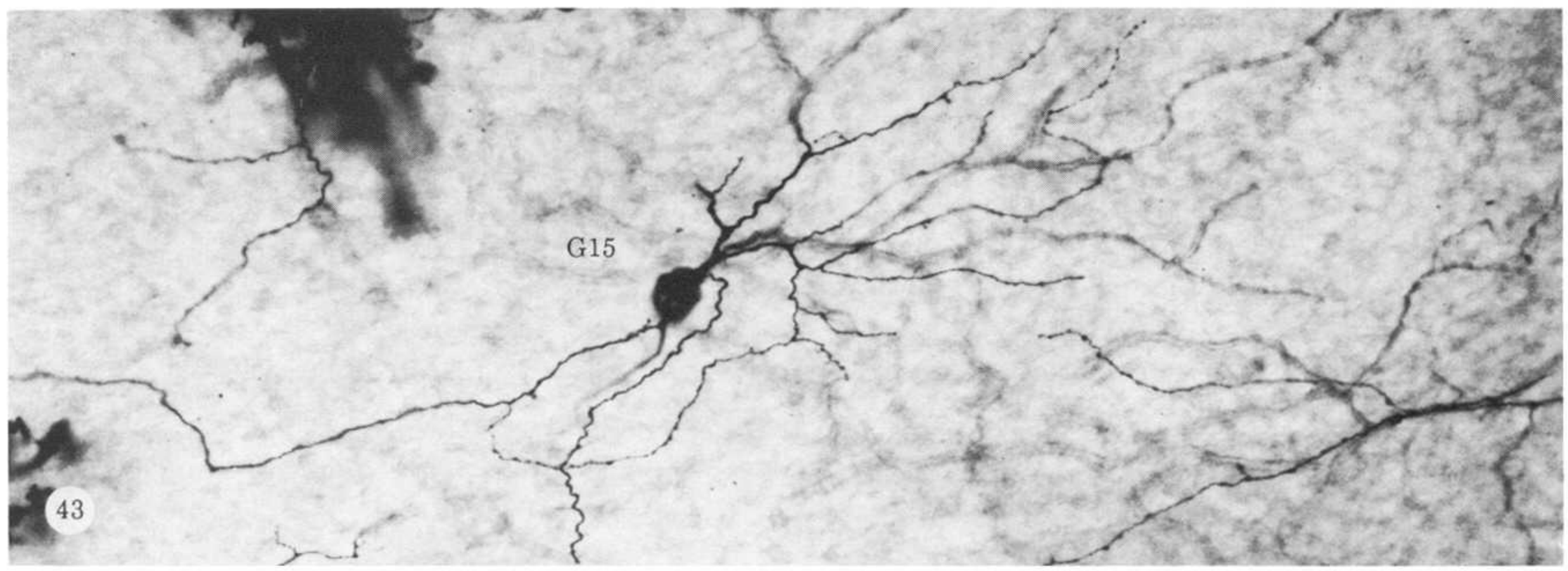

43

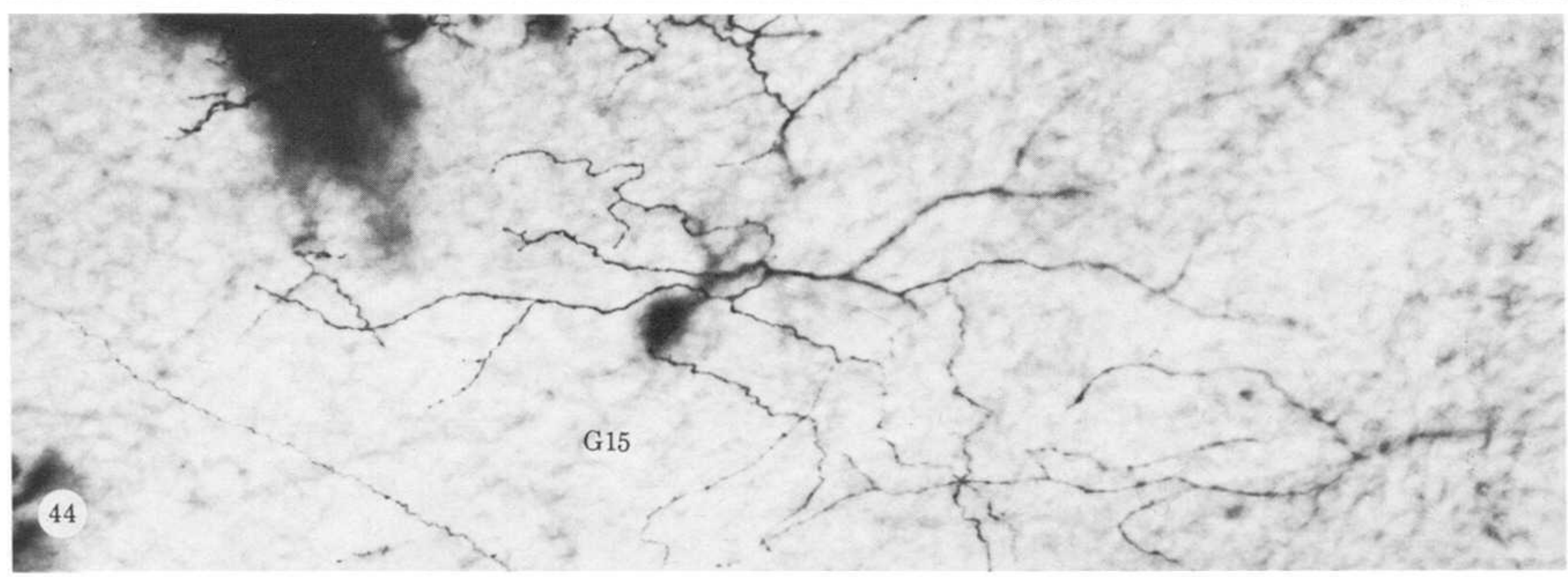

44

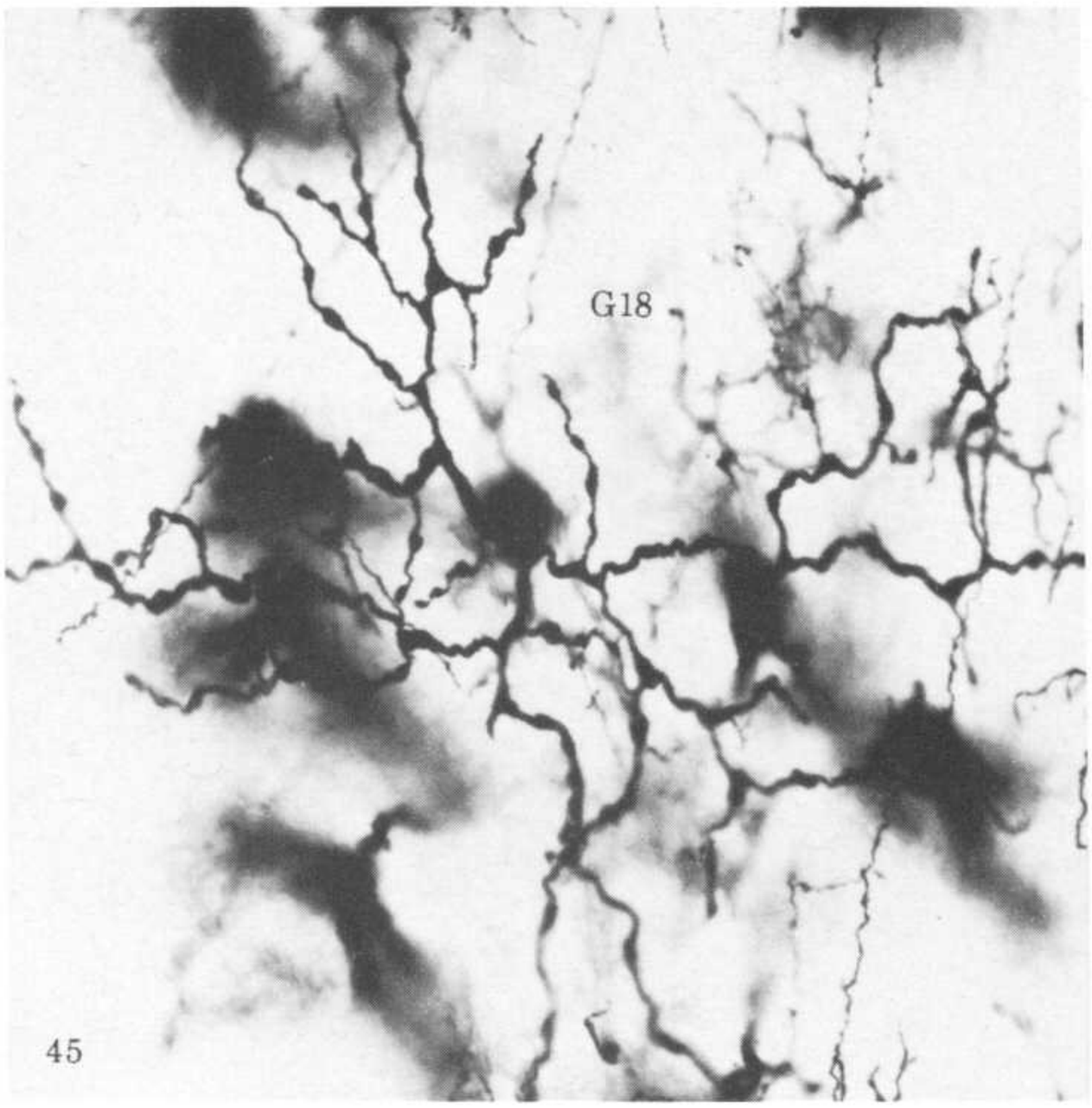
G18
45

G19
47

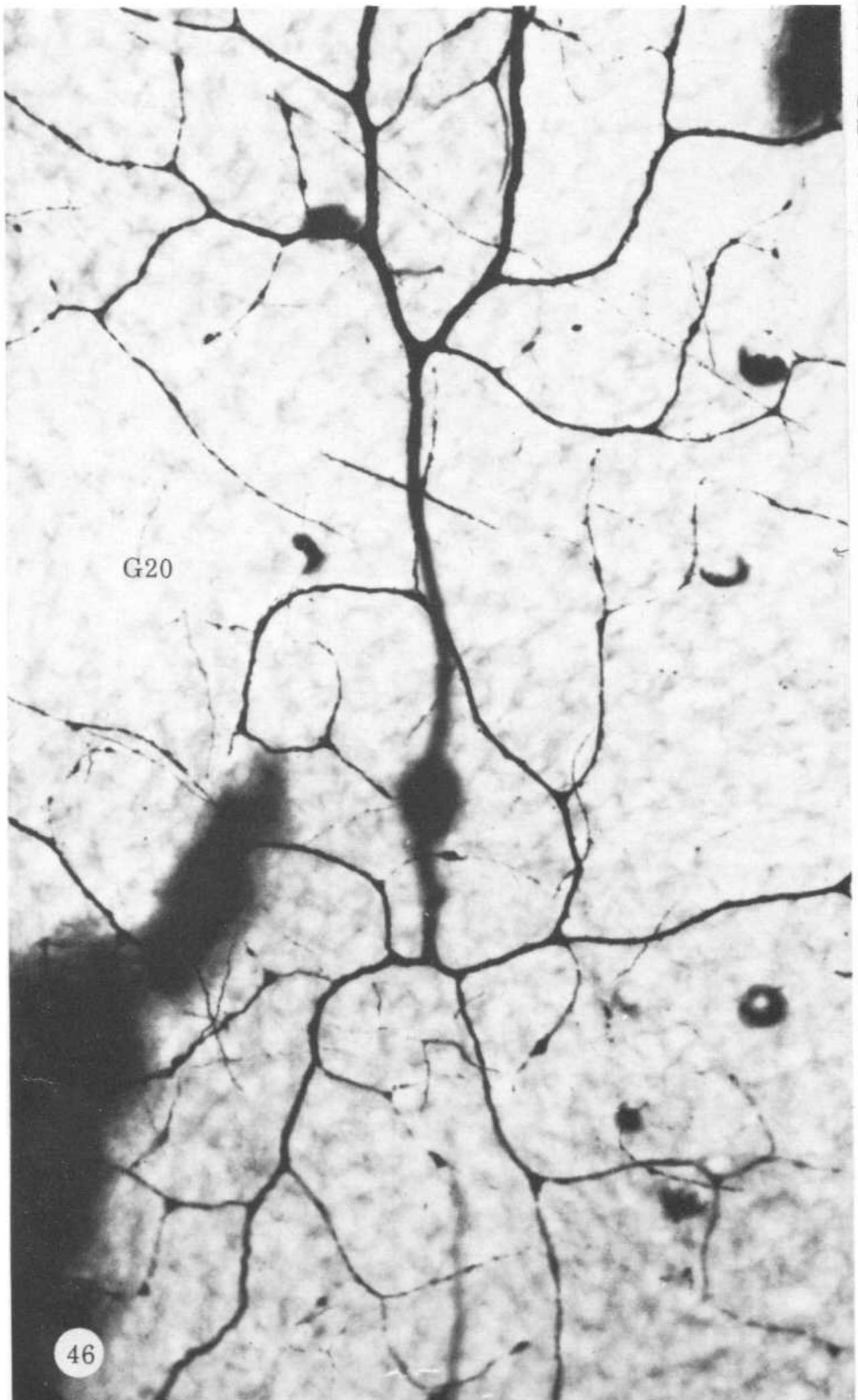
G20
46

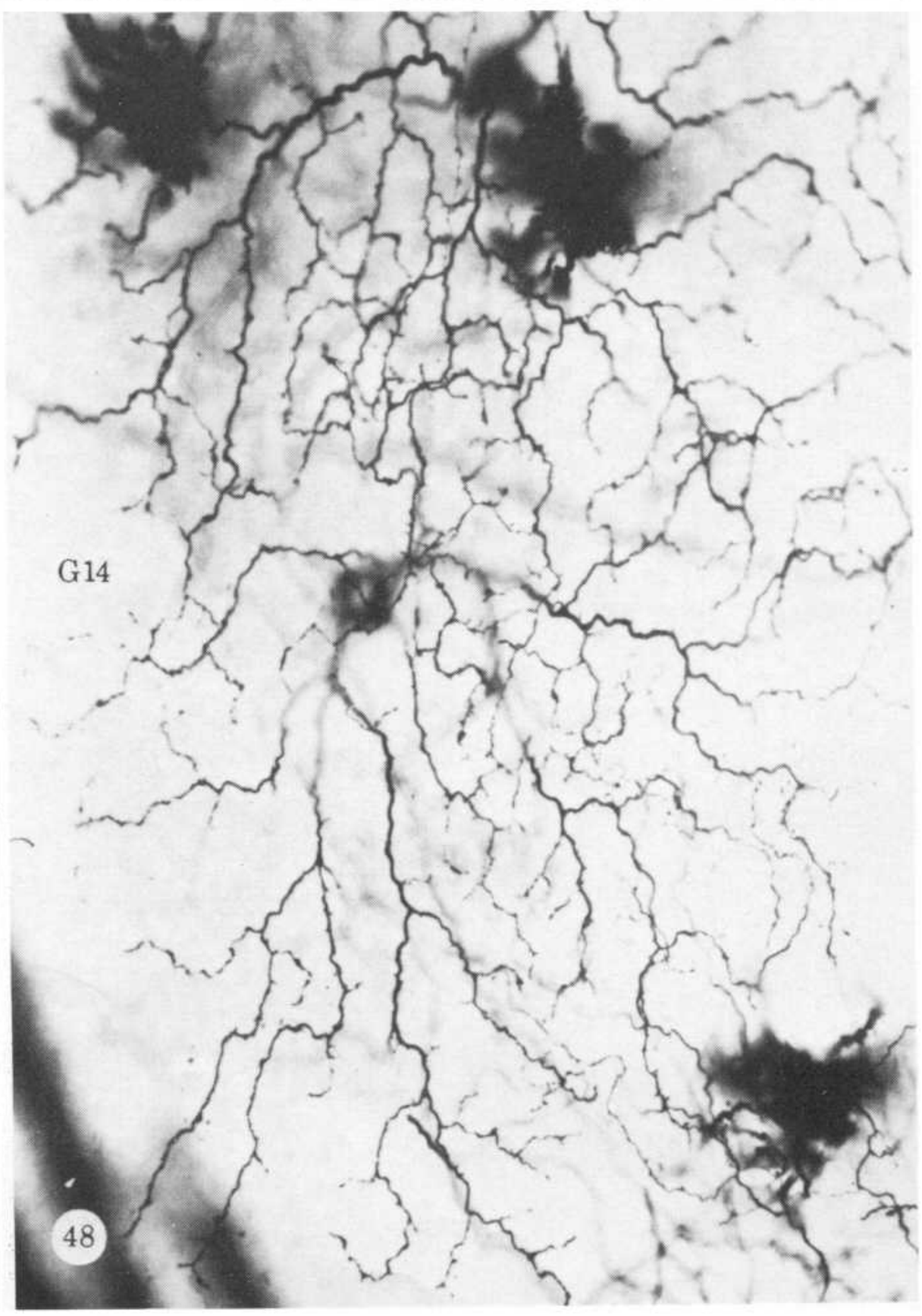
G14
48